

A STUDY OF CONVECTIVE HEAT  
TRANSFER FROM HIGH TEMPERATURE  
COMBUSTION PRODUCTS.

THESIS SUBMITTED FOR THE DEGREE OF DOCTOR OF PHILOSOPHY  
BY RALPH CONOLLY

UNDER THE SUPERVISION OF PROFESSOR F.M.PAGE,

Dr.R.G.TEMPLE AND Dr.R.M.DAVIES.

UNIVERSITY OF ASTON IN BIRMINGHAM - JUNE 1971

THESIS  
536.25  
CON

19 NOV 71 144657

ML

## ABSTRACT

The prediction of heat transfer rates from fuel-oxygen flames to solid surfaces is complicated by the wide variations in physical properties encountered in the gas phase and by the energy transfer which results from the diffusion and recombination of dissociated species. Consequently the conventional methods for the assessment of heat fluxes are found to be inadequate when applied to combustion systems.

A research programme was therefore initiated to carry out extensive experimental and theoretical studies of heat transfer from high temperature combustion products. Convective heat transfer coefficients have been measured at the stagnation point of an axially symmetrical blunt body immersed in the flames of a number of common fuel gases burning with pure oxygen. Theoretical predictions have been made for the full range of conditions covered experimentally. A numerical solution of the appropriate boundary layer conservation equations has been obtained and a method for the modification of the established relationship for heat transfer at low temperature levels has been proposed. Both approaches enable the extreme property variations and the diffusion-recombination effects to be taken into account when estimating the heat flux. Good agreement between experiment and the two prediction methods has been achieved in most cases.

Because of its potential value in design calculations the suggested empirical method has been tested over a wider range of conditions. Heat transfer from stoichiometric flames to small spheres has been measured at surface temperatures ranging to 1600K. It has been found that the proposed prediction method provides quite acceptable agreement with the experimental data.

## CONTENTS

1.	INTRODUCTION	1
1.1	Historical Background to the Project	
1.2	Objectives	
2.	CALCULATION OF THERMOPHYSICAL PROPERTIES	5
2.1	Equilibrium Composition of the Flame Gases	
2.2	Enthalpy and Heat Content	
2.3	Flame Temperature	
2.4	Specific Heat	
1.	Frozen specific heat	
2.	Equilibrium specific heat	
2.5	Density	
2.6	Viscosity of Combustion Product Mixtures	
1.	Calculation for pure non polar gases	
2.	Calculation for pure polar gases	
3.	The viscosity of gas mixtures	
2.7	Thermal Conductivity of Gases	
1.	Pure components	
2.	Mixtures of gases	
3.	THEORY OF HEAT TRANSFER WITH VARIABLE FLUID PROPERTIES	21
3.1	Previous Work	
1.	Systems without dissociation	
2.	Systems involving dissociation	
3.	Experimental investigations	
3.2	Proposed Modification of Low Temperature Relationships	
3.3	Proposed Numerical Solutions	

4.	INITIAL EXPERIMENTAL WORK	41
4.1	Burners	
4.2	Gas Metering System	
4.3	Equipment for Temperature Measurement	
4.4	Velocity Measurement	
4.5	Heat Transfer Probe Design	
4.6	Hydrogen Atom Concentrations	
5.	RESULTS FOR STAGNATION POINT WORK	58
5.1	Flame Temperature Measurements	
5.2	Hydrogen Atom Concentrations	
5.3	Velocity Measurements	
5.4	Heat Transfer Coefficients	
6.	HEAT TRANSFER TO SURFACES AT ELEVATED TEMPERATURES	64
6.1	Theoretical Background	
6.2	Experimental Work	
	1. Heat transfer coefficient measurements	
	2. Fuels and burners	
	3. Temperature and Velocity Measurements	
6.3	Evaluation of Data	
	1. Sensible heat gain of probe	
	2. Conduction from support wires	
	3. Direct flame radiation	
	4. Radiation losses	
6.4	Verification of the Experimental Method Used	
7.	RESULTS OF STUDIES AT ELEVATED SURFACE TEMPERATURES	74
8.	ALTERNATIVE CORRELATION PROCEDURES	75
8.1	Methods used for dissociated air	
8.2	Methods used for pure components	
8.3	Approximation based on hydrogen atom Lewis numbers	

9.	HEAT TRANSFER FROM NON-STOICHIOMETRIC FLAMES	82
9.1	Hydrogen-oxygen system	
9.2	Methane-oxygen system	
10.	DISCUSSION	88
10.1	Hydrogen Atom Concentrations	
10.2	Stagnation Point Studies	
1.	Experimental measurements	
2.	Comparison with numerical solutions	
3.	Comparison with empirical prediction	
4.	Comparison with the results of Kilham and Purvis	
10.3	Measurements at High Surface Temperatures	
1.	Experimental measurements	
2.	Comparison with empirical prediction	
10.4	Heat Transfer from Non-Stoichiometric Flames	
11.	CONCLUSIONS	105
	ACKNOWLEDGEMENTS	106
APPENDIX 1	Data used for transport property calculations Tabulated thermophysical properties of combustion product mixtures	
APPENDIX 2	Derivation of transformation equations used in numerical solution procedure	
APPENDIX 3	An application of the work to the economics of electrically augmented flames	
	BIBLIOGRAPHY	

NOMENCLATURE

$A_b$	area of bead thermocouple	$m^2$
$c$	velocity of light in vacuum	$m/s$
$C_p$	specific heat at constant pressure	$J/kgK$
$C_v$	specific heat at constant volume	$J/kgK$
$D$	diffusion coefficient	$m^2/s$
$D_b$	body diameter	$m$
$E$	equivalence ratio	-
$f$	ratio of velocities $u/u_a$	-
$G$	mass velocity of approach stream	$kg/m^2 s$
$Gr$	Grashof number ( $\beta g \rho^2 D_b^3 \theta / \mu^2$ )	-
$g$	acceleration due to gravity	$m/s^2$
<u>or</u>	enthalpy ratio $I/I_a$ in numerical solutions	-
$H$	enthalpy of fluid excluding kinetic energy term	$J/kg$
$H_{chem}$	dissociation enthalpy	$J/kg$
$h$	heat transfer coefficient	$W/m^2 K$
<u>or</u>	Planck's constant	$W$
$I$	enthalpy of fluid including kinetic energy term	$J/kg$
$k$	Boltzmann constant	$J/K$
$Le$	Lewis number [ $D/(\lambda/\rho C_p)$ ]	-
$M$	molecular weight	-
$Nu$	Nusselt number ( $hD_b/\lambda$ )	-
$P$	static pressure	$N/m^2$
$Pr$	Prandtl number ( $C_p \mu / \lambda$ )	-
$q$	heat flux	$W/m^2$
$R$	ideal gas constant	$J/kg\text{-mole K}$
$R_b$	boost ratio for augmented burners (electrical input/ chemical input)	-
$r$	radius	$m$

$r_b$	body radius	m
St	Stanton number ( $h/GC_p$ )	-
T	absolute temperature	K
u	velocity component parallel to surface	m/s
v	velocity component perpendicular to surface	m/s
x	distance from stagnation point measured along the surface	m
$\bar{x}$	transformed x co-ordinate	-
y	distance measured perpendicularly from surface	m
$\beta$	volumetric coefficient of expansion	1/K
<u>or</u>	velocity gradient at stagnation point	1/s
$\epsilon$	intermolecular force constant	
$\theta$	temperature differential	K
$\eta$	transformed y co-ordinate	-
$\delta$	boundary layer thickness	m
$\lambda$	thermal conductivity	W/mK
$\mu$	shear viscosity	Ns/m <sup>2</sup>
$\nu$	kinematic viscosity	m <sup>2</sup> /s
$\rho$	density	kg/m <sup>3</sup>
$\sigma$	intermolecular force constant	
$\Omega$	collision integral	

### Superscripts

- ° denotes values applicable to reference state
- ' denotes differentiation with respect to  $\eta$
- \* denotes values at mean film temperature
- denotes averaged values

## Subscripts

- ε refers to electricity
- e denotes values at boundary layer edge
- eq denotes equilibrium values
- f denotes chemically frozen values
- g refers to fuel gas
- H denotes values applicable to hydrogen atoms
- i denotes species i
- j denotes species j
- o refers to oxygen
- R denotes reaction values
- s denotes values in the free stream
- w denotes wall values

## 1. INTRODUCTION

### 1.1 Historical Background to the Project

At its inception in 1967, the primary objective of this work was to study the problem of heat transfer from high temperature flames to cooler surfaces. The need for research into this topic became apparent with the development of an expanding market for oxygen particularly within the steelmaking industry. The adoption of refining processes based on the direct oxidation of impurities had led to the construction of progressively larger liquefaction plants for the production of oxygen. The economies effected on running expenses and overheads associated with the increased scale of operation secured a progressive decline in the cost of this commodity.

Previously oxygen had been comparatively expensive so that its use in combustion was economically viable in only a limited number of applications where high flame temperatures were essential. These included the technologically important fields of glassworking and the cutting and welding of metals, but the small scale of each individual operation did not justify an extensive scientific study of the heat transfer process. This state of affairs was abruptly changed by the availability of oxygen at significantly lower prices which opened up new possibilities for the use of fuel-oxygen flames in industry.

One application which appeared to be feasible was the preheating and assisted melting of steel scrap in electric arc furnaces. It was proposed that large capacity fuel-oxygen burners be used to supplement the electrical power input and permit high metal throughputs without endangering the maximum demand restrictions agreed with the electricity suppliers. In addition it was found that gas burners operating with an excess of oxygen were capable of refining the molten steel without forming the large quantities of red oxide fume generated by conventional oxygen-lancing.

Other spheres of activity involved the possibility of providing for supplementary firing in open hearth installations and for oxygen enrichment in the reverberatory furnaces used for melting and refining certain non-ferrous metals. Limited trials of the "Fuel-Oxygen-Scrap" process for steelmaking were also carried out in which oxygen-oil burners provided the sole source of heat input to the refining furnace.

Consequently a number of the major fuel and oxygen suppliers became interested in the subject of heat transfer from high temperature systems and in methods for its prediction. The research project instigated at the Gas Council Midlands Research Station was designed to study the problem in detail and the work carried out forms the basis of this report. During the course of the investigation, it became apparent that the problems encountered with fuel-oxygen flames were but one aspect of the more general field of heat transfer with large temperature and property gradients. For this reason the natural gas-air system was included in the studies, a move which was particularly appropriate following the exploitation of the reserves discovered beneath the North Sea. The extension of the original programme was also demanded by the need for comparison with conventional systems in order to assess the potential benefits to be gained by employing oxygen.

## 1.2 Objectives

It is evident that the ability to make reliable predictions of the heat transfer from flames would be a valuable asset, particularly in the design and evaluation of possible new processes and the optimisation of existing operations. It is frequently desirable that the heat flux obtained with a combustion appliance should be known. This may be necessary to check that the performance of the equipment will meet the required specification, or to ensure that the materials of construction will be adequate for the purpose and not adversely affected by overheating.

At the present time, however, it is clear that the design and operation of gas-fired heat transfer equipment is based very largely on accumulated practical experience rather than on established scientific principles. This is an inevitable consequence of the dearth of experimental data applicable to high temperature systems, particularly in the fields of natural and forced convective heat transfer, and to the lack of accurate prediction methods for use in such environments.

This situation is in striking contrast to that observed under the relatively low temperature conditions which characterise traditional chemical engineering processes. For these, very extensive practical investigations have been carried out and a large number of reliable empirical relationships established. These facilitate the confident prediction of heat and mass transfer rates for many common geometrical and fluid combinations and, as such, are invaluable for design purposes. The difficulties which prevent the extension of these relationships to the high temperature conditions in flames, apart from the shortage of experimental data, stem from the large variations in physical properties which are frequently characteristic of heat transfer from combustion products. These variations hinder the use of empirical equations in their usual forms by introducing difficulties in the definition of the appropriate conditions for the evaluation of fluid properties, a problem particularly acute where large temperature gradients are present.

An additional complicating factor arises when considering the heat transfer from the higher temperature flames which result from the use of oxygen enrichment. At the temperature levels found in these flames dissociated material forms an appreciable proportion of the combustion product mixture. This creates further difficulties both in the evaluation of thermophysical properties and in the prediction of the heat

transfer rates obtained from the flames in practice.

Clearly, one important objective of heat transfer theory lies in the development of sound bases for predictions under conditions where the precise experimental information is not available. In principle estimates may be achieved by taking one of two distinctly separate approaches. The first of these takes advantage of the established theory of boundary layers. The appropriate conservation equations may be solved, usually by machine computation, for virtually any desired conditions provided that all the requisite input parameters can be both identified and quantified. However, since each problem must be treated independently it is evident that the rate of advancement will necessarily be restricted.

On the other hand progress may be made more swiftly with the generalisation of existing data into compact working relationships. In many cases the important variables may be readily identified and incorporated into dimensionless groups with immediate simplifications to the problem of data correlation. Extrapolation by such practices is however, potentially hazardous since unsuspected peculiarities may exist in the unfamiliar system, and a serious loss of accuracy may result. Some compromise inevitably results whereby the concepts developed in the theoretical approaches complement the empiricism of the practical methods while the latter provide stimuli for further theoretical advancement.

Consequently, the purpose of this research project has been to study the process of forced convective heat transfer between flames and solid surfaces from both experimental and theoretical standpoints. An attempt has been made to provide a practical method enabling the numerous correlation equations established for low temperature situations to be extended to combustion systems.

## 2. CALCULATION OF THERMOPHYSICAL PROPERTIES

The desire to predict the magnitude of heat transfer from high temperature gas streams immediately introduces a demand for sound data on the gas-phase thermodynamic and transport properties. The quantities represented by the shear viscosity, the thermal conductivity and the diffusion coefficients are closely associated with all interphase convective heat transfer processes and their accurate determination becomes an essential pre-requisite for the application of a reliable heat transfer theory.

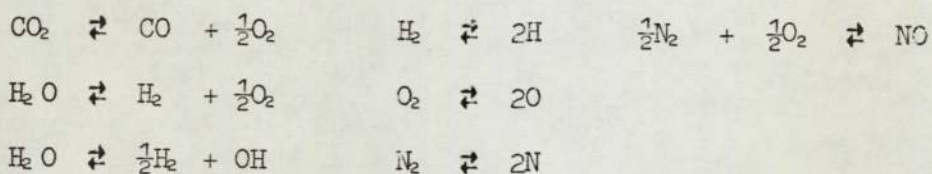
At low temperature levels (up to 1200 K) this demand has been largely satisfied by the careful measurements of numerous investigators. The wide range of fluids and temperatures encountered in the industrial, military and commercial fields has resulted in the generation of a correspondingly large volume of literature reporting the experimental work. This is constantly surveyed by the Thermophysical Properties Research Centre at Purdue University which correlates and cross references the data, and from time to time issues recommended values for general use.

Unfortunately, the available methods for direct measurement of gas properties are in many cases totally unsuited for measurements at elevated temperatures. Recourse to a theoretical approach then has to be made. The monumental work of Hirschfelder, Curtiss and Bird (1) provides the basis for much of present day transport property theory although further advancements have since been made, particularly at the higher temperature levels. However, experimental measurement of the physical properties of the various components in combustion product systems remains as an important check on the validity of theoretical arguments. It is clear that, to be entirely satisfactory, the theory of high temperature thermophysical properties must reduce to the familiar as well as predict the unfamiliar. This theory is inevitably rather complex so that only a broad outline of the procedure used in practical

calculations can be given. The data obtained for use in the present studies has been tabulated and the information is presented for the whole range of fuel-oxidant combinations in Appendix 1.

### 2.1 Equilibrium composition of the flame gases

The calculation of equilibrium combustion product compositions is an essential step in the prediction of the thermodynamic and transport properties of the mixture. The equilibria of greatest importance in stoichiometric hydrocarbon flames may be represented by the following expressions:



It can be seen that a total of 11 species may be present in the gas mixture. The mole fractions of each component may be obtained by a simultaneous solution of the seven equations derived from the equilibria listed with those from overall mass balances on each of the four elemental species present. Appropriate equilibrium constants have been listed in the JANAF thermochemical tables (2) for a wide range of temperatures. As the presence of non-linear equations precludes any direct solution the use of an iterative approach is necessary. The application of the Newton-Raphson method has been fully described by Francis and Toth (3) and found to be entirely satisfactory for the mixtures studied in this work. The equilibrium constants available permit the evaluation of gas compositions for temperatures between 400 and 4000K at 200K intervals.

### 2.2 Enthalpy and heat content

The enthalpy of the combustion product mixture at any specified temperature level can be evaluated from a simple summation of the contributions from each individual species. A convenient table of the enthalpy values for the components of most combustion systems has been

published in reference (3) using a common base temperature of 288K. Although these were used in the early stages of this work certain minor revisions have since been made and the appropriate data is listed in Appendix 1.

In many practical combustion calculations the use of enthalpy data in this form may be somewhat inconvenient. Many calculations are carried out on a volume rather than a mass basis so that the use of heat content data referred to a unit volume of combustion products under STP conditions may be preferred. Since the mean molecular weight of the mixture is affected by dissociation reactions the information is usually based on the 'undissociated' volume. This is the volume applicable to temperatures below 1400 K where the only components are  $N_2$ ,  $CO_2$  and  $H_2O$ . The volume reduced to standard conditions is then constant for any given fuel-oxidant mixture and being independent of temperature greatly simplifies many calculations.

### 2.3 Flame temperature

The adiabatic flame temperature of a particular fuel-oxidant combination may be obtained from a straightforward heat balance over the combustion process. The net calorific value of the fuel gas is imparted to the combustion products so that, in the absence of any losses, the heat content at flame temperature, ( $I_{undiss}$ ), may be calculated from

$$I_{undiss} = C_n / P$$

$C_n$  is the net calorific value of the fuel and  $P$  is the volume of cold combustion products resulting from the combustion of a unit volume of cold fuel. The required information may then be read directly from a plot of the 'undissociated' heat content against temperature.

### 2.4 Specific heat

The equilibrium concentrations of dissociated species in flame gases exhibit a strong temperature dependence. This can be seen by reference

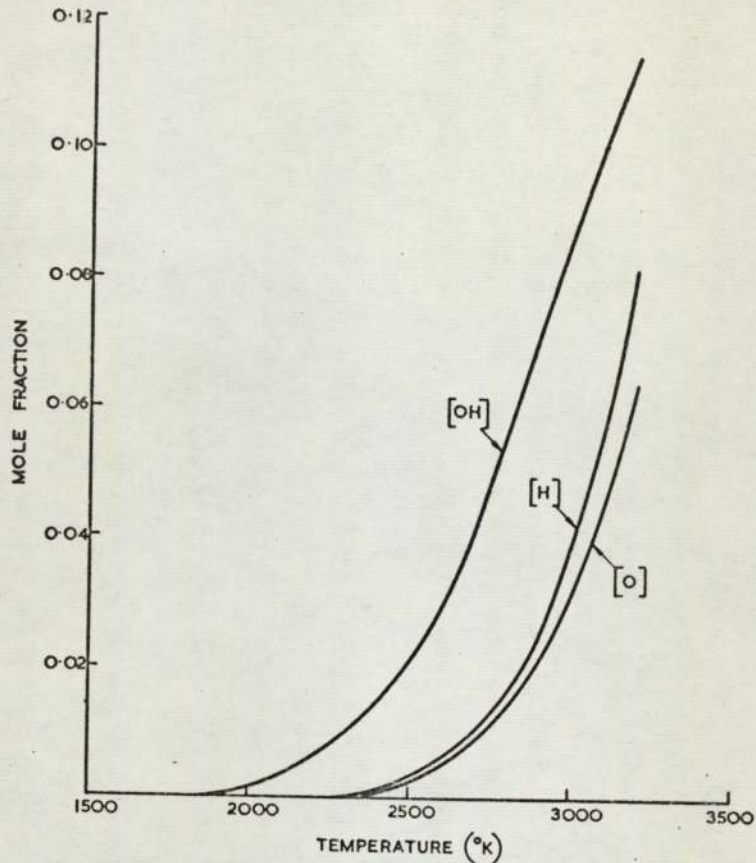


FIG 1 EQUILIBRIUM CONCENTRATIONS OF DISSOCIATED SPECIES IN STOICHIOMETRIC METHANE-OXYGEN COMBUSTION PRODUCTS.

to Fig. 1 which shows the variations predicted for the combustion products of a stoichiometric mixture of methane and oxygen. As a result of the high dissociation energies involved the rate of change of enthalpy with temperature is by no means linear. In consequence, two distinct specific heats can be defined depending on whether equilibrium is maintained or a frozen composition is assumed.

#### 2.4.1 Frozen specific heat

For this case a summation of the contributions from each of the constituent species is all that is required. For a multicomponent mixture this will

be given by

$$C_p = \sum_1 c_i x_i M_i/M_o$$

where  $c_i$  is the concentration of species  $i$

#### 2.4.2 Equilibrium specific heat

The specific heat of a fluid for equilibrium conditions is defined as

the gradient of the enthalpy curve  $\left(\frac{\partial H}{\partial T}\right)_p$ . With the machine

computation of thermophysical properties this may conveniently be achieved either by numerical differentiation using Stirling's formula or from a polynomial fit to the enthalpy data.

### 2.5 Density

The density of the flame gases at any desired temperature may be determined from the appropriate value of the mean molecular weight assuming ideal gas behaviour.

### 2.6 The Viscosity of Combustion Product Mixtures

The calculation of the thermodynamic properties mentioned so far is a relatively straightforward process with a well established theoretical background to which only trivial modifications are likely in the future. The close correspondence between the measured and predicted flame temperatures after taking into account radiative and conductive losses is indicative of the accuracy expected. The theoretical values and the calculated compositions are closely inter-related so that the agreement of predicted flame temperatures with experiment inspires confidence in the remaining predictions. On the other hand, the situation with regard to viscosity and thermal conductivity is much less satisfactory and needs to be examined more fully. In order to bring out the approximations involved, the estimation of the viscosity of pure components as well as of mixtures will be described in some detail.

A number of empirical relationships of varying degrees of sophistication have been proposed for the interpolation and extrapolation of the existing experimental data for viscosity. Many of these may be satisfactory under certain circumstances but for the most part the Chapman-Enskog theory for dilute gases has been used with the greatest success. This theory has been expounded in great detail in a multitude of publications, the principal one being that of Hirschfelder, Curtiss and Bird referred to earlier. In its strictest form only molecules undergoing elastic (rigid

sphere) collisions and having spherically symmetrical force fields governing the attraction and repulsion effects are considered. It is therefore of greatest relevance for monatomic gases but in most cases suitable modifications can be made so that polar molecules and inelastic collisions can be included. The stipulation of dilute gases can in some circumstances remain as an important restriction although it is usually complied with in combustion systems employing flames at atmospheric pressure.

### 2.6.1 Calculation of viscosity for pure nonpolar gases

The Chapman-Enskog theory gives the viscosity of a pure non-polar gas at a particular temperature in terms of the molecular weight of the gas and some temperature dependent parameters governing the molecular interactions.

$$\mu = \frac{2.6693 \times 10^{-6} (MT)^{0.5}}{\sigma^2 \Omega^{(2,2)*}} \dots\dots (1)$$

where  $\mu$  is the viscosity (Ns/m<sup>2</sup>)

M is the molecular weight

T is the temperature (K)

$\sigma$  is the collision diameter (Å)

$\Omega^{(2,2)*}$  is a collision integral.

The quantity  $\Omega^{(2,2)*}$  is a temperature dependent function which incorporates the interaction potentials of the colliding molecules. The asterisk (\*) indicates that its value is taken relative to that obtained assuming a rigid sphere collision. Values of this function can be calculated in only a few restricted cases since the interaction parameters are not readily obtained. For practical purposes reference is made to experimental data and a proposed form of the potential function assumed. The adjustable parameters in this function are then manipulated to give a reasonable fit to any experimental data available and subsequently used for extrapolation purposes. One of six potential functions have been used in the majority of transport property calculations. These range considerably in their complexity with the simplest versions giving the

least realistic picture of the intermolecular forces.

The simplest model is that which considers the colliding molecules to be rigid non-interacting spheres having an effective collision diameter of  $\sigma$ . The potential energy is thereby considered to be zero for  $r > \sigma$  and infinite for  $r < \sigma$ . This model is clearly unrealistic and for accurate work has been discarded.

The next two spherically symmetrical interaction functions are those which take into account the purely repulsive forces between molecules which are associated with their electron clouds and ignore the gravitational and electrostatic attractions. These are the inverse power potential:

$$\phi(r) = d/r^\delta$$

and the exponential repulsive potential:

$$\phi(r) = Ae^{-r/\rho}$$

Here  $r$  represents the distance between the two nuclei while  $d$ ,  $A$ ,  $\delta$  and  $\rho$  are constants for a given pair of molecules. The omission of the attractive forces naturally introduces errors, although these will become less significant at high temperature levels. The increased energy of the species then results in more penetrating collisions and correspondingly higher repulsive forces. The value of  $\delta$  is a measure of the resistance of the molecule to distortion during a collision, a value of  $\delta = \infty$  reducing the inverse power potential to the rigid sphere model. For most molecules the value of  $\delta$  lies between 9 and 15 depending on this resistance.

A further variation, the Sutherland model, represents the molecules as rigid spheres but in addition includes an attractive potential inversely proportional to the separation of the two electron clouds

$$\phi(r) = \infty \quad \text{for } r < \sigma$$

$$\phi(r) = -\epsilon(\sigma/r)^\gamma \quad \text{for } r > \sigma$$

Evaluation of collision integrals using this model can prove to be inordinately complex. However, the exclusion of high powers of  $\epsilon$  from the strict treatment enables a good approximation to be obtained which

eventually gives the viscosity as

$$\mu = \mu_{rs} / (1 + S_{\mu}/T)$$

$\mu_{rs}$  is the viscosity calculated from the rigid sphere model while  $S_{\mu}$  is a quantity which depends on the exact value of  $\gamma$  used, the necessary data having been calculated by Kotari (4).

The simpler potential functions described above are useful in the prediction of transport property data especially for interpolation procedures. For extrapolation purposes the more complex Lennard Jones (6-12) or Modified Buckingham (Exp-6) potentials have been found most valuable, and of these the former has gained the wider acceptance. This takes the form

$$\phi(r) = 4\epsilon \left[ (\sigma/r)^{12} - (\sigma/r)^6 \right] \dots\dots (1)$$

The adjustable parameters here are  $\epsilon$ , which represents the depth of the potential well (or the maximum energy of attraction) and  $\sigma$  which represents the value of  $r$  for which  $\phi$  becomes zero. This is illustrated by Fig. 2. The calculation of the requisite collision integrals based on this

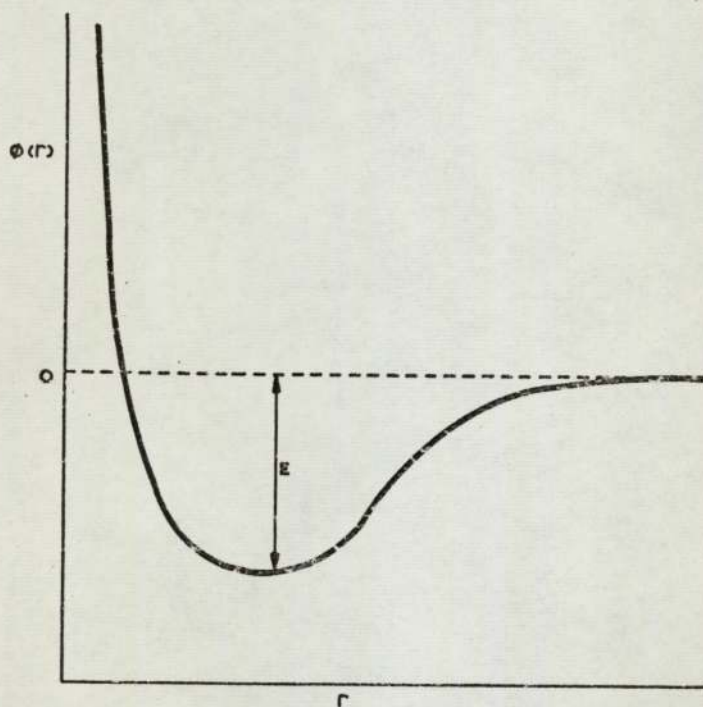


FIGURE 2. REPRESENTATION OF THE LENNARD JONES (6-12) POTENTIAL FUNCTION USED IN TRANSPORT PROPERTY CALCULATIONS

expression have been obtained independently by several workers and a close correspondence between the various sources has been obtained. Tabulated values of  $\Omega^{(2,2)*}$  have been given in reference (1) in terms of the reduced temperature  $kT/\epsilon$ . The two data fitting functions  $\epsilon/k$  and  $\sigma$  have been obtained for many common gases and recommended values are also listed.

Although widely used in practice, the Lennard Jones (6-12) function suffers from an overestimation of the repulsive forces represented by the  $(\sigma/r)^{12}$  term. This drawback is partially overcome by the Modified Buckingham version, which is a three parameter expression given by

$$\phi(r) = \left[ \epsilon / (1 - 6/\alpha) \right] \left\{ (6/\alpha) \exp \left[ \alpha (1 - r/r_m) \right] - (r_m/r)^6 \right\}$$

This allows superior data fitting but in most cases the experimental information is not, in itself, of sufficiently high accuracy to warrant the additional expenditure of effort. However collision integrals for this function have been computed by Mason (5) and are available if needed.

In view of its widespread acceptance elsewhere and the greater availability of the required input data, the Lennard Jones (6-12) potential has been used throughout for the calculations needed in this work. The appropriate modifications enabling polar molecules to be included have been made as described below.

### 2.6.2 Calculation of viscosity for pure polar gases

The Lennard-Jones function describing molecular interactions is found to break down when the data for polar gases and for long chain molecules such as n-octane are examined. This is not unexpected since in neither case do the force fields approximate to the spherically symmetrical conditions assumed in the theory. The numerical evaluation of the desired collision integrals for use with Equation (1) then becomes exceedingly difficult owing to the introduction of angular dependent effects. Monchick and Mason (6) have described a method whereby this difficulty may be circumvented by the inclusion of a term which takes into account the dipole

moments and non-symmetrical force fields. More generally known as the modified Stockmayer potential this takes the form

$$\phi(r) = 4\epsilon \left[ (\sigma/r)^{12} - (\sigma/r)^6 \right] - (\eta^2/r^3)\zeta$$

Monchick and Mason hold the value of the angular dependent quantity  $\zeta$  fixed so that, provided  $\eta$  be known, the required integrals can be obtained and averaged for all values of  $\zeta$ .

### 2.6.3 The viscosity of gas mixtures

The thermophysical and transport properties of various combustion product mixtures have been computed by several major organisations although in many cases the results have not been published. As stated previously, the thermodynamic data can in most cases, be taken to be quite reliable, although doubts arise when one considers the accuracy of the transport properties represented by thermal conductivity and viscosity. The calculation of both of these quantities can be achieved using purely theoretical arguments but the complexity of the procedure required renders it unsuitable for practical use, except where monatomic gases are concerned.

Consequently, recourse to certain simplified relationships is necessary. An approximate formula for the viscosity of a gas mixture was originally presented by Sutherland (7) and later modified by Wassiljewa (8)

$$\mu_{\text{mix}} = \sum_{i=1}^n \frac{\mu_i}{1 + \sum_{\substack{j=1 \\ j \neq i}}^n \phi_{ij} x_j/x_i}$$

Originally developed in 1904, this expression is still widely used in present day calculations although the form of the function  $\phi_{ij}$  (the so-called Wassiljewa coefficient) has been modified by various authors. Wilke (9), Buddenberg and Wilke (10), and later Francis (11) have obtained expressions for this coefficient which incorporate empirical correction terms. Using the Lennard-Jones function these generally provide quite

satisfactory agreement with the available experimental information the version suggested by Francis proving to be especially good in this respect. The quantity  $\phi_{1j}$  is given by

$$\phi_{1j} = \left( \frac{\sigma_{1j}}{\sigma_{11}} \right)^2 \frac{\Omega_{1j}^{(2,2)}}{\Omega_{11}^{(2,2)}} * \left( \frac{2M_j}{M_1 + M_j} \right)^{1/3}$$

On the other hand, Brokaw (12) has recently attempted to improve the theoretical approach by the development of new formulae based on the rigorous Chapman-Enskog kinetic theory. Because of the very limited number of approximations introduced in Brokaw's approach, the values of viscosity calculated from these formulae agree closely with predictions obtained from truly rigorous theory. However, it seems that the accuracy is less good when experimental data is considered and the use of the simple expression developed by Francis may be preferable from a practical point of view.

This has been shown by Davies (13) in a critical comparison of the two methods. While it appears that the use of Brokaw's approach may give marginally better predictions where binary mixtures of polar molecules are concerned, the equation proposed by Francis proves to be slightly superior for most polar/non-polar binary and polar ternary mixtures. It is therefore of particular value when combustion product viscosities are required since the calculation invariably involve both classes of molecules. Its comparative simplicity is, however, the main attraction and this encourages its continued use for the viscosity calculations needed in this work.

## 2.7 Thermal conductivity of gases

### 2.7.1 Pure components

The classical theory put forward by Hirschfelder, Curtiss and Bird has been found adequate in the prediction of thermal conductivity data for pure monatomic gases. Rigorous kinetic theory gives a first approximation

$$\text{as } \lambda = \frac{25TC_v}{16M\Omega^{(22)}}$$

In this expression  $C_v$  represents the specific heat of the gas under constant volume conditions while  $M$  is the atomic weight and  $\Omega^{(22)}$  a collision integral. As for the case of viscosity the latter is closely associated with the potential energy of interaction and a similar series of potential functions may be used in its evaluation. In the majority of cases the adjustable fitting parameters are best obtained from experimental viscosity data. This arises from the practical difficulties encountered with the measurement of thermal conductivity, particularly at higher temperature levels.

Although satisfactory for pure monatomic gases the classical theory proves to be inadequate when polyatomic gases and their mixtures are involved. A number of workers have endeavoured to extend the range over which the simple theory will suffice by taking into account the exchange between translational energy and the various internal degrees of freedom. These effects were first considered by Eucken (14) and later by Chapman and Cowling (15), Shäfar (16) and Meixner (17). A correction to the monatomic conductivity was proposed whereby the influence of a temperature gradient on the internal energies of the molecules could be included. The local temperatures are associated with corresponding equilibrium internal energy states and a form of concentration gradient established. Eucken proposed a prediction method into which the resulting self diffusion process could be incorporated. Unfortunately the values obtained from the Hirschfelder Eucken theory have invariably been found to be significantly higher than experimental measurements.

In an attempt to improve the basis for the prediction of thermal conductivity Mason and Monchick (18) have recently derived expressions applicable to both polar and non polar gases. This appears to be a

noteworthy improvement on the earlier methods although at the present time the data required is not always available. For the components present in hydrocarbon combustion products, most of the information needed has been published and predictions using this method can be made for most cases of industrial interest. Mason and Monchick's treatment takes the thermal conductivity determined from the Hirschfelder - Eucken theory to be a first approximation to the true value. A second approximation is then made by including the effects of resonant exchanges of energy in polar molecules and of finite relaxation times in other polyatomic species. The method proposed has proved to be very useful in transport property calculations for pure components where a high degree of accuracy is required. Its complexity precludes a fuller description here since it has been discussed in detail in the reference quoted above.

### 2.7.2 Mixtures of Gases

Like that for viscosity, the theoretical treatment for the thermal conductivity of gas mixtures is inordinately complicated. At modest temperature levels a rigorous solution for mixtures of monatomic gases is tractable, but is too involved for general use. The situation with polyatomic gases becomes correspondingly worse and although a rigorous theory has been developed its use can hardly be contemplated at the present time. In consequence developments have paralleled those for viscosity calculations and a number of approximate methods have been suggested.

Of these, the one proposed by Hirshfelder has most frequently been used. This assumes a full equilibration between the internal and translational degrees of freedom and takes the form

$$\lambda_{mTx} = \lambda_{mTx}^{\circ} + \frac{\sum_i (\lambda_i - \lambda_i^{\circ}) (X_i/D_{i1})}{\sum_j (X_j/D_{1j})}$$

Here  $\lambda_{mTx}^{\circ}$  represents the translational thermal conductivity of the mixture and is calculated from the overall composition, various properties

of the individual components and the diffusion coefficients. The quantities involved in the second part of the expression can also be evaluated entirely from theory but are more usually obtained by way of experimental measurements of diffusion coefficients or viscosities.

It has been found that the relationship outlined above is capable of realistic estimates of mixture conductivities for simple binary and ternary mixtures where force constants derived from experimental work are available. Where such information has not been obtained or where complex mixtures are involved, the predictions are found to be rather less reliable. For such cases a number of semi-empirical relationships have been proposed which are generally modified forms of the Sutherland-Wassiljewa equation:

$$\lambda_{mix} = \sum_i \frac{x_i \lambda_i}{\sum_j x_j \phi_{ij}} \quad \dots (2)$$

The predictions resulting from the use of the variations proposed by Francis (3), Lindsay and Bromley (19), and Brokaw (20) have been studied in detail by Davies (13). Davies found that the formula put forward by Francis proved to be at least as effective as the other, more complicated, versions in predicting the available information for both polar and non-polar mixtures. It can be seen that the equation for the Wassiljewa coefficient in this case,

$$\phi_{ij} = \left[ \frac{\sigma_{ij}}{\sigma_{ii}} \right]^2 \left[ \frac{2M}{M_i + M_j} \right] \left[ \frac{\Omega_{ij}^{(2,2)}}{\Omega_{ii}^{(2,2)}} \right] \quad \dots (3)$$

takes a similar form to the expression for viscosity calculations, the only difference being in the exponent to the term involving molecular weights.

Unfortunately Eqs. (2) and (3) above cannot be applied directly to calculations for high temperature combustion products. This is because flames, particularly those burning with oxygen, contain appreciable concentrations of dissociated material. Under equilibrium conditions

calculations indicate that the species H, OH and O constitute upwards of 15% by volume of stoichiometric methane-oxygen combustion products at the calculated adiabatic flame temperature of 3050K. As a result of the high dissociation energies involved, it is clear that an appreciable proportion of the total energy of the system is incorporated in the heats of dissociation for the radicals present. Since the equilibrium concentrations of such species are strongly dependent on temperature, the presence of a cooler surface creates steep concentration gradients within the boundary layer. A diffusion of dissociated species ensues and subsequent recombination, either in cooler regions of the boundary layer or at the wall, releases the heat of dissociation. The heat transfer is thereby increased and the phenomenon can be looked upon as an enhancement of the thermal conductivity of the mixture beyond that expected from the usual intermolecular collision processes.

A first approximation to the effective equilibrium thermal conductivity of a chemically active mixture may be estimated from data for the frozen and equilibrium specific heats. It can be shown that the frozen and equilibrium conductivities of a mixture having a unity Lewis number are related by the equation

$$\lambda_{e,q} = \lambda_f \frac{C_{p,e,q}}{C_{p,f}}$$

The simple formula quoted above can be quite valuable where rapid order of magnitude estimates are required, but suffers from the restrictions imposed on Lewis numbers. Because of these limitations a more sophisticated approach is necessary for accurate work on combustion product mixtures since very much higher Lewis numbers are encountered. In this respect the calculation method devised by Brokaw (21) would seem to be most appropriate. In this the effective total conductivity is determined from the sum of two parts. The value arising from the normal conduction process,  $\lambda_f$ , is supplemented by an additional quantity called

the reacting conductivity,  $\lambda_R$ , which accounts for heat transfer by diffusion and recombination.

$$\lambda_{e,q} = \lambda_f + \lambda_R$$

The frozen thermal conductivity,  $\lambda_f$ , may be calculated from the formulae given in Eqs. (2) and (3) above while the second term,  $\lambda_R$ , may be determined by using the original method described by Brokaw in reference (21).

The concept of a reacting thermal conductivity is especially valuable in calculations for combustion systems. At high temperature levels the contributions to heat transfer arising from the diffusion and recombination of species other than hydrogen atoms can be considerable. These are included when Brokaw's method is employed and should lead to more accurate values for the transport property in question.

Reacting conductivities have been determined for all the six fuel oxidant combinations of interest, excellent agreement with the independent calculations of Svehla (22) having been obtained in the case of stoichiometric hydrogen-oxygen combustion. However, it is noticeable that the values for the total thermal conductivity,  $\lambda_{e,q}$ , diverge from those quoted by Svehla at the lower temperature levels. This arises from the use of rather different input data for these conditions. For the purposes of this work the availability of experimental data for steam was recognised and curve fitting procedures were available to allow this information to be included in the calculations for temperatures below 2000K. On the other hand, the calculations carried out by Svehla were based entirely on theoretical considerations with no reference to measured data. The values and sources of the force constants used in the present calculations are tabulated in Appendix 1.

### 3. THEORY OF HEAT TRANSFER WITH VARIABLE FLUID PROPERTIES

#### 3.1 Previous Work

The heat transfer occurring between gas streams and solid surfaces is a field which has attracted an enormous amount of attention over the years. The process is of such practical importance that a vast and detailed literature exists on the subject. Many aspects of the problem have been resolved, but it is notable that the theory of heat transfer under the severe temperature conditions encountered in combustion systems has escaped intensive study for many years. This has arisen from a lack of real industrial interest which has only recently been dispelled by an increased awareness that a solution to the problem would be of direct practical value.

In order to survey the relevant work which has been published, it is convenient to divide the subject of variable property heat transfer into three sections. The first of these encompasses the lower temperature ranges where dissociation is absent, the second includes the effects of dissociation while the third covers the limited amount of work involving combustion product mixtures.

##### 3.1.1 Systems without dissociation

Numerous studies of heat transfer have been carried out at modest temperature levels and two general methods for correlating experimental data seem to have gained quite wide acceptance. In the first of these a reference temperature is selected and used in the evaluation of the dimensionless groups so frequently encountered in heat transfer calculations. Although this reference temperature is sometimes taken to be that of the wall or of the free stream, it is more usually defined as the arithmetic mean of these values. Thermophysical properties evaluated at this temperature are then said to represent

the mean film conditions.

The second method requires that the results obtained from a purely constant property solution be modified by a term which accounts for the variations across the boundary layer. The constant property relationship may need to be evaluated at any of the usual temperatures but free stream conditions are generally favoured. The effects of property variations are then accommodated by taking the ratio of some physical quantity at the surface temperature to the value appropriate to either the mean film temperature or that of the free stream. For the majority of correlations applicable to gases, the appropriate physical property is assumed to be the shear viscosity,  $\mu$ , or the density-viscosity product,  $\rho\mu$ . The ratio can frequently be reduced to a simple function of temperature by making use of the power law dependence of these quantities on the absolute temperature. The general form of correlation equation may then be represented by

$$\text{Nu} = A\text{Re}^x\text{Pr}^y (T_w/T_s)^z$$

These approaches have proved to be quite successful for heat transfer problems involving both laminar and turbulent flow of gases through tubes. Similar methods have been used to correlate experimental data obtained for the impingement of gas streams on solid surfaces.

For the case of flow inside tubes an enormous volume of material has been published but only a very small proportion of this is relevant to systems which involve large temperature gradients. One of the more comprehensive works dealing with tube flow is that of Perkins and Worsoe-Schmidt (23). These authors have reported detailed experimental measurements of friction factors and heat transfer coefficients under quasi steady state conditions. Precooled nitrogen in turbulent flow was passed through a heated tube where the ratio of the absolute temperatures at the wall and in the free stream ranged from 1.25 to 7.54.

The results were correlated using the second of the two methods

outlined above, that incorporating a correction factor based on the temperature ratio. In order to allow for entry effects, the two forms of correlation equation included a multiplying factor  $\{1 + (L/D)^{-0.7} (T_w/T_s)^{0.7}\}$  which successfully coped with all of the experimental data. The expressions proposed were

$$Nu_s = 0.024 Re_s^{0.83} Pr_s^{0.4} (T_w/T_s)^{-0.7} \{1 + (L/D)^{-0.7} (T_w/T_s)^{0.7}\}$$

and

$$Nu_w = 0.023 Re_w^{0.83} Pr_w^{0.4} \{1 + (L/D)^{-0.7} (T_w/T_s)^{0.7}\}$$

for bulk and wall conditions respectively. Here the wall Reynolds number was defined in terms of the total mass flow,  $w$ , and the temperature ratio:

$$Re_w = (4w/\pi D \mu_w) (T_s/T_w)$$

In fully developed flow (large  $L/D$ ) the quantity represented by the expression in curly brackets reduces to unity, the temperature ratio term remaining then being associated with powers of  $-0.7$  and  $-0.8$  respectively.

Similar work by Humble, Lowdermilk and Desmon using air as the heat transfer medium indicated a slightly higher valued exponent of  $-0.55$  for the heating case, although the range of temperatures covered was not nearly as extensive. (24).

On the other hand, the analytical results of McEligot, Smith and Bankston (25) for strong heating of gases in turbulent flow through tubes seem to indicate that the exponent does not remain constant. From a comparison of their results with those of Perkins and Worsoe-Schmidt it appears that a dependence on the magnitude of the temperature ratio exists. At comparatively modest temperature levels this may conveniently be ignored and yet still enable good agreement to be obtained with experiment. A possible explanation of this behaviour may lie in a slight departure from the simple power law relationship used in the theoretical work to describe the variation of viscosity with

temperature. In the case of nitrogen or air, such a relationship proves to be reasonably satisfactory but with high temperature combustion products the situation is very much altered by the effects of dissociation. The increase of viscosity with temperature is attenuated or even reversed by the formation of low molecular weight species. These have viscosities appreciably lower than those of the remaining components and their formation tends to mask the effect of increasing temperature. This constitutes an important difference between the two systems so that the simple approaches which prove successful at low temperature levels might break down if applied to flames.

A second difference lies in the mechanism of heat transfer. The highest temperature encountered in the studies with nitrogen was about 1200K whereas combustion product mixtures frequently involve values in excess of 3000K. Furthermore, in the downstream region where corrections for entry effects become smaller, the highest temperatures recorded by Worsoe-Schmidt were very much reduced. Thus an appreciable proportion of the heat flux may be carried by dissociated species in a combustion system but this could not occur in the studies using nitrogen since the temperatures involved were far too low.

Taylor (26 and 27) has examined the heating of pure components inside circular tubes at rather higher temperature levels. These were sufficient to cause appreciable dissociation of molecular species adjacent to the wall, but the close similarities with the work described above makes it most convenient to discuss the two papers at this stage. In both cases hydrogen and helium were used as the fluid media but these were precooled in a liquid nitrogen bath for the second set of measurements.

The earlier paper was concerned with the measurement of local values of heat transfer coefficients applicable to flow of the gases through an electrically heated tungsten tube having a length to diameter ratio

of 77. In this study the local Reynolds number varied between 7,600 and 39,500 indicating that turbulent flow conditions would prevail throughout. A maximum surface temperature of just over 3100K was recorded.

From these studies Taylor concluded that the most satisfactory correlation was provided by the expression

$$Nu^* = 0.021 (Re^*)^{0.8} (T_s/T^*)^{0.5} (Pr^*)^{0.4}$$

where \* designates film values.

The corresponding low temperature relationship for the Reynolds number range in question is that proposed by Colburn,

$$Nu_s = 0.023 (Re^*)^{0.8} (Pr_s)^{0.33}$$

For the Prandtl number range applicable to hydrogen and helium ( $\sim 0.7$ ) this expression bears an obvious similarity to that put forward by Taylor.

The difference in the numerical constant is accounted for by the slight variation in the exponent to the Prandtl number term. Taylor's approach appears to permit the use of the low temperature equation in situations where large temperature differentials exist. This is achieved by employing film values throughout and attaching a modifying factor,  $T_s/T^*$ , directly to the Reynolds number.

In his later paper Taylor has obtained a somewhat improved correlation of similar heat transfer data measured in virtually the same test facility as before. The equation used to describe the heat transfer introduced a wall to free stream temperature ratio raised to a power which was dependent on the axial position of the point in question.

$$Nu_s = 0.021 Re_s^{0.4} Pr_s^{0.4} (T_w/T_s)^{-[0.23 + 0.00191/b]}$$

For flow through hexagonal tubes a similar form of equation, but with different constants in the exponential term was found to be satisfactory to within about 20% by Slaby and Mattson (28). However, McEligot and Smith (29) are of the opinion that the correlation of data by this method is unnecessarily complex except for the special case of a developing flow so that this approach has not been given more than a cursory examination.

For the laminar flow condition, both theoretical and experimental data have been produced. The first analytical approach was made by Deissler (30) but his results did not correspond to available experimental data chiefly because of the assumed velocity and temperature profiles. Under variable property conditions it is clear that the changing gas temperatures lead to radial velocity components so that a fully developed flow situation is never reached. Worsoe-Schmidt (31) has improved the analysis by allowing for this and has indicated that the influence of temperature ratio should be very small but act in the same direction as for turbulent flow. This conclusion has been verified experimentally, principally by Kays and Nicoll in their much quoted work on air flowing through circular tubes (32).

The position regarding stagnation point situations and external boundary layers in laminar flow has been summarised quite neatly by Kays (33). Drawing on the analytical solutions by Cohen and Reshotko (34) he has concluded that the cases of heating and cooling must be treated separately and recommends the use of exponents to the temperature ratio given in the table below.

Table 1

Recommended Values of the Exponent to the Temperature Ratio ( $T_w/T_s$ ) for Gases in Laminar External Boundary Layers

Flow Situation	$T_w/T_s > 1$	$T_w/T_s < 1$
$U_\infty = \text{constant}$	- 0.01	0
Stagnation Pt.	0.1	0.07

The important point to notice here is that the dependence on temperature ratio seems to be much stronger in the case of stagnation point heat transfer than for situations which involve the flow of gases over a surface. Furthermore it can be seen that the correction factors

tend to operate in opposite directions for the two geometrical arrangements. Because of this, heat transfer to a stagnation point must be considered separately since correlations proposed for other systems are unlikely to hold for this particular case.

### 3.1.2. Systems involving dissociation

It has already been mentioned that the theory of heat transfer from dissociated combustion products has been developed to only a limited extent. On the other hand the related problem with dissociated air has been the subject of considerable attention for more than a decade, chiefly in connection with the various space exploration programmes. This arises from the need to control or minimise the heating effects encountered during the re-entry of space vehicles to the earth's atmosphere. The rapid conversion of kinetic energy to heat as the accompanying shock wave passes through the gases may cause appreciable dissociation and ionisation of the boundary layer, with the attendant effects of high heat transfer rates and severe property gradients.

In the course of the research effort a number of papers dealing with these topics have emerged. Some of these papers are directly relevant to the present work and their main features and limitations are outlined below.

Since the greatest rates of heat transfer to an object travelling at hypersonic speeds may be expected in the neighbourhood of the forward stagnation point, the majority of authors have concerned themselves with this restricted case. Two distinctly separate lines of approach appear to have predominated.

The first of these has been concerned with the adaption of relationships originally designed for heat transfer under comparatively low temperature conditions and modest temperature differentials. A large number of such relationships have been produced, covering a wide

range of geometrical and fluid combinations. Although the majority have resulted from the correlation of experimental data, a limited number have been obtained from purely theoretical considerations. In view of their widespread acceptance for low temperature situations, the development of suitable modifications permitting their use at higher temperature levels is clearly an attractive prospect.

The formulae referred to above usually take the form  $Nu = f(Gr, Pr)$  or  $Nu = f(Re, Pr)$  depending on whether natural or forced convection processes dominate the heat transfer. Sibulkin (35) has obtained a theoretical expression for the particular case of forced convective heat transfer at the            forward stagnation point of a sphere. Applicable to constant property incompressible flow conditions, this takes the form

$$Nu = 1.32Pr^{0.4} Re^{0.5} \dots (4a)$$

or  $St = 1.32Pr^{-0.6} Re^{-0.5} \dots (4b)$

The corresponding expressions for the heat flux being

$$\dot{q} = 1.32Pr^{0.4} Re^{0.5} \lambda \Delta T / D_b \dots (5a)$$

and  $\dot{q} = 1.32Pr^{-0.6} Re^{-0.5} G C_p \Delta T \dots (5b)$

The extension of equations such as that put forward by Sibulkin was first considered by Rosner (36). Using Rosner's approach the stagnation point heat flux for equilibrium conditions becomes

$$\dot{q} = 1.32Pr^{-0.6} Re^{-0.5} G \Delta H [1 + (Le_f - 1) \Delta H_{chem} / \Delta H]^{0.6} \dots (6)$$

In this expression some allowance for property variations within the boundary layer has been made. In effect a mean specific heat has been introduced by the separate enthalpy term since  $\bar{C}_p \Delta T = \Delta H$ . In addition the term in parentheses involving Lewis numbers and dissociation enthalpies acts as a correction to thermal conductivity used in the Prandtl number and provides for the energy transfer which occurs by the diffusion and recombination of active species.

An interesting point arises from Eq (6) for the case of unit Lewis numbers when diffusion-recombination heat transfer occurs at the same rate as the usual conduction processes, ( $Le_f = D/[\lambda/\rho C_p]_f$ ). Under these conditions the heat flux can be seen to be directly proportional to the overall enthalpy difference. In such a case the driving force for heat transfer would best be represented by the overall enthalpy difference rather than by the temperature difference. For non-unity Lewis numbers a similar conclusion may be drawn provided that an equilibrium Prandtl number be defined as

$$Pr_{eq} = Pr_f [1 + (Le_f - 1) \Delta H_{chem} / \Delta H]^{-1}$$

Equation (6) can then be written as

$$\dot{q} = 1.32 Pr_{eq}^{-0.6} Re_s^{-0.5} G \Delta H$$

Rosner has pointed out that in many systems the major part of the heat flux attributed to dissociated species is carried by hydrogen atoms because of their high diffusion coefficients. As a result it may be possible to introduce further approximations into the equations listed above by defining Lewis numbers on the basis of hydrogen atom diffusion only and restricting the term  $\Delta H_{chem}$  to these species alone. The heat transfer rate can then be estimated from

$$\dot{q} = 1.32 Pr^{-0.6} Re^{-0.5} G \Delta H \{1 + (Le_H - 1) \Delta H_{chem H} / \Delta H\}^{-0.6} \dots (7)$$

All of the expressions listed above embody certain simplifying assumptions concerning the transport properties of the fluid which, although quite reasonable for heat transfer from dissociated air, may be invalid for high temperature combustion products. Particularly important in this context are the effects, arising from the multicomponent diffusion of the various active species, of variable Lewis and Prandtl numbers. In the case of heat transfer from dissociated air streams to cold surfaces, the use of constant frozen Lewis and Prandtl numbers of 1.4 and 0.71 respectively may be a useful approximation. However, it has been shown by Davies and Toth (37) that the frozen Prandtl and H-atom Lewis numbers for fuel-oxygen

combustion products can vary substantially between adiabatic flame temperature and the sink temperature of 400K. Consequently, the application of such formulae must be made with utmost caution.

The second, and possibly more fruitful approach to the problem has made use of numerical solution methods. The pioneering work in this field was carried out by Lees (38) with the application of numerical methods to the solution of the appropriate laminar boundary layer conservation equations. Lees considered the simplified case where physical property variations through the boundary layer were such that a constant, near unity Prandtl number could be assumed together with a Lewis number of unity and a constant value of the product of density and viscosity. In addition implicit within the derivation are the assumptions that chemical equilibrium prevails throughout and that the ratio of free stream to wall temperature is large.

A similar treatment incorporating certain worthwhile refinements was made by Fay and Riddell (39) who, by removing the restrictions of unit Lewis number and of a constant density-viscosity product, produced results which were more nearly representative of heat transfer from dissociated air. The equation fitted to their numerical results for equilibrium conditions takes a similar form to that proposed by Rosner.

$$\dot{q} = 1.32 \text{Pr}_f^{-0.6} \left( \frac{\rho_w \mu_w}{\rho_s \mu_s} \right)^{0.1} \text{Re}_s^{-0.5} G \Delta H [1 + (\text{Le}^{0.52} - 1) \Delta H_{chem}/H_s] \dots (8)$$

The predictions obtained from this solution have been tested against experimental shock tube studies by Rose and Stark (40) and in general good agreement seems to have been obtained for air. Unfortunately the restriction of constant Prandtl and Lewis numbers remains as an unwelcome requirement when combustion product mixtures are to be considered. Furthermore, a simplification similar to that introduced by Fay and Riddell's assumption that the air stream consisted of two species only, air 'atoms' and air 'molecules' is probably inadmissible in this case.

A final point concerns the validity of the method by which density and viscosity variations in the boundary layer are accommodated. In the

case of heat transfer from dissociated air it was found that the effective value of the density-viscosity product was related to the wall and free stream conditions. Fay and Riddell found that the expression

$$(\overline{\rho\mu})^{0.55} = (\rho_s \mu_s)^{0.55} (\rho_w \mu_w / \rho_s \mu_s)^{0.1}$$

was adequate for this purpose and included it in the derivation of Eq (8). However, it is evident from sample calculations on combustion product mixtures that such a manoeuvre is unsuitable when heat transfer from flames is to be predicted. This is shown by Table 2 which compares the values of  $(\overline{\rho\mu})^{0.55}$  calculated directly from thermophysical property data with those generated by the expression quoted above

Table 2 : A survey of the error introduced by using Fay and Riddell's approximation in combustion systems  
Stoichiometric Methane-Oxygen Flame at 3000K

$T_w$	$(\overline{\rho\mu})^{0.55}$	$(\rho_s \mu_s)^{0.55}$	$(\rho_w \mu_w / \rho_s \mu_s)^{0.1}$
400	3.073		2.882
800	3.144		2.901
1200	3.208		2.919
1600	3.273		2.942
2000	3.338		2.960

### 3.1.3 Previous Experimental Work

On the practical side it appears that useful experimental results are at a premium. Numerous studies of heat transfer from flames have been reported, but the majority of these have been concerned with specific engineering aspects of the problem rather than with the development of a heat transfer theory. As a result, the detailed information needed for a more basic understanding of the subject has not often been collected although their value in helping to solve practical problems cannot be denied. However, the lack of data frequently means that the results of

such investigations are difficult to interpret from a theoretical point of view.

The conversion of appliances to natural gas firing, both in this country and overseas, has formed the primary stimulus for a large proportion of the experimental work. Comparative assessments of performance before and after conversion has formed a large part of this, with the very nature of the topic precluding much in the way of theoretical studies.

A typical example of the work carried out is provided in the paper published by Gronegress and Rosser (41). This reports industrial experience with various burner designs used in the flame hardening processes common to the fabrication of many engineering components. The performance of natural and towns' gas versions of each of four burner types were compared so that their suitability for industrial use could be assessed. Component feed rates and the depth of heat penetration into the metal were studied and, although these were naturally dependent on the prevailing heat transfer rates, only qualitative information can be extracted.

Parallel difficulties arise in the interpretation of experimental studies concerned with the relative merits of different fuels in given heating applications. Fay (42) has examined the distribution of heat flux when propane, acetylene and MAPP\* flames impinge normally on a flat surface. This geometrical arrangement is not amenable to theoretical treatment as the effects of differing flame shapes prevent more than a superficial examination of the data. Similar aerodynamic complications exist in the practical studies performed by Reed (43) and Ivernel (44) on hydrogen-oxygen and natural gas-oxygen flames respectively. Likewise the papers by Davies (45) and by Harker (46) dealing with heat transfer

---

\* MAPP is a registered trade mark of the Dow Chemical Company.

from electrically augmented flames also involve complex flow situations because of the inherent non-uniformity of the gas streams generated by these burners.

A comparatively small amount of work has been carried out for the express purpose of improving the current heat transfer theory. In this context the investigations by Kilham (47) and by Dunham (48) must be mentioned. The first of these was concerned with the possible mechanisms of energy transfer from flame gases. The rates of heat transfer to refractory cylinders were estimated and it was shown that with carbon monoxide-air flames the bulk of this occurred by radiation and forced convection. However, in hydrogen-air flames it appeared that up to 24% of the energy transfer was contributed by the recombination of atoms and radicals within the boundary layer. The work carried out by Dunham was of a somewhat similar nature again using hydrogen and carbon monoxide burning with air. In this case a stagnation point geometry was used and the results reinforced the conclusions reached by Kilham.

Investigations with higher temperature combustion products have been carried out using various fuel gases, notably hydrogen, methane, propane and acetylene. Stoichiometric combustion with oxygen has generally been favoured. However, Giedt, Cobb and Russ (49) have concerned themselves with the heat transfer resulting from the passage of the combustion products of a rich acetylene-oxygen flame over the surface of a flat plate mounted parallel to the flow direction. This work was followed by a further report by Giedt and Woodruff (50) using a similar test facility but one which permitted surface temperatures to reach 2000K.

Unfortunately the similarity of the two experimental rigs does introduce a certain amount of confusion since, for the earlier work, the boundary layer was assumed to be turbulent from its point of inception. This is at variance with the statement in the later paper that a laminar flow regime could be assumed. A private communication failed to

resolve this matter and although further experimental information was supplied little could be done to clarify the issue.

Another paper which seemed pertinent to the present research effort was the early publication by Anderson and Stresino (51). This covered measurements of the heat transfer from flames impinging on flat and cylindrical surfaces using various methane, propane and hydrogen oxygen mixtures together with a limited number using methane-air. The distribution of heat flux was obtained by a mathematical inversion of data gathered from both a simple tube probe and a segmented flat plate. It was admitted that the method used for the processing of the results would necessarily accentuate any errors in the data but the values presented represent one of the few sources in which actual fluxes are listed.

With one of the flames of interest the quoted gas velocity must be questioned. This arises in the hydrogen-oxygen case where experimental difficulties demanded the calculation of this quantity. The velocity was deduced from the flow rates of the fuel and oxygen using the diameter of the burner exit to define the flow area. The appropriate figures were  $12.11 \times 10^{-3} \text{ m}^3/\text{s}$  ,  $6.06 \times 10^{-3} \text{ m}^3/\text{s}$  and 9.525 mm respectively. If a flame temperature of 3040K be assumed (adiabatic  $\sim 3073\text{K}$ ) then a simple calculation can be made since the mixture density is then  $60.87 \times 10^{-3} \text{ kg/m}^3$

The total input rate corresponds to  $9.74 \times 10^{-3} \text{ kg}$  of mixture each second and this necessitates an exit velocity of 2245 m/s. This differs markedly from the figure of 1402 m/s quoted in the paper and cannot be explained by the flame temperature being lower than the assumed 3040K. To account for the exit velocity given, a temperature of about 2300K would be required. This is far too low to be more than a remote possibility for a stoichiometric hydrogen-oxygen mixture. Even if this temperature were correct, the quoted heat fluxes would then appear to be much too high for such a flame when compared with the other mixtures reported

in the same paper.

One of the most recent experimental studies was that performed by Brim and Eustis (52). This was designed specifically to study the effects of property variations on heat transfer. Measurements of heat flux were obtained at a number of stations along a thick walled copper tube through which combustion products were passed. These were generated by an ethanol-oxygen burner which initially fired into a plenum chamber lined with refractory brick. This acted as a calming section and ensured that the products entering the instrumented tube would be in equilibrium. Nitrogen dilution was used to control the temperature of the inlet gas, a maximum of 2515K being attained. Turbulent flow was assumed throughout and most of the data were correlated within  $\pm 6\%$  by the expression

$$Nu_s = 0.021 Re_s^{0.8} Pr_s^{0.6}$$

Although this does not acknowledge any dependence on the ratio of wall and free stream temperatures it is clear from the paper that such an influence begins to appear at the highest ratios of  $T_s/T_w$ . Under these conditions the discrepancy between the measured data and the correlation equation rises to nearer 15%, probably reflecting the onset of dissociation.

The final work of interest was published by Kilham and Purvis (53) shortly after the completion of the first draft of this thesis. Measurements of heat transfer were reported for methane and propane flames burning with various proportions of oxygen. Heat fluxes were determined at the forward stagnation point of a hemispherically ended blunt body using a similar transient technique to that employed in the corresponding part of this work. Seven mixture compositions were taken and a single mass velocity used in each case. Three data points were obtained for the fuel rich flames of both propane and methane while the remaining run was carried out with a slightly lean methane flame.

In order to correlate the experimental results, a procedure based

on Fay and Riddell's modification to <sup>the</sup> method of Rosner was used. The expression quoted was equivalent to

$$\dot{q} = \frac{1.32}{D} \mu_s \left( \frac{\rho_w \mu_w}{\rho_s \mu_s} \right) (\overline{Pr})^{-0.6} \left[ 1 + (Le - 1) \frac{\Delta H_{chem}}{\Delta H} \right] \Delta H$$

The predictions obtained from this relationship were then compared with the experimental results. It was concluded that the true heat transfer rate lay intermediate to the values obtained for unit Lewis numbers and those taking Lewis numbers based on the diffusion of hydrogen atoms only. Further discussion of this paper has been deferred until Section 10 where a comparison of experimental results has been made.

### 3.2.1 Proposed Modifications of Low Temperature Relationships

In view of the differences between the problems encountered in heat transfer from dissociated air and from high temperature combustion products it is clear that somewhat modified approaches are likely to be necessary. In the present studies both numerical and semi-empirical methods have been used and in each case modifications have been made which should enable more realistic account to be taken of the thermophysical property variations involved. The relevant theory can be greatly simplified by confining the investigations to a stagnation point situation, at least for the initial stages of the work. This largely eliminates aerodynamic complications and enables differences in heat transfer arising from the use of various fuels to be identified more easily.

When attempting to extend the range of existing heat transfer relationships it is first suggested that a value of equilibrium Prandtl number be used which incorporates the effects of non-unity Lewis numbers which vary with temperature. In this respect it would seem that the evaluation of Prandtl numbers using equilibrium thermal conductivities calculated by Brokaw's method would be appropriate. In order to provide for the wide variations in Prandtl number and other thermophysical

properties it is felt that some form of averaging is necessary. Since the variation over the range between flame and sink temperatures is non-linear, a weighted average based on the numerical integration of the property with respect to temperature could well be a suitable choice.

Thus for any property  $\alpha$

$$\bar{\alpha} = \frac{1}{T_s - T_w} \int_{T_w}^{T_s} \alpha \, dT \quad \dots\dots (9)$$

The majority of expressions available for the prediction of heat transfer at low temperature levels are based on correlations involving dimensionless groups of variables. For situations where forced convection predominates the equations are frequently in the form of simple relationships for the Nusselt or Stanton numbers. When expressions involving the latter are to be modified for application to high temperature problems it seems reasonable to define the effective value of this group in terms of an averaged specific heat, the prevailing heat transfer coefficient and the mass velocity of the approach stream. In this way the general procedure suggested by previous workers is followed and the simplification  $\bar{C}_p = \Delta H / \Delta T$  can again be introduced. This maintains a similarity with the proposals of both Rosner and Fay and Riddell shown in Eqs. (7) and (8). The use of averaged conductivity values defined by Eq. (9) forms the corresponding simplification for relationships expressed in Nusselt number form.

Three general methods for correlating measurements in high temperature combustion systems are proposed. The first of these bases the required physical property data on the average conditions in the boundary layer, and leads to equations which for stagnation point heat transfer takes the form

$$\bar{St} = 1.32 \bar{Pr}^{-0.6} \bar{Re}^{-0.5}$$

and  $\bar{Nu} = 1.32 \bar{Pr}^{0.4} \bar{Re}^{0.5}$

The second considers that the flow pattern around the heated object is determined largely by the free stream Reynolds number. This is retained but the remaining quantities are averaged in the manner suggested above.

$$St = 1.32 \bar{Pr}^{-0.6} Re_s^{-0.5}$$

$$Nu = 1.32 \bar{Pr}^{0.4} Re_s^{0.5}$$

The final suggestion again takes averages of the physical properties of the combustion products but includes a modified Reynolds number

$$St = 1.32 \bar{Pr}^{-0.6} (\bar{\mu}/\mu_s) Re_s^{-0.5}$$

$$Nu = 1.32 \bar{Pr}^{0.4} (\bar{\mu}/\mu_s) Re_s^{0.5}$$

The predictions from each of these forms of equation have been assessed in order to ascertain which leads to the most satisfactory correlation of experimental results. In practice it is found that the third of these methods proves to be the most successful.

### 3.2.2. Proposed numerical solutions

The important features of the numerical solutions for combustion systems may be seen by reference to the boundary layer equations for flow over an axially symmetrical blunt nosed body. For thin boundary layers, that is where the boundary layer thickness is very much smaller than the characteristic dimension of the heated object, these equations are as follows:

global continuity for  $\delta \ll r_b$  is defined by

$$\frac{\partial}{\partial x} (\rho u r) + \frac{\partial}{\partial y} (\rho v r) = 0$$

conservation of momentum by

$$\rho u \frac{\partial u}{\partial x} + \rho v \frac{\partial u}{\partial y} = - \frac{\partial p}{\partial x} + \frac{\partial}{\partial y} (\mu \frac{\partial u}{\partial y})$$

and  $\frac{\partial p}{\partial y} = 0$

conservation of energy, neglecting thermal diffusion, by

$$\rho u \frac{\partial I}{\partial x} + \rho v \frac{\partial I}{\partial y} = \left( \lambda_f \frac{\partial T}{\partial y} \right) + \frac{\partial}{\partial y} \left\{ \frac{\mu}{2} \left( 1 - \frac{1}{Pr} \right) \frac{\partial u^2}{\partial y} \right\} + \frac{\partial}{\partial y} \left\{ \sum_i \rho D_i (H_i - H_i^\circ) \frac{\partial c_i}{\partial y} \right\}$$

where  $I = H + \frac{1}{2} u^2$

and  $H = \sum_i c_i (H_i - H_i^\circ)$

In the above  $\lambda_f$  is the frozen thermal conductivity of the mixture while the summation term represents the diffusion - recombination effects mentioned previously. In the case of heat transfer from combustion products considered here, the energy equation may be modified to avoid the explicit appearance of diffusion terms. This may be accomplished with the use of equilibrium conductivities incorporating the chemical reaction term.

$$\rho u \frac{\partial I}{\partial x} + \rho v \frac{\partial I}{\partial y} = \frac{\partial}{\partial y} \left( \lambda_{e,q} \frac{\partial T}{\partial y} \right) + \frac{\partial}{\partial y} \left\{ \frac{\mu}{2} \left( 1 - \frac{1}{Pr} \right) \frac{\partial u^2}{\partial y} \right\}$$

There is in the general case, no intrinsic advantage to be obtained from this substitution since  $\lambda_{e,q}$  is still dependent on the species diffusivities, and the local concentration gradients. In the present case since values for  $\lambda_{e,q}$  had already been calculated some saving in computing time could be achieved.

The boundary layer equations presented above are a set of non linear partial differential equations. As such they are not easily solved except in restricted circumstances where conditions permit the elimination of certain terms and enable ordinary differential equations to be produced. Such a situation exists close to a stagnation point where, from symmetry considerations, the thermophysical properties must be functions of the displacement from the surface only, and largely independent of  $x$ . An approximate solution can then be obtained, provided that a co-ordinate transformation can be found such that the velocity and enthalpy profiles remain similar to themselves over distances corresponding to several boundary layer thicknesses. This implies that

changes occurring in the x direction are small compared with those in the y direction. In such a system it then becomes possible to separate the dependent variables so that ordinary rather than partial differential equations are produced. Thus a transformation from (x, y) to ( $\bar{x}$ ,  $\eta$ ) co-ordinates is required such that

$$u(x, \eta) = u_e(\bar{x}) f'(\eta)$$

and 
$$I = I_e g(\eta)$$

The derivation of the necessary transformations, which follows the procedure outlined by Fay and Riddell, Lees, Dorrance (54) and others shown in Appendix 3, leads to the transformed equations:

$$\left(\frac{C}{Pr} g'\right)' + fg' = \left\{ Cf' f'' \left(\frac{1}{Pr} - 1\right) \frac{u_e^2}{I_e} \right\}' + \frac{2\bar{x} f' g}{I_e} \frac{\partial I_e}{\partial \bar{x}}$$

and

$$(Cf'')' + ff'' + \frac{\partial \bar{x}}{\partial x} \frac{\partial u_e}{\partial \bar{x}} \left\{ \frac{\rho_e}{\rho} - (f')^2 \right\} = 0$$

where  $C = \frac{\rho \mu}{\rho_e \mu_e}$  and ' denotes differentiation with respect to  $\eta$ .

These equations may then be solved by finite difference methods over small increments of  $\eta$  taking various initial guesses for  $f''(0)$  and  $g'(0)$  until the conditions at the boundary layer edge are satisfied:

$$f'(\infty) = 1, \quad g(\infty) = 1 \quad \text{and} \quad g'(\infty) = 0$$

The necessary thermodynamic and transport property values were fed into the computer program in the form of polynomial fits to the data calculated earlier. These polynomials were obtained with the aid of a library program of General Electric Information Services Ltd and included up to 11<sup>th</sup> order terms to ensure smooth and accurate fitting.

It is most important to note that the derivation of the set of equations given above has required that chemical equilibrium should prevail throughout the system. For the free stream this should be a very good approximation since temperature gradients caused by heat losses to the environment should be very small. Coupled with the fact that equilibration in fuel oxygen flames is very rapid because of the high temperature levels this should mean that departures from equilibrium will be restricted

to the immediate neighbourhood of the visible reaction zones. This behaviour has been confirmed by Baxendale et al. (55) in work on hydrocarbon oxygen flames. The behaviour of the boundary layer itself is not so readily predicted and the accuracy of the numerical solutions should provide the best indication of whether or not such an assumption can be justified. An invariant elemental composition across the layer is also implicitly assumed when equilibrium thermal conductivities are specified.

The solution procedure outlined above permits local enthalpy and velocity profiles to be evaluated in the vicinity of the stagnation point of an axisymmetric body exposed to a particular gas stream. These profiles are initially determined for values of  $\eta$  across the boundary layer and because 'similarity' is assumed in this region they will be virtually independent of  $x$ . For the data obtained to have a more practical significance it becomes necessary to introduce the inverse transformation.

$$y = \frac{(\bar{2x})^{1/2}}{\rho_e r u_e} \int_0^{\eta} \frac{\rho_e}{\rho} d\eta$$

Using this relationship and the values of enthalpy and velocity applicable to the boundary layer edge it is then possible to obtain the variation of these quantities with position. Provided the assumption that chemical equilibrium prevails is valid, the thermodynamic state of the boundary layer is then defined and with it the variation of temperature and of all other thermophysical properties.

The heat flux received by the surface may be determined from the following expression

$$q = \lambda_w \left( \frac{\partial T}{\partial y} \right)_w = \frac{\lambda_w}{C_{p_w}} H_e g'(\eta_w) \left( \frac{\partial \eta}{\partial y} \right)_w$$

and the related heat transfer coefficients deduced from a knowledge of flame and wall temperatures.



## 4. INITIAL EXPERIMENTAL WORK

### 4.1 Burners

In order to provide reliable data for the development of prediction methods it is essential that any experimental equipment used should be well designed and adequate for the tasks demanded of it. In the case of heat transfer from high temperature flames it is evident that the use of a uniform combustion product stream would greatly simplify theoretical arguments. As a result the first stage in the experimental programme was the provision of such a stream.

After an extensive survey of available burner designs it was thought that a surface mixing type would prove to be most useful. Premixed versions were discarded because of instability with respect to lightback, particularly in the case of hydrogen-oxygen combustion. Tunnel burners were rejected on the grounds of excessive refractory wear at the high temperature levels, and because of the inherently non-uniform velocity profile produced.

A number of attempts were made to design a burner suitable for the range of fuels in question. It was found that the mixing of the fuel and oxygen presented difficulties and rather long, non-uniform flames resulted. After numerous enquiries of burner manufacturers, a commercial glassworking burner produced by the Carlisle Burner Corporation was suggested. This consisted of a tightly packed bundle of steel capillary tubes through which oxygen was supplied, surrounded by a close fitting jacket for the fuel gas. There was also provision for a small premixed flame at the centre of the burner. A schematic diagram is shown in Fig. 3 and a typical flame in the photograph facing this page. It can be seen that excellent combustion quality was obtained, with the small reaction zones resembling the flame cones of

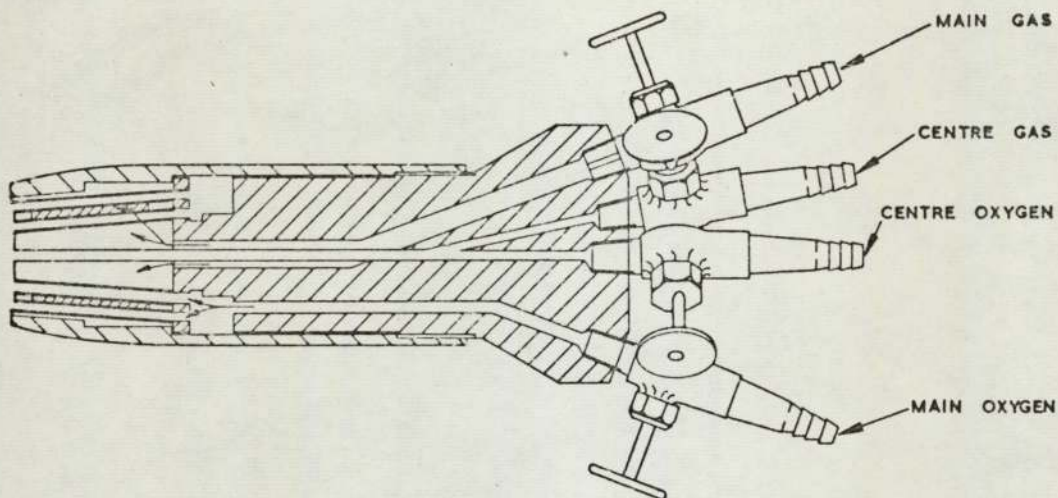


FIG.3 BURNER (SCHEMATIC DIAGRAM)

premixed burners. The flame was exceptionally quiet and took on a laminar appearance being some 300mm high and about 30mm in maximum width. The burner was always fired vertically upwards so that flame buoyancy effects would have as little effect as possible on the experimental results. The experimental work with natural gas and air was carried out using a simple design of burner where the flame was stabilised on a steel plate 40mm in diameter in which a large number of closely spaced 1.6mm diameter holes had been drilled.

Significant variations in throughput, giving rise to Reynolds numbers of from 50-500, were possible for all fuels. In the case of carbon monoxide, however, a marked tendency to lift had to be countered by the provision of a small annular diffusion flame at the outer edge of the main flame.

## 4.2 Gas Metering System

In order to reduce to a minimum the uncertainties which might arise from fluctuations in fuel quality, particular attention was paid to the purity of the gases supplied to the test rig. Propane, ethylene and carbon monoxide were conveniently obtained from high pressure cylinders using the 'CP' grade throughout. Supplied by Air Products Ltd these had the minimum purity levels specified in Table 3. The use of

Table 3 - Purity of gases supplied to experimental rig.

Fuel Gas	Minimum Purity %	Max. Levels of Impurities ppm by volume
CH <sub>4</sub>	99.1	CO <sub>2</sub> , 3500; C <sub>2</sub> H <sub>6</sub> 2000; traces of N <sub>2</sub> , C <sub>3</sub> H <sub>8</sub> , O <sub>2</sub>
C <sub>3</sub> H <sub>8</sub>	99.4	C <sub>4</sub> H <sub>10</sub> , 5500; C <sub>3</sub> H <sub>6</sub> , 500.
C <sub>2</sub> H <sub>4</sub>	99.8	CH <sub>4</sub> , 1500; C <sub>2</sub> H <sub>6</sub> , 50; N <sub>2</sub> , 50; CO <sub>2</sub> , 30; C <sub>2</sub> H <sub>2</sub> , 10; O <sub>2</sub> , 10.
CO	99.5	CO <sub>2</sub> , 200; O <sub>2</sub> , 20; N <sub>2</sub> , 75.
H <sub>2</sub>	>99.9	O <sub>2</sub> , 1; CO + CO <sub>2</sub> , 1;
O <sub>2</sub>	99.8	N <sub>2</sub> , 2000.

similar cylinders of hydrogen proved to be impracticable in view of the higher flowrates required with this fuel. Instead a supply was drawn from the high pressure laboratory system which was fed in turn from a bank of 20 cylinders each containing 60 standard cubic metres of the gas.

The greatest difficulties were experienced with the provision

of a suitable natural gas supply. The laboratory services were fed from a storage tank containing liquefied Algerian natural gas which was periodically replenished by a road tanker delivering from the Gas Council's Canvey Island Terminal. As delivered, this fuel contained appreciable proportions of higher hydrocarbons in addition to methane. The tendency of the lighter fractions to boil off preferentially from the storage facility resulted in a corresponding enrichment of the liquid with the higher homologues. Consequently the composition of the gas circulated to the laboratories varied with time and this had pronounced effects on the stoichiometric air requirements of the fuel. These effects were especially noticeable when the liquid level in the storage tank was low, and it was decided to restrict operation on natural gas to the period when the tank was virtually full. At a later date CP methane was used on the fuel oxygen studies but the natural gas supply was retained for the fuel-air work in view of the higher throughputs demanded by the relevant burner.

Oxygen and air were drawn from the fixed laboratory supply mains. The air was taken from the high pressure circuit to avoid the pulsations in pressure which are invariably present in the low pressure system. The supply was governed down to  $30\text{kN/m}^2$  using Hale Hamilton equipment consisting of a regulator in series with two RL1M controllers. The latter had the characteristic that a fall in the inlet pressure resulted in a rise at the outlet while an increased inlet pressure produced no change at the outlet. Thus the two controllers arranged in series effectively isolated the rig from disturbances generated by other equipment operating off the same line.

All supplies originating from high pressure cylinders were governed down to  $20\text{kN/m}^2$  using standard regulators. The natural gas was reduced from  $900\text{kN/m}^2$  to a pressure corresponding to a few

centimetres of water using a Fisher S201 unit in conjunction with a non-return valve. It was found that very precise control of the supplies derived from cylinders was afforded by the use of a Hale Hamilton L15S regulator, again with a RL1M controller. The gases were then fed to a bank of rotameters which provided for accurate metering of the fuel and oxidant fed to the burners.

Flow rates were adjusted by fine-control needle valves mounted before the metering tubes. It was found from experience that valves of the diaphragm type were generally unsatisfactory because the coarseness of control and the relaxation of the diaphragms made precise setting of flowrates more difficult.

Calibration of the rotameters was carried out by comparison with wet gas meters which had previously been tested at the Gas Standards Branch of the Ministry of Technology. It was reported that the meters used were accurate to within 0.8% after the usual corrections for ambient conditions had been applied. In spite of the large reduction in pressure between the various supply mains and the test rig, it was found that the gases were invariably metered at ambient temperature which remained virtually constant. This convenient state of affairs arose by virtue of the lengthy pipe runs involved and the fact that the laboratory concerned was acoustically, and hence thermally, insulated. No warming coils were required and temperature corrections to the indicated flowrates were included in the scales attached to the metering tubes. The range of supply rates covered was determined primarily by considerations of burner stability and combustion quality and varied from fuel to fuel. In the case of hydrogen - oxygen combustion a considerable range of throughputs was possible with fuel rates between 5 and 100 litres/minute being accommodated without difficulty. With

carbon monoxide and methane the range was rather more restricted being from 3 to 12 litres/minute for the latter.

#### 4.3 Equipment for Temperature Measurement

Conventional line reversal equipment was employed for all measurements of flame temperature. A number of background sources were used in the course of the experimental programme and either sodium or lithium was introduced to provide the spectral line for reversal. Initially a carbon arc lamp was chosen for the measurements on fuel-oxygen flames using the red lithium line at 670.7nm. The effective temperature of the continuous spectrum was adjusted by the rotation of a continuously variable neutral density wedge placed between the lamp and the flame (Fig. 4). This filter was driven by a small reversible electric motor operating at 10 revolutions per hour and controlled by potentiometers mounted near to the spectroscope. A calibration of effective temperature against angular displacement was then obtained using a high range 'Optix' pyrometer.

The use of lithium as the reversing species was dictated by the presence of appreciable quantities of sodium in the standard grade of lamp carbons. High purity electrodes were tried but considerable wandering of the anode crater made accurate measurement exceedingly difficult. Doping the rods with potassium salts was suggested but proved to be ineffective. Difficulties arising from the insensitivity of the human eye in the red region of the spectrum at high light levels were encountered throughout and correspondingly low accuracy was expected. It was thought that the errors and uncertainties involved probably amounted to  $\pm 100\text{K}$ . An error of this magnitude would be completely unacceptable in view of the strong temperature dependence of calculated radical concentrations. The great influence

- |                   |                  |
|-------------------|------------------|
| 1 CARBON ARC LAMP | 5 IRIS DIAPHRAGM |
| 2 IRIS DIAPHRAGM  | 7 LENS           |
| 3 NEUTRAL WEDGE   | 8 STOP           |
| 4 LENS            | 9 SPECTROSCOPE   |
| 5 BURNER          |                  |

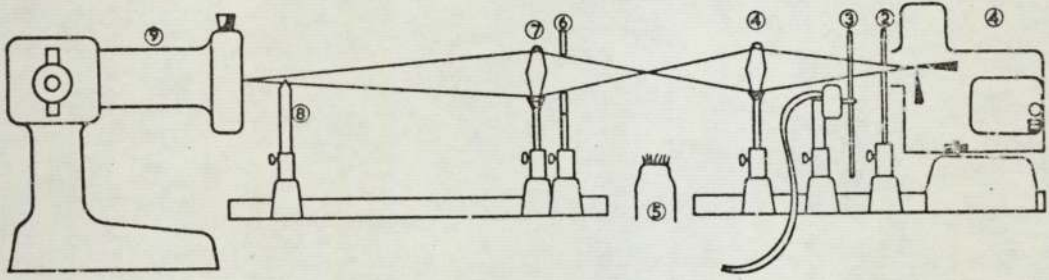
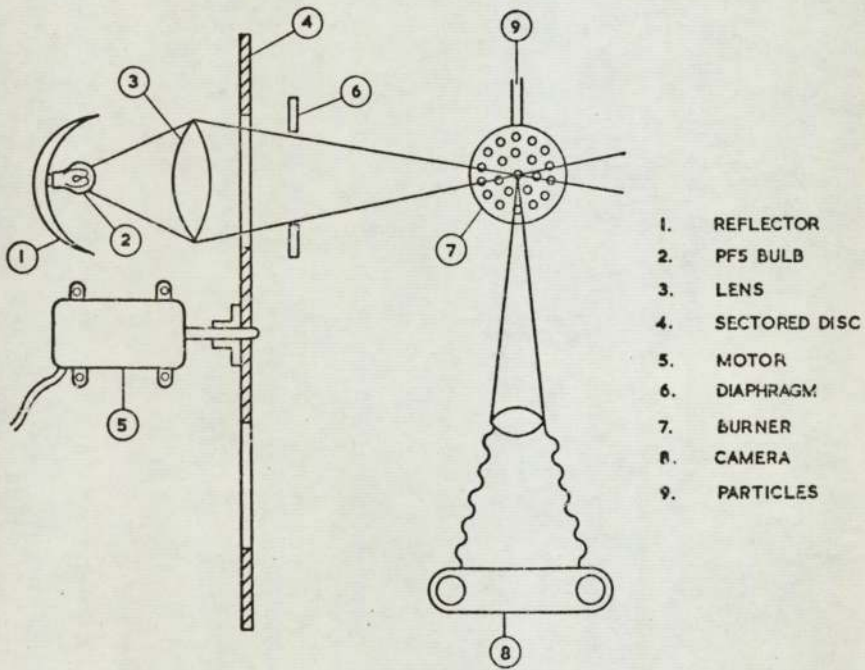


FIGURE 4. EQUIPMENT FOR TEMPERATURE MEASUREMENT BY LINE REVERSAL



- |                  |
|------------------|
| 1. REFLECTOR     |
| 2. PF5 BULB      |
| 3. LENS          |
| 4. SECTORED DISC |
| 5. MOTOR         |
| 6. DIAPHRAGM     |
| 7. BURNER        |
| 8. CAMERA        |
| 9. PARTICLES     |

FIGURE 5. PARTICLE TRACK EQUIPMENT

which dissociated species exert on the overall heat transfer process demands that their concentration be known with confidence. For this reason attempts were made to improve the temperature measuring system.

Fortunately a new design of tungsten filament lamp became available at the appropriate time. Designed by Quinn and Barber (56) for precise pyrometry up to 3000K, this lamp was manufactured at the Hirst Research Centre of the General Electric Company Ltd. The new design overcame many of the difficulties inherent in the use of traditional strip filament lamps as a high temperature standard. The problems of emissivity changes over a period of time and of temperature gradients across the strips were virtually eliminated by the use of a tubular filament 2mm in diameter and 45 mm long. A bundle of fine tungsten wires was situated at the centre of this tube to act as the radiating surface. By the inclusion of a restricting aperture 0.75mm in diameter at the end of the filament, substantially black body radiation was produced.

Quinn and Barber have shown the stability of the lamp to be better than  $\pm 0.1K$  making it highly suitable as a reference source. A current/temperature calibration was carried out by the National Physical Laboratory, reproducing the International Practical Scale of Temperature to within 0.2%. The inherent calibration error is therefore  $\pm 6K$  at the operating level of around 3000K. The calibration was made through the appropriate lens from the line reversal system in order to obviate the need for any transmissivity measurements.

Current was supplied by a 10V, 100A Hewlett Packard power supply in conjunction with two 2V heavy duty accumulators. A maximum current of 68A was drawn, this representing an overload condition demanding extrapolation of the current temperature relationship. Current was measured using a high-accuracy potentiometer connected across a standard resistor in the circuit.

The sodium carbonate supplied for the temperature measurements was

added axially through the small premixed flame in the centre of the fuel-oxygen burner. In the case of the premixed natural gas-air flame a separate seeded fuel supply was made to the centre burner port. In both cases a small electromagnet was used to vibrate the steel supply pipe, into which a small quantity of the appropriate alkali metal carbonate had been introduced. This resulted in sufficient material being carried forward in the gas stream to colour the centre zone of the flame. The addition of seed material as an aerosol was considered preferable to the atomisation of a solution, the latter method giving rise to appreciably lower flame temperatures because of the added moisture.

#### 4.4 Velocity Measurements

Local velocities in the natural gas-air flames were determined from measurements of the pressure head developed by the flowing gases. Open ended quartz tubes were used and the pressure generated was recorded on a direct reading micromanometer. This had previously been calibrated against an absolute instrument having a resolution corresponding to a head of 0.01mm of water. The gas velocity was then obtained from the relationship given in reference (57).

$$V = 1.52 \sqrt{\frac{\Delta P}{\rho}}$$

where  $\Delta P$  is the dynamic pressure  $N/m^2$

$\rho$  is the gas density  $kg/m^3$

$V$  is the gas velocity  $m/s$

Velocities in the fuel oxygen flames were determined in an identical manner using a water cooled copper probe.

In order to check that the velocities deduced from the total pressure heads were sufficiently accurate a supplementary set of measurements were carried out using a particle track technique. It was found that satisfactory results could be obtained using high output PF5 flash lamp

illumination in conjunction with moderate speed film (400ASA), using the arrangement depicted in Fig. 5. Light from the flash bulb was synchronised with the camera shutter using the 'M' system, and chopped by the rapidly rotating stroboscopic disc. This had six 3<sup>rd</sup> segments removed to provide light pulses for the illumination of the particles. The camera was mounted perpendicular to the direction of illumination and recorded the position of particles at each successive light pulse. The speed of rotation was determined by arranging for a photocell to supply a signal to the marker input of a high speed chart recorder once each revolution. At a chart speed of 3m/s it was found that a satisfactory trace was obtained. The electric motor, rated at 100W, drove the lightweight disc at approximately 26,000 R.P.M. providing exposures of 24 $\mu$  sec duration. The particles used were of alumina or magnesia and were carried into the flame as an aerosol.

Excellent agreement between the two experimental methods was obtained and for convenience the measurement of pressure heads was used in most cases.

#### 4.5 Probe design for stagnation point heat transfer measurements

The calorimeter used for the measurement of heat flux is illustrated in Fig. 6. A small plug of copper/1% beryllium alloy was mounted in the nose of a hemispherically ended cylindrical probe, 12.7 mm in diameter, made from stainless steel. Three sharpened stainless steel pins were used to suspend the plug centrally in a narrow air gap with a minimum of thermal contact area. A thermocouple mounted on the rear surface of the copper element was used to monitor the temperature change. The output from the thermocouple was fed via a suitable resistance network to a UV recorder which had previously been calibrated to enable the temperature history to be obtained from the trace. The freezing points

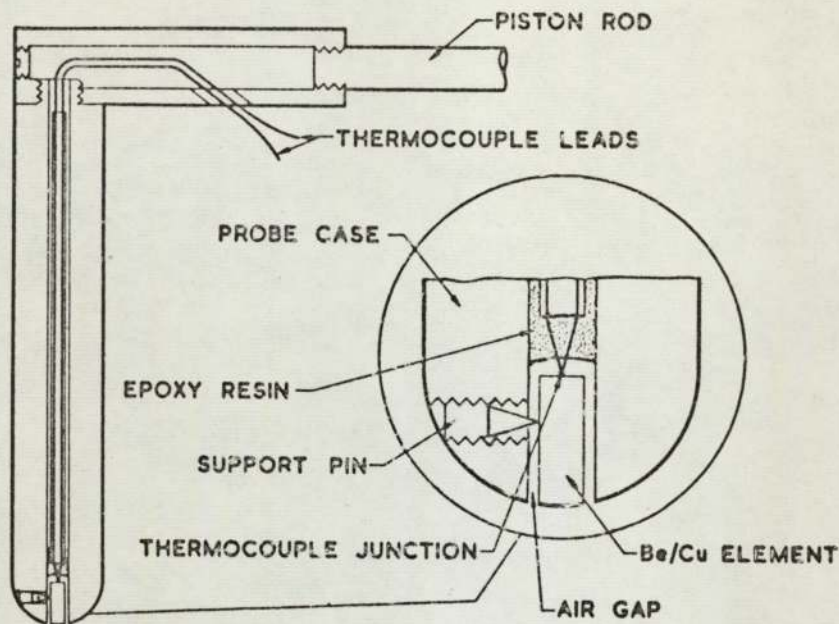


Figure 6. Sectional diagram showing construction of stagnation point probe

of pure lead and pure tin together with the boiling points of water and of sulphur were used to cover the operating range of the calorimeter. The centre section of the probe was filled with an epoxy resin to prevent circulation of flame gases past the sides of the plug.

The method of operation consisted of briefly inserting the probe into the flame using a pneumatic actuator in conjunction with suitable timing circuits. Measurements were made with the probe axis collinear with that of the flame. The time for a set temperature rise at the rear surface of the plug was recorded. From a knowledge of dimensions and thermal properties it was then possible to calculate the heat flux to the front face of the copper plug by solving the one-dimensional transient heat conduction equation.

It is important to point out at this stage that the chosen design of heat transfer probe does not represent the ideal geometry for theoretical studies. In retrospect a true sphere would have been preferable to the

hemispherically ended cylinder which was used in practice. This arises from the original intention to draw comparisons between various modified forms of Sibulkin's original relationship and measurements taken in flames. The relationship in question is given by

$$Nu = 0.763 Pr^{0.4} D_1(\beta/v)^{0.5}$$

Here  $\beta$  represents the velocity gradient at the stagnation point and for a sphere is given by  $3U_\infty/D_1$ . This leads to the proportionality constant of 1.32 when expressed in conventional Nusselt number form:

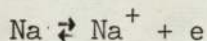
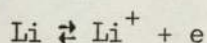
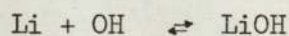
$$Nu = 1.32 Pr^{0.4} Re^{0.5}$$

For the hemisphere-cylinder combination the value of the velocity gradient cannot strictly be represented by  $3U_\infty/D_1$  and probably lies between this value and the  $8U_\infty/3D_1$  which is appropriate to a Blasius half body. This point was overlooked at the time of the experimental work, although the precaution of testing Sibulkin's relationship against experiment was made. Heat transfer rates were determined for the stagnation point probe cooling from 450K in a uniform laminar air stream. A wide range of fluid velocities was covered and in all cases it was found that the measurement agreed closely with predictions derived from Sibulkin's expression for a sphere. The maximum discrepancy noted was only 4% and curiously enough, the theoretical predictions generally resulted in a slight underestimation of the measured flux. This is the reverse of what might be expected from the inadvertent use of the quantity  $3U_\infty/D_1$ , although several possible explanations for this behaviour can be suggested. The most likely of these would be errors in the thermal properties of the calorimetric insert at the probe tip and errors introduced in the calibration of the recording equipment. However, it is extremely fortunate that the two influences act in opposite directions and conveniently cancel out. This obviates the need to calibrate the probe and permits quantitative comparisons to be drawn between expressions which are strictly applicable to spheres and the experimental measurements taken in flames.

#### 4.6 Hydrogen atom concentrations in the flame gases

It has already been mentioned that the presence of dissociated species in fuel-oxygen flames has an important bearing on the mechanism and rate of energy transfer to a cooler surface. Consequently, it was deemed necessary to check whether or not excess concentrations of free radicals might be present at the positions where heat transfer was to be measured. Significantly higher than equilibrium concentrations would be unacceptable if prediction methods were to be tested realistically. Since the major part of the diffusive heat flux from combustion products is usually carried by the hydrogen atoms present, concentration measurements were obtained for that species.

The experimental determination of hydrogen atom concentrations in flames takes advantage of the differing stabilities of alkali metal hydroxides at high temperatures. While sodium is largely present in atomic form, lithium has a very much greater tendency to form the stable hydroxide LiOH. This feature can be used to obtain the concentration of OH, and subsequently of H, by referring to equilibrium constants for the reactions listed below



Briefly, the experimental technique was to introduce a known concentration of a sodium salt into the flame and to measure the intensity of the emitted radiation from the yellow line at 589.0nm. A similar measurement was then made with lithium addition using the red line at 670.8nm. The equipment required is shown in Fig. 7. Light from the flame was interrupted by a rotating sector disc and focussed by the lens onto the entrance slit of a quartz spectrograph. The spectrum

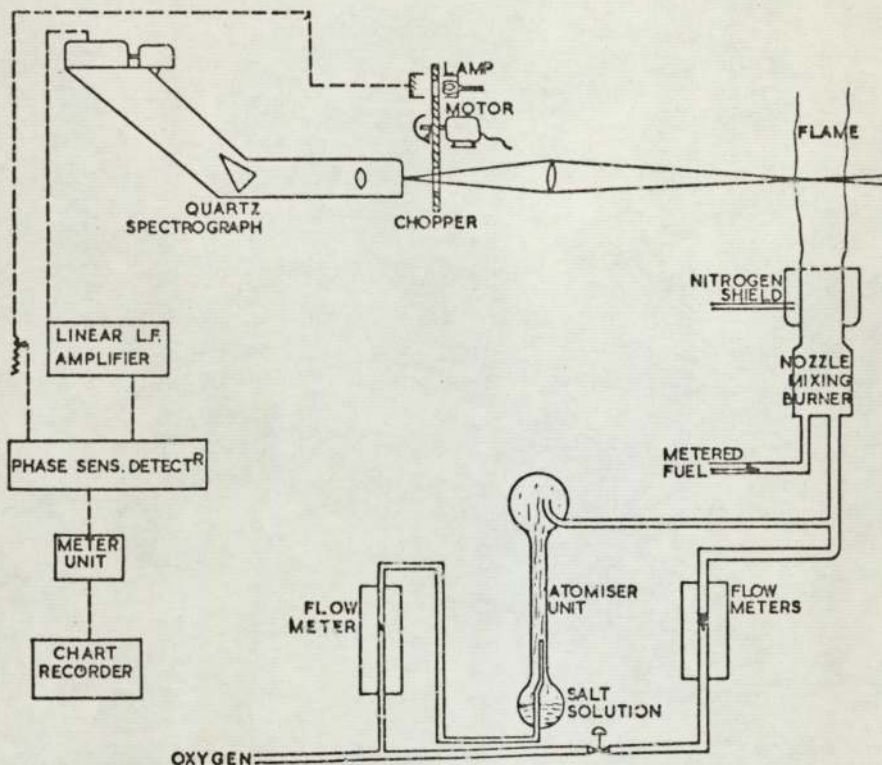


FIGURE 7. EQUIPMENT FOR THE MEASUREMENT OF HYDROGEN ATOM CONCENTRATIONS

produced was scanned by a high gain photomultiplier driven by an electric motor. The output from the photomultiplier tube was fed to a linear low frequency amplifier and then to a phase sensitive detector. A second signal corresponding to the chopping frequency was supplied by a light source and photocell mounted on either side of the stroboscopic disc. The phase sensitive detector was tuned to this frequency to eliminate background noise arising from the amplification circuits and the resultant signal fed to a metering unit and a chart recorder. The latter was chosen to give a deflection directly proportional to the input signal. A knowledge of the photomultiplier response characteristic, obtained from an independent calibration against a tungsten strip lamp, enabled the absolute intensities of the sodium and lithium lines to be compared.

On the treatment of Mitchell and Zermansky (58) it can be shown that

the intensity of a resonance spectrum line emitted by a hot gas column is given by

$$I = \frac{8\pi\alpha hc}{\lambda^3} \exp(-hc/\lambda kT) \int_0^{\infty} \{1 - \exp(-K_{\nu} l)\} d\nu$$

For the low concentrations of alkali metals considered in this work the effects of self absorption can be neglected and the expression quoted reduces to

$$I = \frac{8\pi\alpha hc}{\lambda^3} \exp(-hc/\lambda kT) \frac{\pi e^2}{Mc} Nfl$$

where:

I	is the intensity	$\nu$	the frequency
$\alpha$	an instrument constant	$K_{\nu}$	the absorption coefficient at $\nu$
h	the Planck constant	T	the absolute temperature
$\lambda$	the line wavelength	k	the Boltzmann constant
l	the column thickness	c	the velocity of light
e	the electronic charge	N	the number of ground state metal atoms/cm
m	the electronic mass	f	the oscillator strength of the transition

In the present case the measured intensities of the sodium and lithium resonance lines  $I_{Na}$  and  $I_{Li}$  can therefore be related to the concentrations of ground state atoms present in the flame gases.

$$\frac{I_{Na}}{I_{Li}} = \left(\frac{\lambda_{Li}}{\lambda_{Na}}\right)^3 \frac{[Na] f_{Na}}{[Li] f_{Li}} \exp\left\{\frac{hc}{kT} \left(\frac{1}{\lambda_{Li}} - \frac{1}{\lambda_{Na}}\right)\right\} \dots\dots (10)$$

Now the relative intensities of the two spectrum lines can be deduced from the peak heights, L, on the chart record and the photomultiplier response characteristic. If P represents the ratio of the output signals obtained for equal absolute intensities at the lithium and sodium wavelengths then

$$\frac{I_{Li}}{I_{Na}} = \frac{L_{Li}}{PL_{Na}}$$

Equation (10) may then be used to evaluate [Li] provided that [Na] be

known. The latter may be determined directly from the well known Saha equation describing thermal ionisation in which the equilibrium constant for the ionisation reaction is expressed as a function of the ionisation potential,  $V$ , and the absolute temperature. In the case of sodium  $K_1 = [\text{Na}^+]^2 / [\text{Na}]$  with  $K_1$  given by

$$\log K_1 = -\frac{5040V}{T} + \frac{5}{2} \log T - 6.1816$$

$$\text{where } V = 5.193 \text{ eV}$$

Similarly the prevailing lithium ion concentration may be deduced from a knowledge of the concentration of unionised material,  $[\text{Li}]$ , and with corresponding equilibrium constant  $K_2$ . In this case

$$K_2 = [\text{Li}^+]^2 / [\text{Li}] \text{ with the appropriate ionisation potential being } 5.391 \text{ eV.}$$

The intensity of light emission remains proportional to the concentration of the radiating species, providing that self absorption can be neglected. Under the conditions used experimentally this is certainly the case so that the measured intensity at the lithium wavelength and that calculated on the assumption that no hydroxide formation or ionisation occurs can be related as follows:

$$\frac{I_{Li\tau} - I_{Li}}{I_{Li}} = \frac{[\text{LiOH}] + [\text{Li}^+]}{[\text{Li}]} = \frac{[\text{LiOH}]}{[\text{Li}]} + \frac{K_2}{[\text{Li}^+]}$$

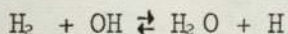
$$\text{but } K_1 = \frac{[\text{LiOH}][\text{H}]}{[\text{Li}][\text{H}_2\text{O}]} \text{ and } K_2 = \frac{[\text{Li}][\text{OH}]}{[\text{LiOH}]}$$

$$\text{so } \frac{1}{[\text{H}]} = \frac{1}{K_1[\text{H}_2\text{O}]} \left[ \frac{I_{Li\tau} P I_{Na}}{I_{Na} I_{Li}} - 1 - \frac{K_2}{[\text{Li}^+]} \right]$$

$$\text{or } [\text{OH}] = K_2 \left[ P \left( \frac{\lambda_{Na}}{\lambda_{Li}} \right)^3 \frac{[\text{Li}\tau] f_{Li} I_{Na}}{[\text{Na}] f_{Na} I_{Li}} \exp \left\{ \frac{hc}{kT} \left( \frac{1}{\lambda_{Na}} - \frac{1}{\lambda_{Li}} \right) \right\} - 1 - \frac{K_2}{[\text{Li}^+]} \right] \dots (11)$$

The equilibrium constant  $K_2$  has been obtained as a function of temperature by Smith and Sugden (59), from theoretical considerations

of the vibrational energy of the lithium hydroxide molecule. The value quoted of  $7.6 \times 10^5 \exp(-102,000/RT)$  may then be substituted into Eq. (11) enabling the hydroxyl concentrations to be evaluated. In order to relate these to the required data for hydrogen atoms it is only necessary to consider the reaction



This is a simple exchange process and, as such, is extraordinarily fast. As a result, the relative proportion of H to OH always remains the same as that for equilibrium conditions irrespective of the thermodynamic state of the overall mixture. As the equilibrium compositions have already been obtained for the calculation of thermodynamic and transport properties, the computation of local hydrogen atom concentrations becomes straightforward.

## 5. RESULTS FOR STAGNATION POINT WORK

### 5.1 Flame temperature measurements

In order to follow the decay of temperature with distance, traverses were made along the axis of typical flames of hydrogen and methane burning with oxygen. The results of these measurements are presented in Fig. 8 together with an indication of the extent of the principal reaction zone in each case. It can be seen that the measured temperature falls only slowly from the maximum value as the distance from this zone is increased. Similar horizontal traverses indicated that the temperature is insensitive to position in the central regions of the flames but, as expected, falls abruptly in the outer edges. It was noted that this region of relatively steady temperature diminishes both with increased height and with higher flowrates. However, it appeared that the constant property zone was sufficiently extensive to permit the use of quite large (12.7 mm) probes without undue concern.

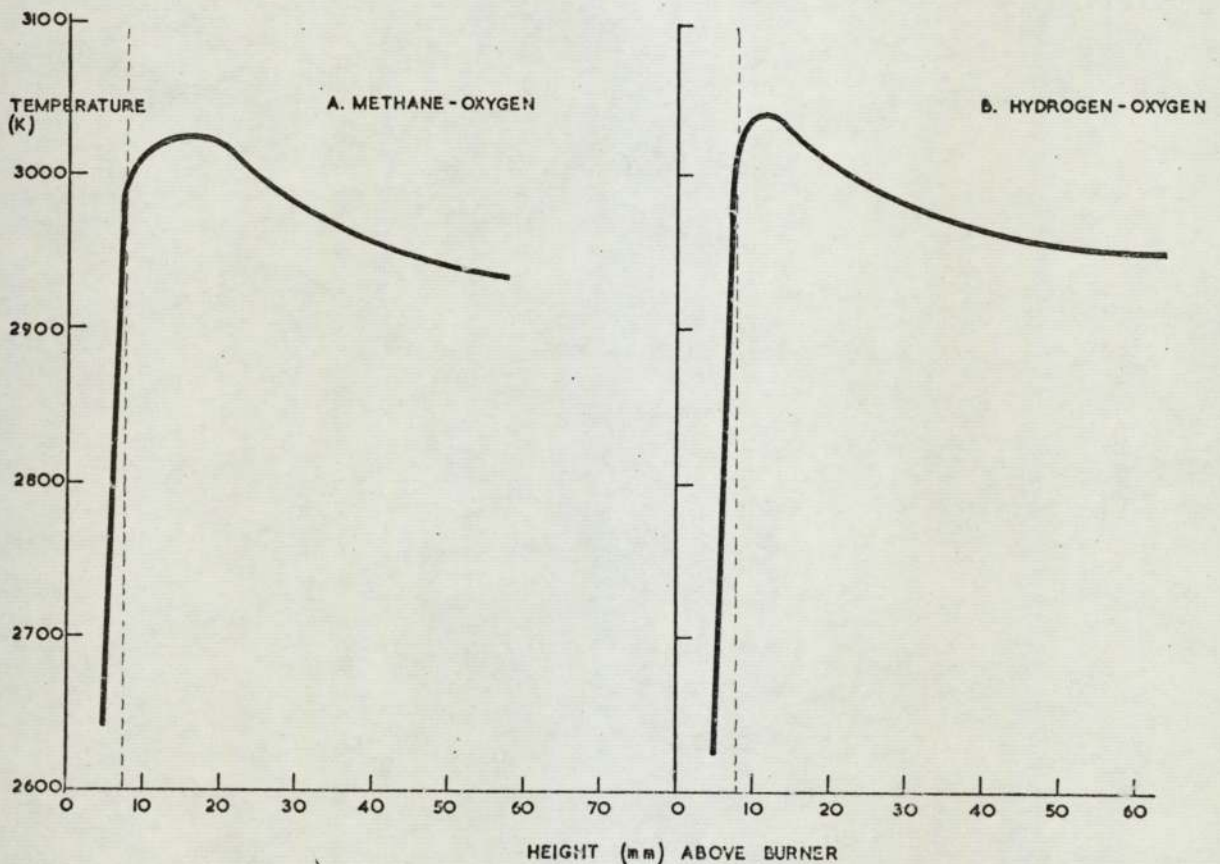


FIGURE 8. TEMPERATURE PROFILES MEASURED ON THE FLAME AXIS.

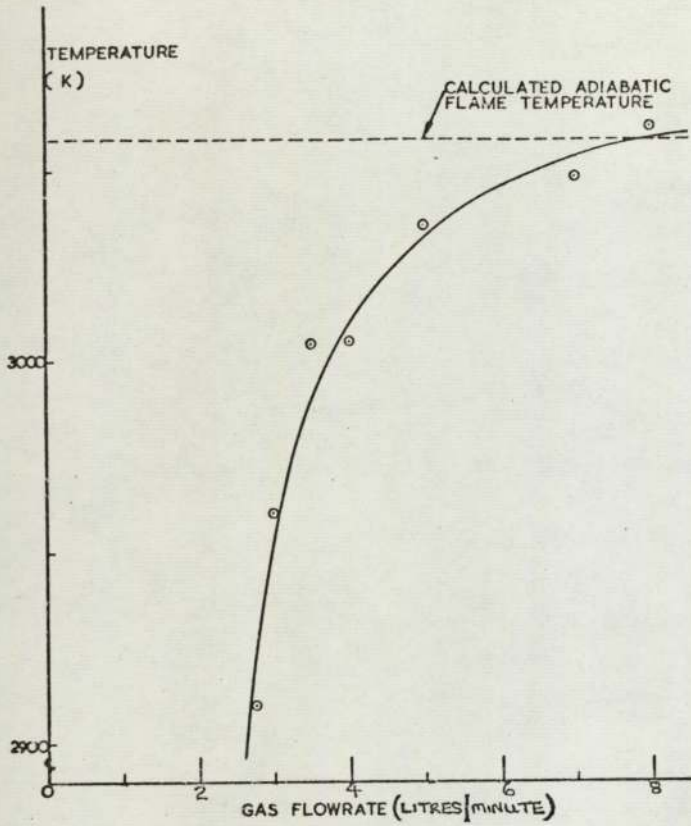


FIG.9 VARIATION OF FLAME TEMPERATURE WITH GAS FLOW NATURAL GAS/O<sub>2</sub>

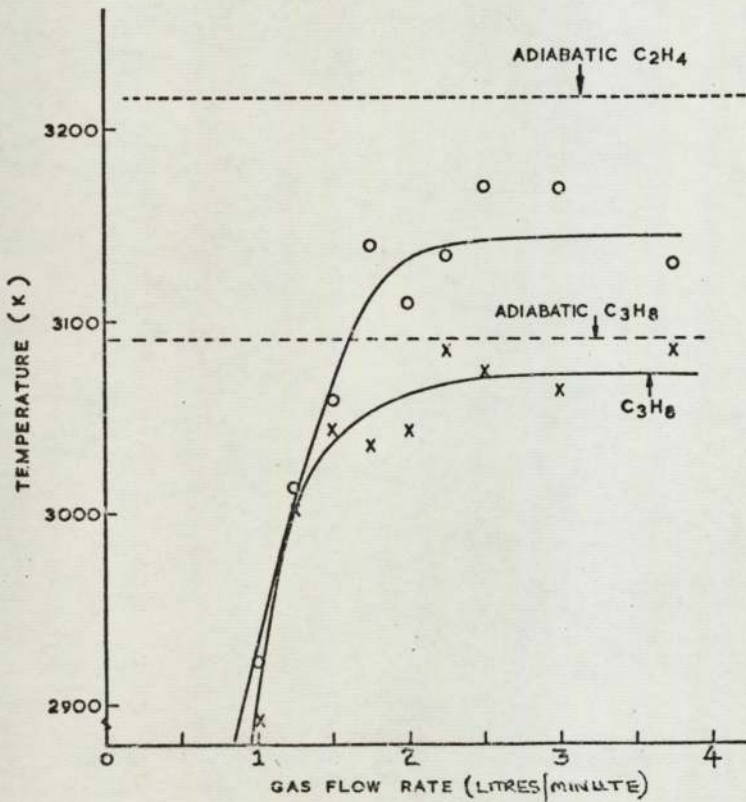


FIG.10 VARIATION OF FLAME TEMPERATURE WITH GAS FLOW PROPANE/O<sub>2</sub> ETHYLENE/O<sub>2</sub>

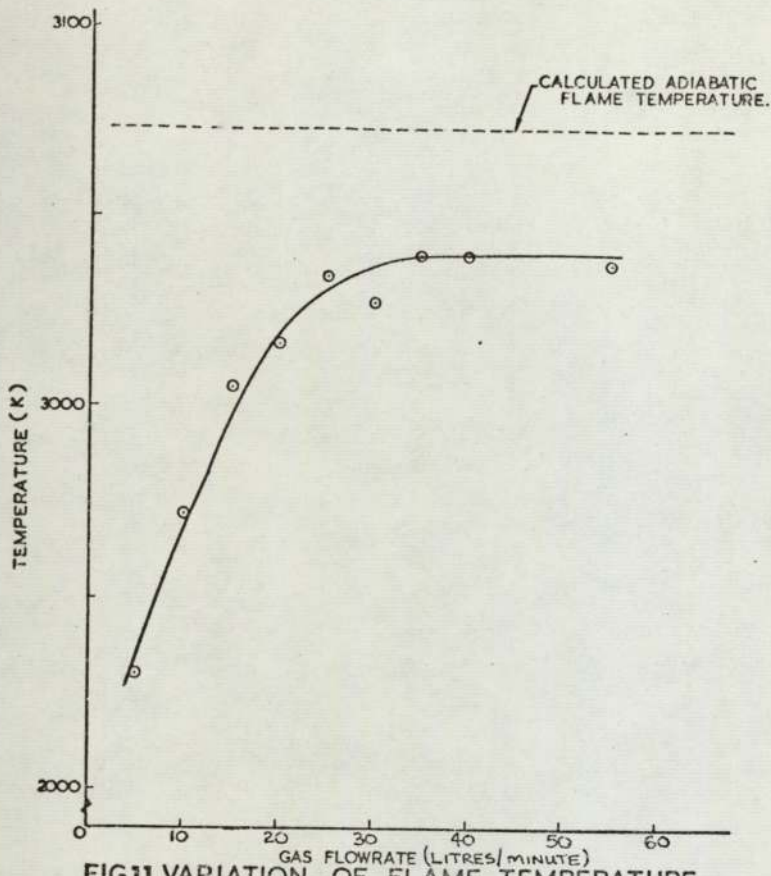


FIG.11 VARIATION OF FLAME TEMPERATURE WITH GAS FLOW HYDROGEN/O<sub>2</sub>

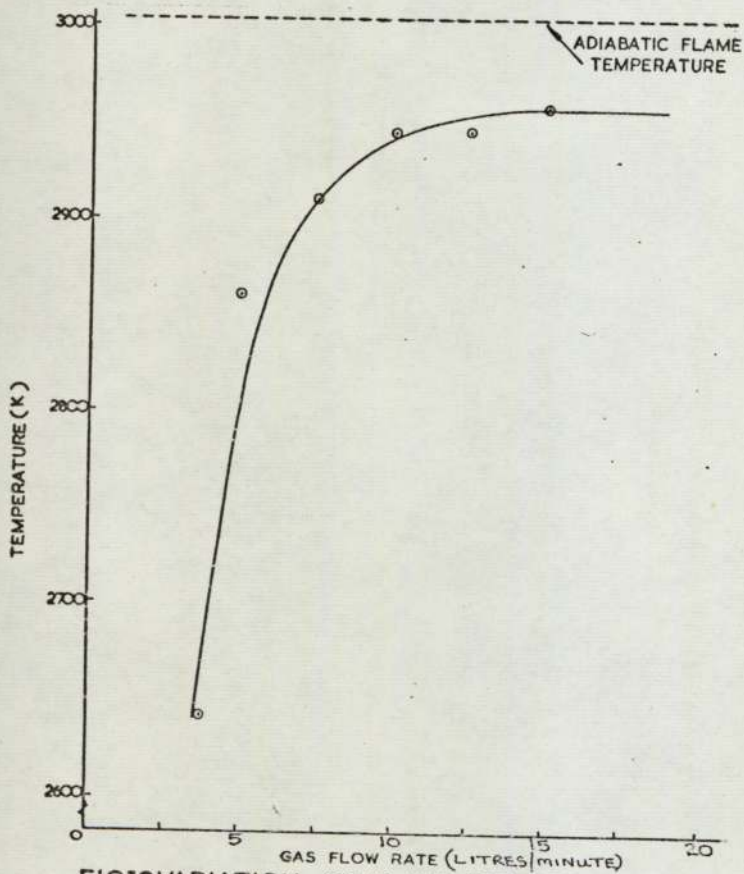


FIG.12 VARIATION OF FLAME TEMPERATURE WITH GAS FLOW CARBON MONOXIDE/O<sub>2</sub>

It was found that the temperature at a given point above the burner rim was constant for any particular fuel over the major part of the range of flow rates used. Below about one third of the maximum flow, a progressive decline in temperature was noted with the lowest value being some 100 to 200K below the maximum. This is shown in Figs. 9 to 12. Over the normal working range of the burner, which includes most of the experimental data, little dependence on thermal throughput was apparent.

The temperatures applicable to the majority of measurements for each fuel-oxygen combination are listed in Table 4 together with the corresponding calculated adiabatic flame temperatures. For convenience, the calculated thermophysical properties of the combustion products at this flame temperature, the cold sink temperature are also listed together with the weighted averages between flame and sink temperature.

## 5.2 Hydrogen atom concentrations

Typical data obtained from the studies of lithium and sodium emission have been plotted against height above the burner in Figs. 13 and 14. Only methane-oxygen and hydrogen-oxygen flames were studied since the measurements had to be completed in a short time on equipment loaned by the Department of Chemistry at Aston University. It can be seen that excess concentrations of hydrogen atoms do not appear to be particularly large. However, it appears that the appropriate region for all the heat transfer measurements would extend from 12 to 17 mm from the burner head. This distance is in keeping with the conclusions reached from the temperature traverses and a separation of 12.7 mm was used throughout.

An independent check on the degree of equilibrium reached in the flames was afforded by an otherwise abortive series of heat transfer measurements carried out before the present project was formulated. The heat fluxes to small platinum/platinum-rhodium thermocouple probes were obtained by a crude analysis of the response curve obtained when suddenly

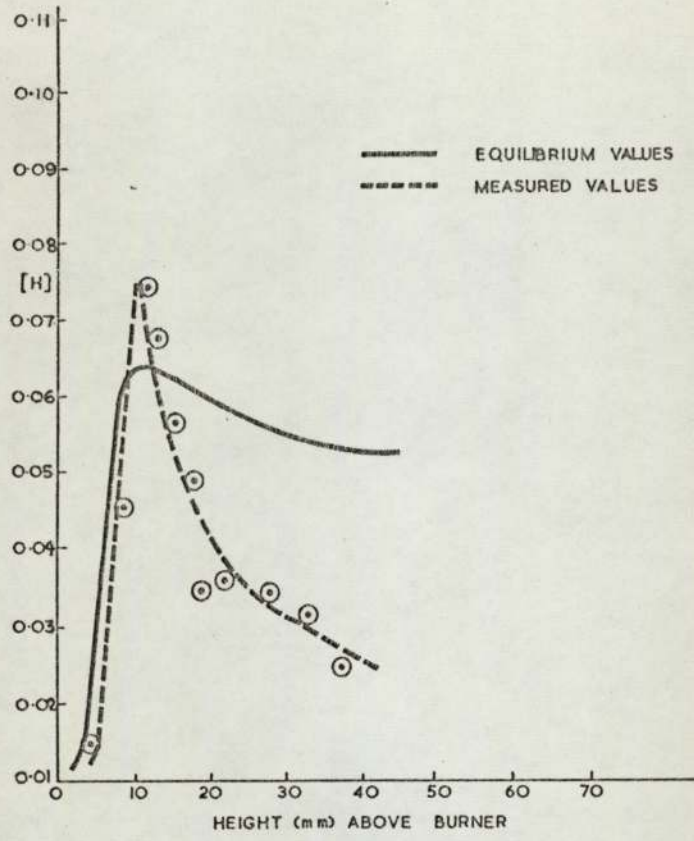


FIG. 13. HYDROGEN ATOM CONCENTRATION IN THE STOICHIOMETRIC HYDROGEN-OXYGEN FLAME

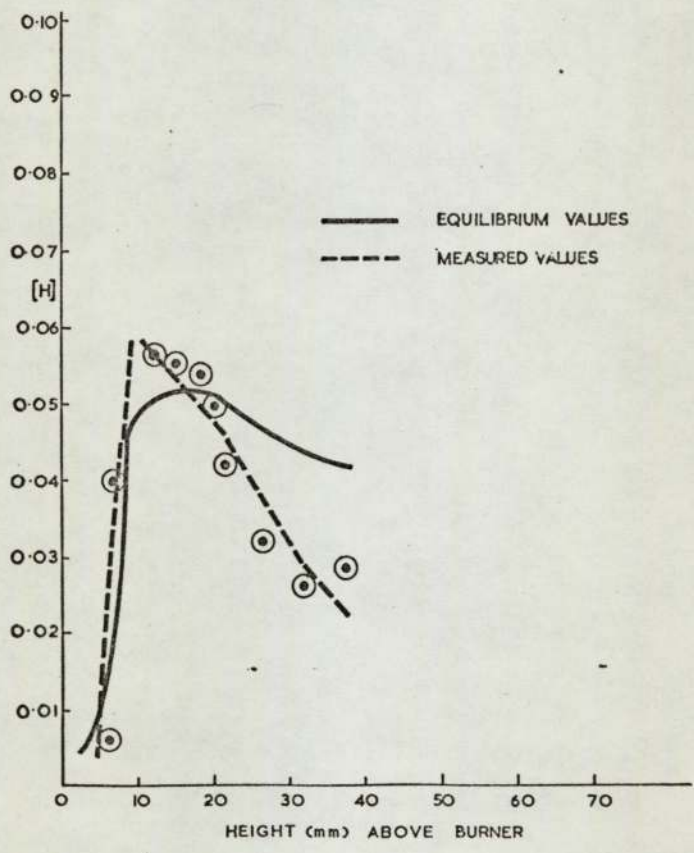


FIG. 14 HYDROGEN ATOM CONCENTRATION IN THE STOICHIOMETRIC METHANE-OXYGEN FLAME

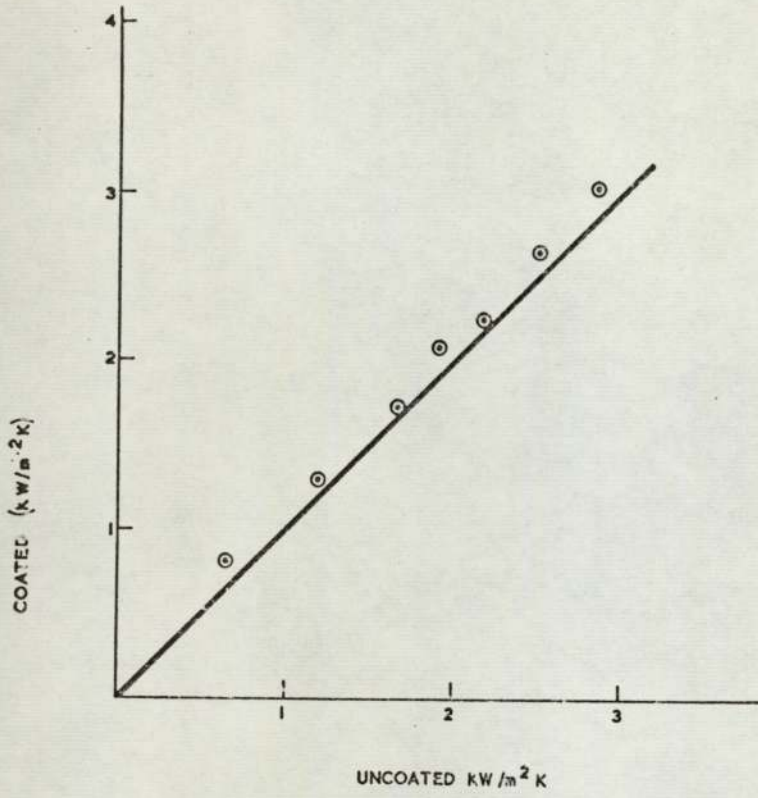


FIGURE 15. MEASURED HEAT TRANSFER TO SILICA COATED AND UNCOATED PLATINUM PROBES.

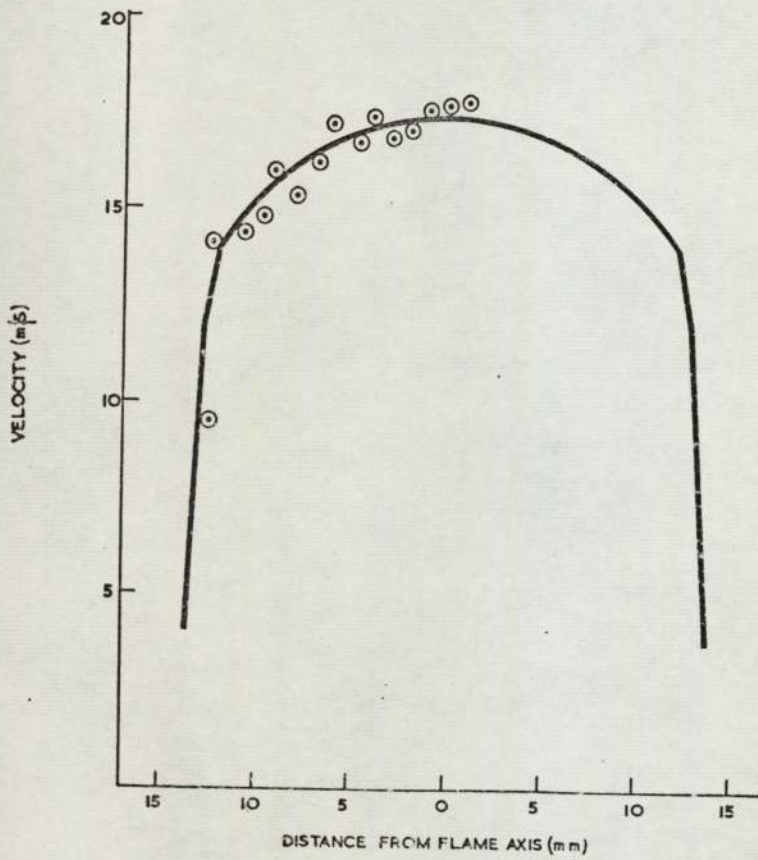


FIGURE 16. TYPICAL VELOCITY PROFILE OBTAINED ON THE CALISILE BURNER 20 mm ABOVE SURFACE

exposed to the flame gases. For research purposes the accuracy of the analysis was decidedly poor and the results obtained were rightly discarded. However, at one stage the effect of surface conditions on the heat transfer rates was investigated. The heat transfer coefficients to probes coated with silica were compared with those to identical probes left uncoated. The data obtained is shown in Fig. 15 and indicates that little difference in response exists.

This tends to indicate that boundary layer recombination of active species predominates, since it would be expected that the two surfaces would catalyse the recombination reactions to differing extents. The thinness of such layers in the experimental system, further emphasises the rapidity at which the chemical changes occur, giving additional weight to the assumption that the bulk gas stream be in equilibrium.

### 5.3 Velocity measurements

Velocity traverses were made using a 3.6 mm diameter water cooled pitot tube and indicate that the central cores of the flames have substantially uniform velocity at the prescribed height above the burner nozzle. This is demonstrated by Fig. 16 which shows the profile obtained in the methane oxygen flame at the maximum throughput used in the experimental programme. At lower thermal inputs the profile was found to be correspondingly flatter.

### 5.4 Heat transfer coefficients

Experimental heat transfer coefficients have been derived from the measured heat fluxes and flame temperatures. The values appropriate to a free stream Reynolds number of 300 are listed in Table 5 for all the five fuel-oxygen flames and for the natural gas-air flame. At this Reynolds number the effects of flame temperature changes were absent for all the combinations studied.

The corresponding predictions from the various modified forms of Sibulkin's original low temperature relationship and from the

numerical solution procedure are also given for comparison. It is clear that satisfactory agreement with experiment is provided by the empirical expression given by Eq. (F) and by the numerical method. The agreement with experimental measurements extends over the whole range of flow rates covered.

A generalised plot covering the whole range of the experimental studies with the stagnation point probe is provided by Fig. 17. On this figure the predictions derived from the suggested empirical method, Eq. (F), are also included. The experimental data are presented in a more readily accessible form in Figs. 18 to 23 where comparisons with the numerical solutions are made. Information on property variations within the heat transfer boundary layer, typical of that obtained from the numerical solutions, is presented in Figs. 24 to 27.

Table 4 : Physical Properties of combustion products at measured flame temperature, the sink temperature of 400K and averaged properties between flame and sink temperature

Property	Fuel/Oxidant					
	$\text{CH}_4/\text{O}_2$	$\text{H}_2/\text{O}_2$	$\text{C}_2\text{H}_4/\text{O}_2$	$\text{C}_3\text{H}_6/\text{O}_2$	$\text{CO}/\text{O}_2$	$\text{NG}^*/\text{Air}$
$T_s$ (adiab)	K	3073	3216	3097	3004	2224
$T_s$ (meas)	K	3040	3144	3072	2957	2200
$\bar{C}_p$	J/kgK	4765	3750	3595	2370	1435
Pr	-	0.7251	0.6373	0.6510	0.6868	0.7337
$\rho_s$	kg/m <sup>3</sup>	$61.0 \times 10^{-3}$	$90.5 \times 10^{-3}$	$90.6 \times 10^{-3}$	0.154	0.152
$\rho_w$	kg/m <sup>3</sup>	0.549	0.945	0.899	1.34	0.847
$\mu_s$	Ns/m <sup>2</sup>	$87.8 \times 10^{-6}$	$89.4 \times 10^{-6}$	$88.2 \times 10^{-6}$	$83.7 \times 10^{-6}$	$67.4 \times 10^{-6}$
$\mu_w$	Ns/m <sup>2</sup>	$13.9 \times 10^{-6}$	$18.0 \times 10^{-6}$	$17.6 \times 10^{-6}$	$19.6 \times 10^{-6}$	$21.0 \times 10^{-6}$
$\bar{\mu}$	Ns/m <sup>2</sup>	$56.5 \times 10^{-6}$	$57.9 \times 10^{-6}$	$57.4 \times 10^{-6}$	$54.4 \times 10^{-6}$	$43.8 \times 10^{-6}$
$\lambda_s$	W/mK	3.78	2.72	2.58	0.899	0.233
$\lambda_w$	W/mK	$26.8 \times 10^{-3}$	$27.5 \times 10^{-3}$	$27.9 \times 10^{-3}$	$24.2 \times 10^{-3}$	$32.6 \times 10^{-3}$
$\bar{\lambda}$	W/mK	0.429	0.625	0.487	0.235	$95.0 \times 10^{-3}$

\* Algerian Natural Gas Evaporated from Liquid Storage. Typical Composition 83.9%  $\text{CH}_4$ , 11.4%  $\text{C}_2\text{H}_6$ , 3.4%  $\text{C}_3\text{H}_8$ , 1.3%  $\text{C}_4\text{H}_{10}$ .

Table 5 : Heat transfer coefficients evaluated from modified forms of Sibulkin's equation and from numerical solutions.  $Re_s = 300$ ,  $T_w = 400K$ .

Expressions from which coefficients have been derived	Heat Transfer Coefficient ( $W/m^2 K$ )						
	$CH_4/O_2$	$H_2/O_2$	$C_2 H_4/O_2$	$C_2 H_6/O_2$	$CO/O_2$	$NG^*/Air$	
(A) $\bar{Nu} = 1.32 \bar{Pr}^{0.4} Re_s^{0.5}$	748	1010	797	738	371	157	
(B) $\bar{St} = 1.32 \bar{Pr}^{-0.6} Re_s^{-0.5}$	743	925	805	739	456	219	
(C) $\bar{Nu} = 1.32 \bar{Pr}^{0.4} \bar{Re}^{0.5}$	931	1270	990	885	460	195	
(D) $\bar{St} = 1.32 \bar{Pr}^{-0.6} \bar{Re}^{-0.5}$	598	740	647	574	366	176	
(E) $\bar{Nu} = 1.32 \bar{Pr}^{0.4} \left(\frac{\mu}{\mu_s}\right) Re_s^{0.5}$	482	642	517	480	241	102	
(F) $\bar{St} = 1.32 \bar{Pr}^{-0.6} \left(\frac{\mu}{\mu_s}\right) Re_s^{-0.5}$	479	588	521	481	296	142	
Numerical Prediction	544	585	520	493	301	152	
Experimental Value	521	611	526	465	256	147	

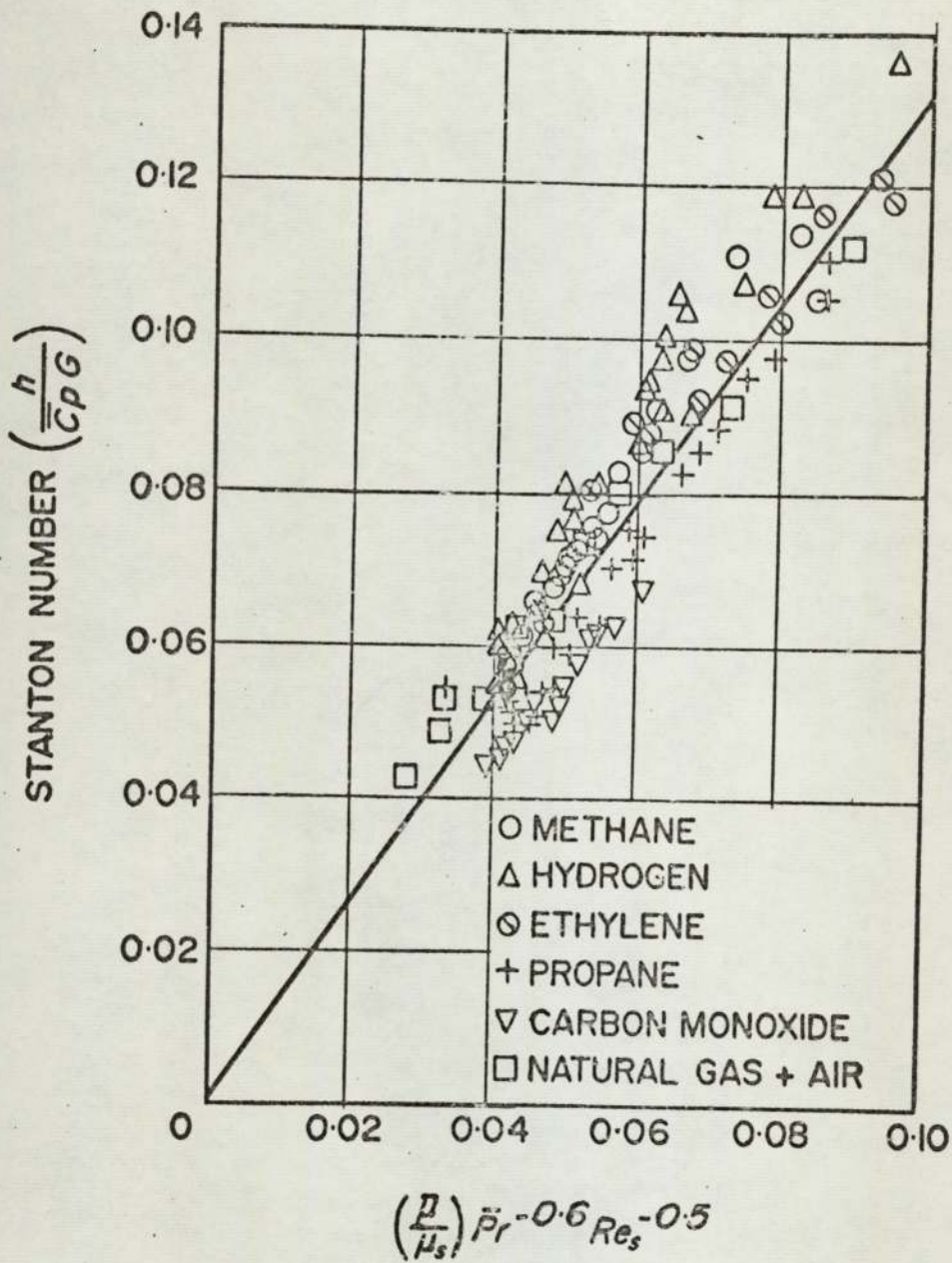


Fig.17. Generalised plot of stagnation point measurements  
 The continuous line represents the proposed  
 empirical correlation.

Experimental data and numerical solutions for stagnation point heat transfer from flames

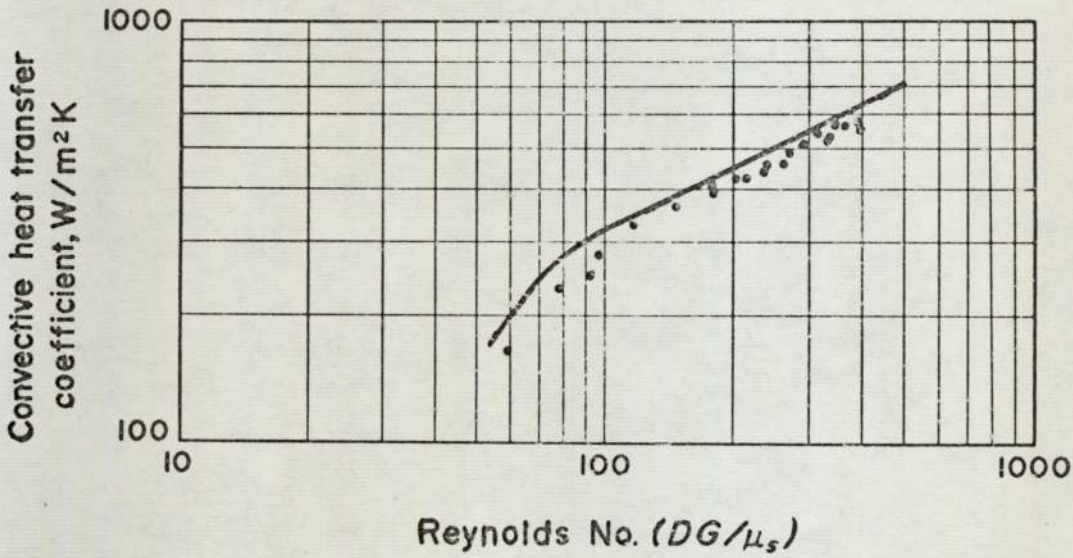


Fig. 18 Stoichiometric methane-oxygen

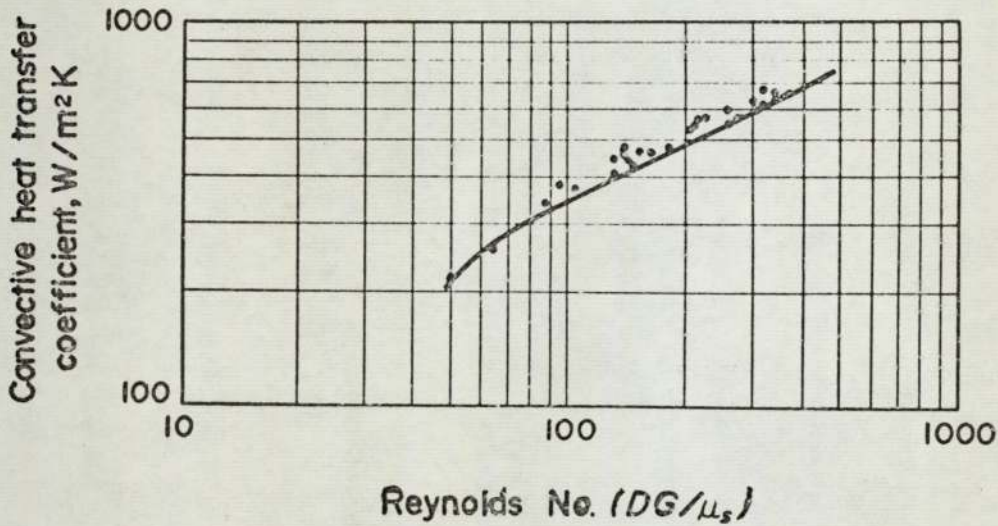


Fig. 19 Stoichiometric hydrogen-oxygen

Experimental data and numerical solution for  
stagnation point heat transfer from flames

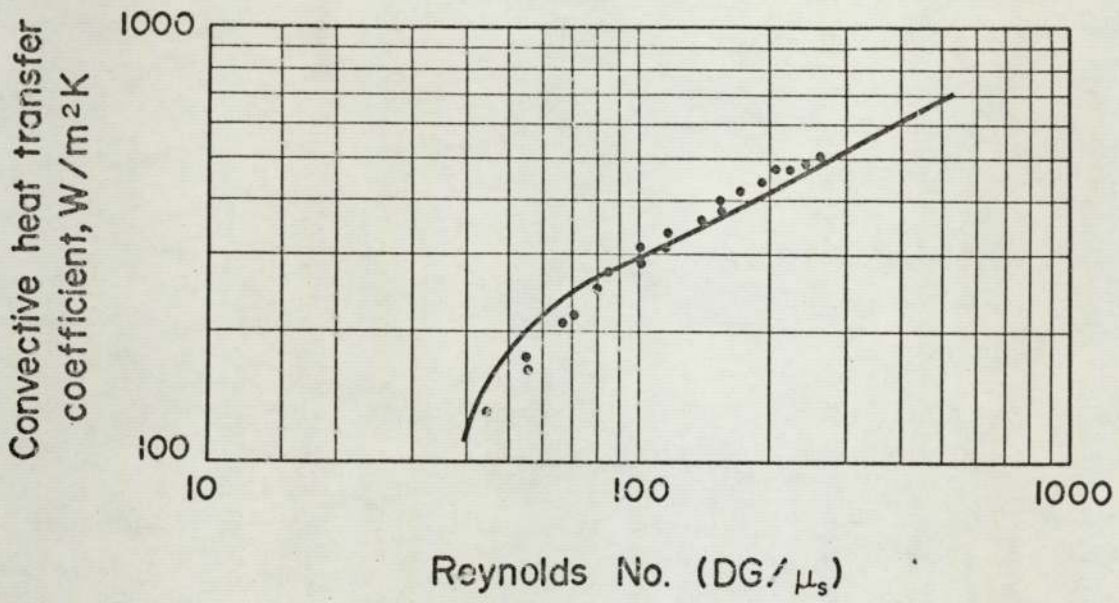


Fig 20 Stoichiometric ethylene-oxygen

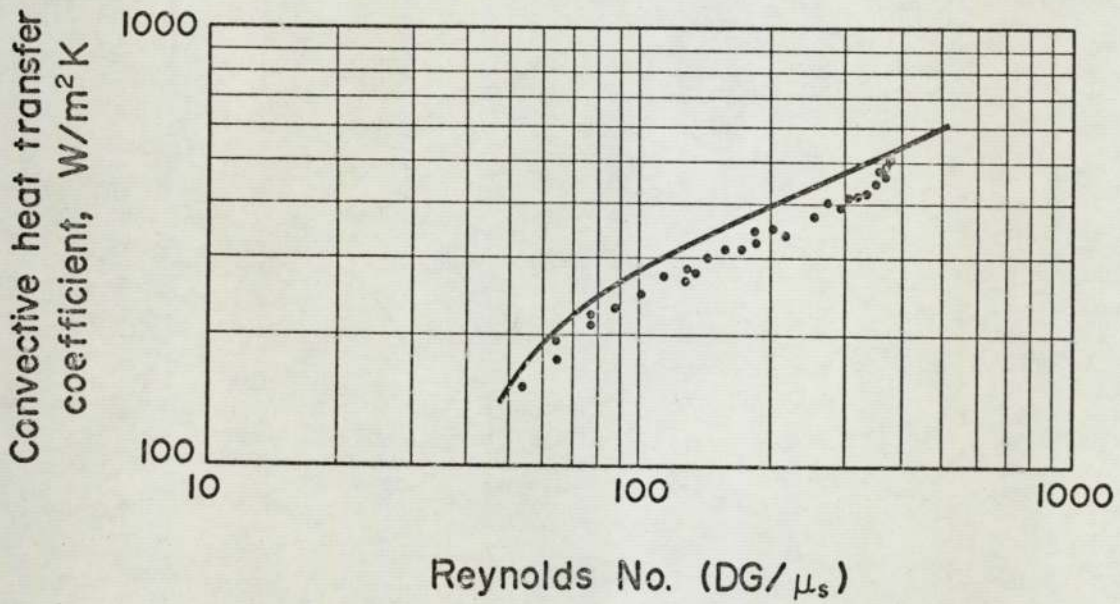


Fig 21 Stoichiometric propane-oxygen

Experimental data and numerical solution for stagnation point heat transfer from flames

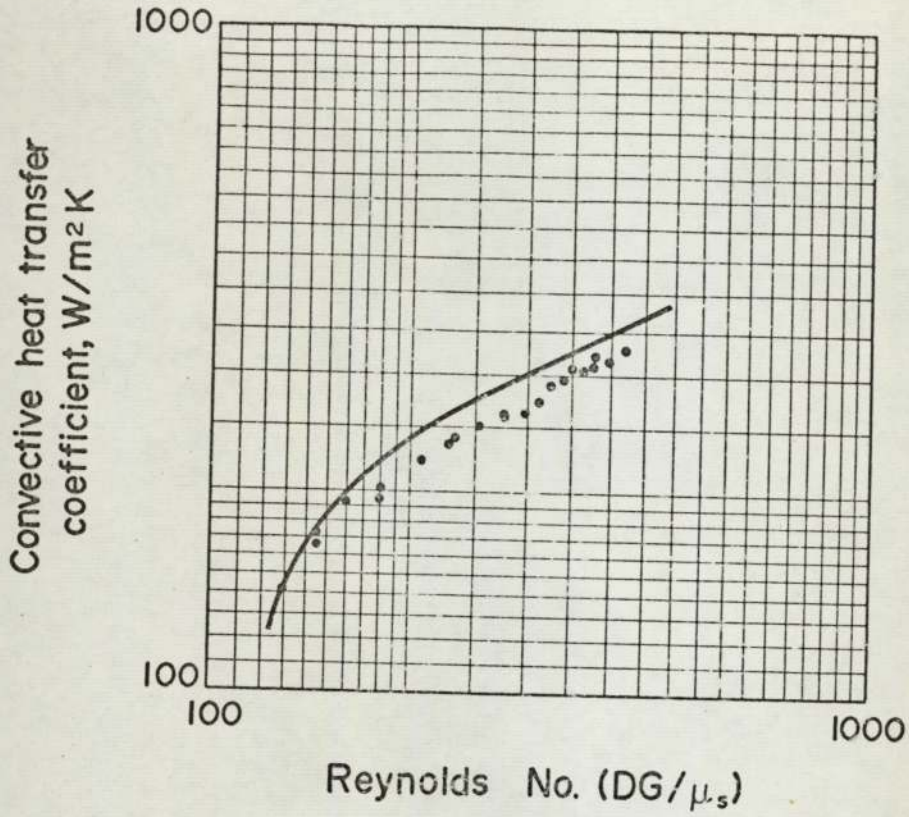


Fig 2 2 Stoichiometric carbon monoxide - oxygen

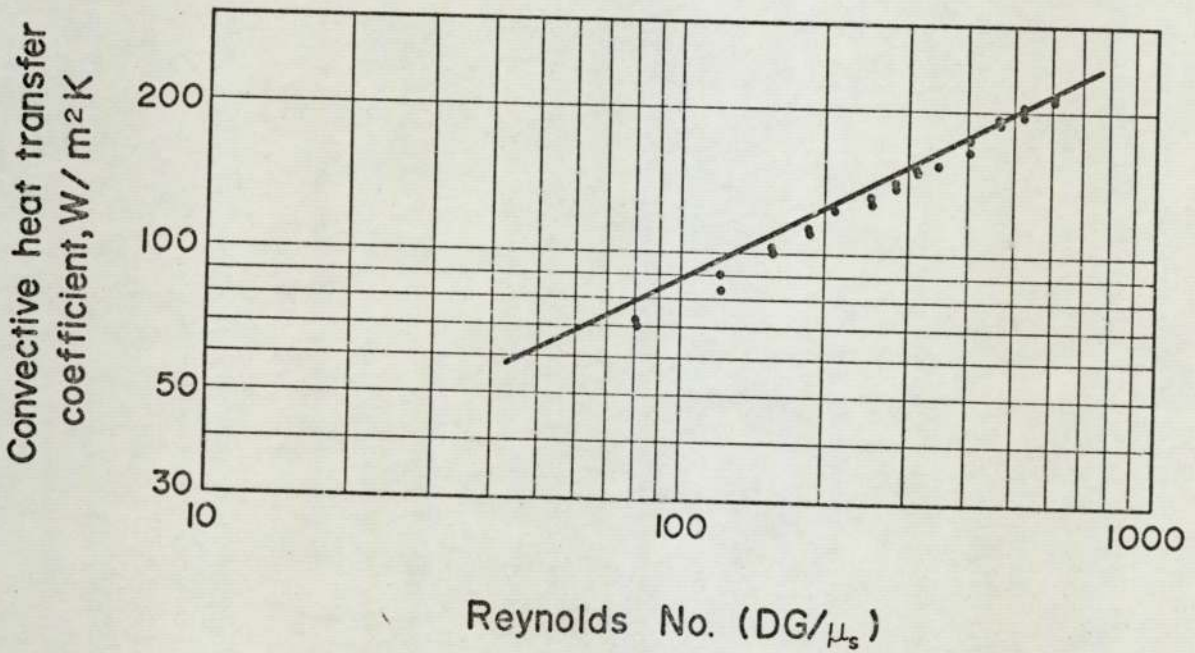


Fig 23 Stoichiometric Algerian natural gas - air

Typical data for numerical solutions  $\text{CH}_4 / \text{O}_2$  system

$T_s = 3023 \text{ K}$ ,  $T_w = 400 \text{ K}$ ,  $\text{Re}_s = 125$

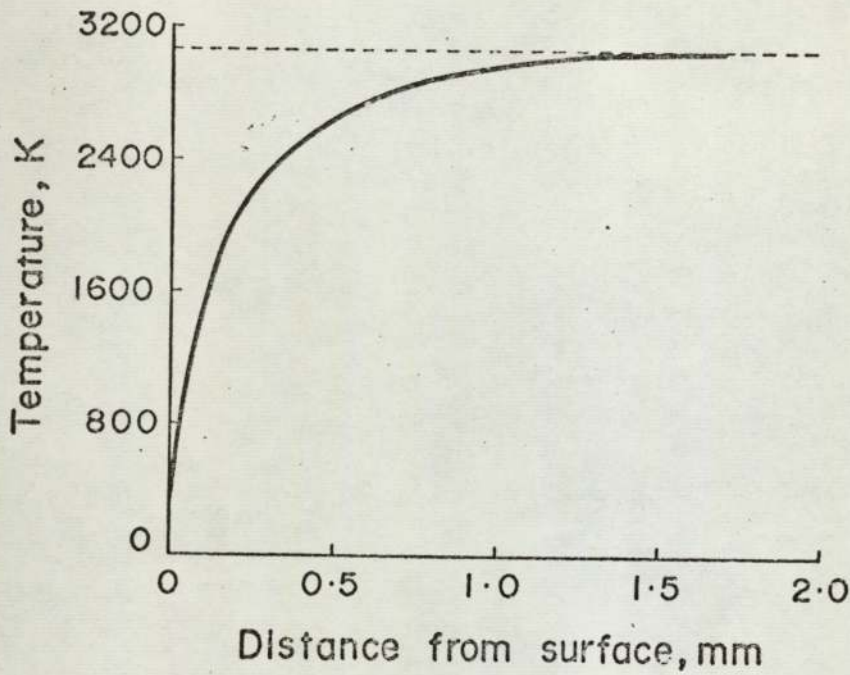


Fig. 24 Temperature profile near the stagnation point

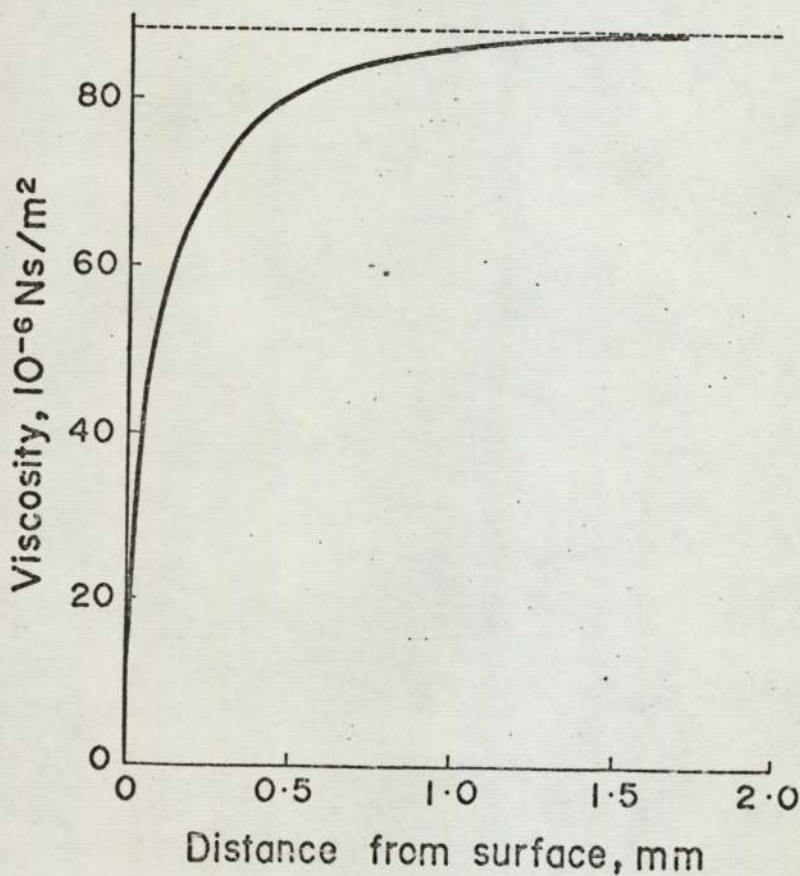


Fig. 25. Viscosity profile near the stagnation point

Typical data for numerical solutions  $\text{CH}_4/\text{O}_2$  system

$T_s = 3023 \text{ K}$ ,  $T_w = 400 \text{ K}$ ,  $\text{Re}_s = 125$

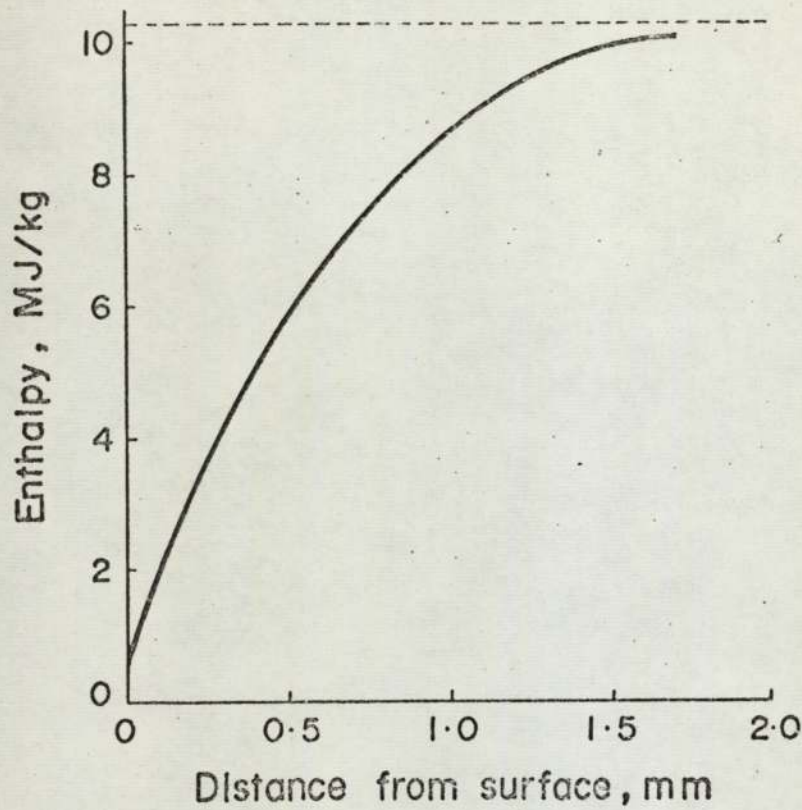


Fig 26 Enthalpy profile near the stagnation point

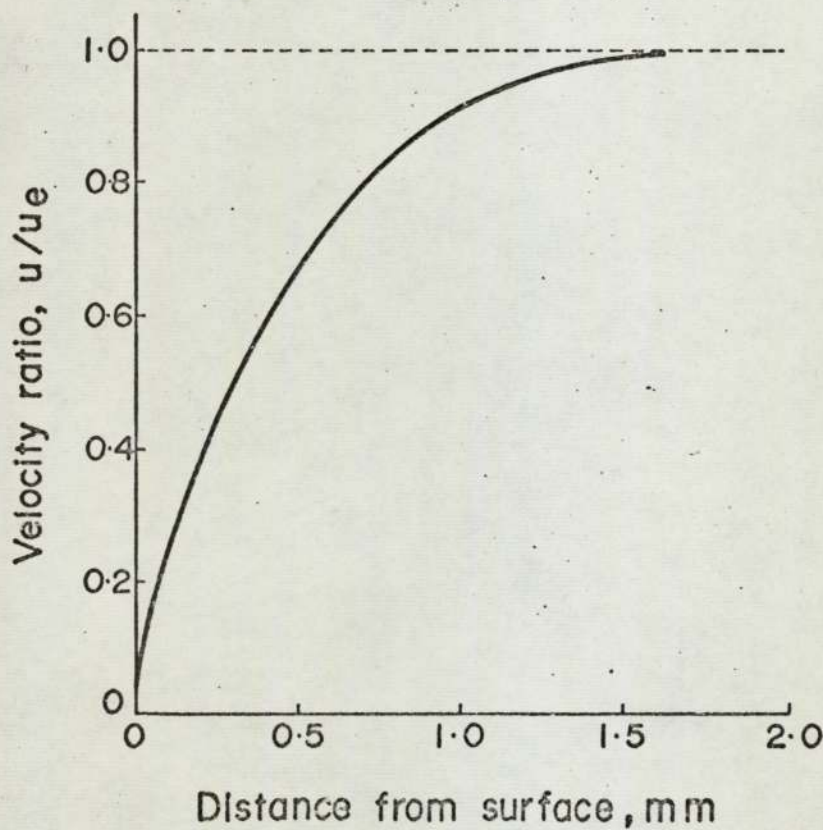


Fig. 27 Velocity profile near the stagnation point

## 6. HEAT TRANSFER TO SURFACES AT ELEVATED TEMPERATURES

It appears that satisfactory prediction of the heat transfer from high temperature flames to the stagnation point of an axially symmetrical blunt body may be obtained in two ways. The first of these is based on the empirical modification of an established relationship describing heat transfer under constant property conditions. The modifications suggested enable the effects of wide ranging variations in thermophysical properties to be incorporated into the prediction method. This has the advantage of providing for rapid estimates of stagnation point heat fluxes obtained with direct flame impingement.

The second approach features the numerical solution of the laminar boundary layer conservation equations. The assumptions necessary in the solution procedure prove to be reasonably well justified, at least for the input data encountered in the present studies. As a result the numerical solution method is more acceptable from a theoretical standpoint than the simpler empirical approach.

Unfortunately the numerical prediction of boundary layer phenomena is of rather limited application at present, and while the flow patterns and heat fluxes can be calculated for simple shapes the method is not available for aerodynamically complex situations. Since these are frequently encountered in engineering practice the provision of a simple empirical prediction method becomes especially attractive. However, the proposed modifications have only been tested under a narrow range of conditions with a clearly defined flow situation and a single low sink temperature of 400K. As a result the conclusions reached may not necessarily be appropriate to conditions where the heated surface is at an elevated temperature, nor to cases where flow separation occurs.

It was felt that a particularly useful extension of the initial studies would be an investigation of the heat transfer to surfaces at elevated temperatures. This affords a convenient means of testing the

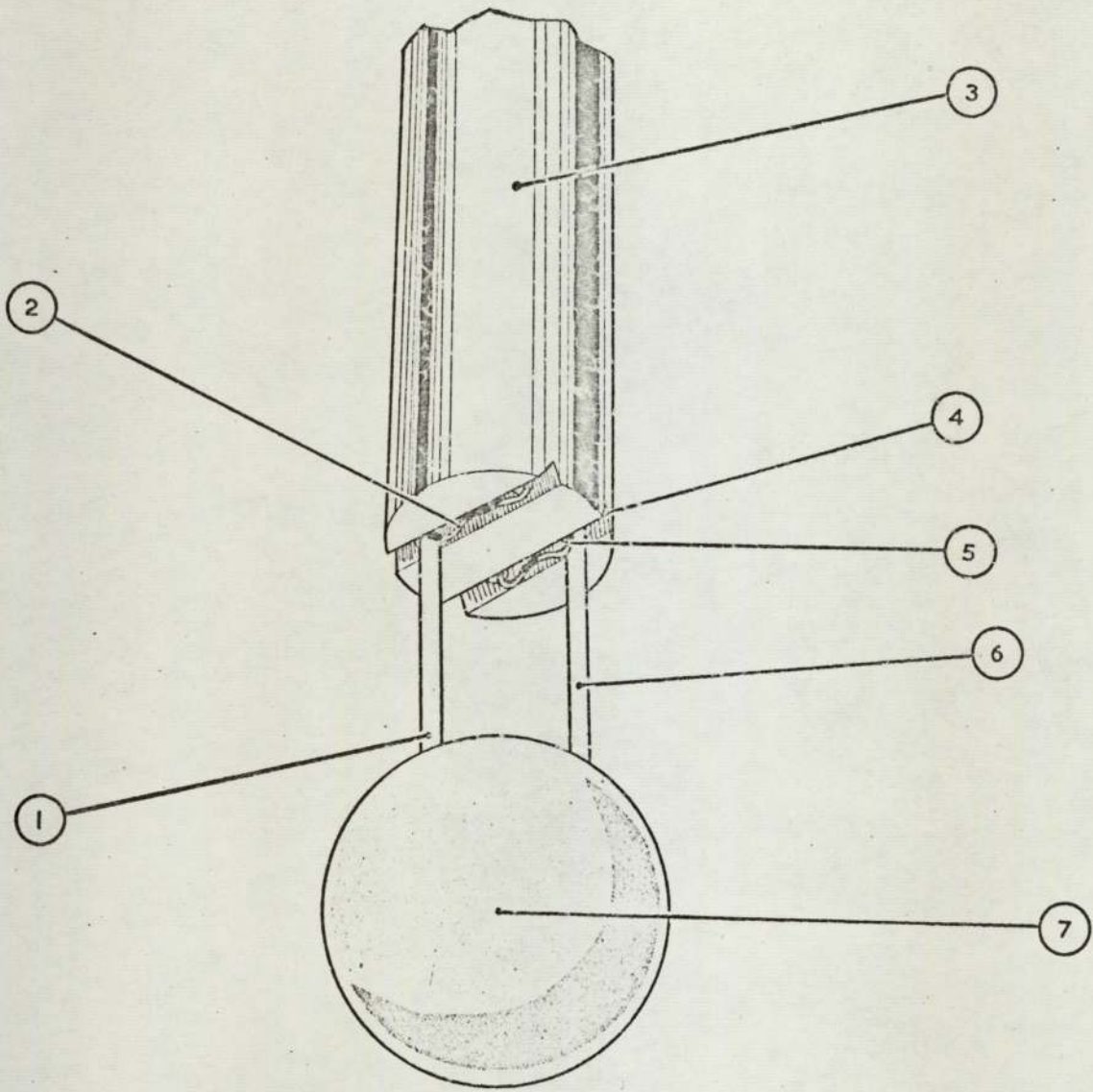
empirical prediction method over a wider range of conditions, while providing data which may have direct practical value. As many metallurgical operations are carried out at temperatures ranging to 1600K, the experimental work was taken to this level. For experimental convenience a spherical geometry was selected, which incidentally provided a situation where flow separation was known to take place.

### 6.1 Theoretical background

As pointed out previously, the energy transfer from high temperature flames arises from normal conduction processes supplemented by the diffusion and subsequent recombination of dissociated species. It is evident, from an inspection of the curves relating the equilibrium concentrations of radical species to the temperature, that little dissociation occurs in combustion products below about 2000K. As a result, the total contribution of the diffusion recombination reactions to the overall heat transfer rate remains substantially constant for surface temperatures below this level. On the other hand the contribution made by purely conductive heat transfer through the boundary layer is dependent on the temperature differentials encountered. It is therefore reasonable to expect that the effects of diffusion - recombination reactions would become progressively more important at higher surface temperatures.

Rowe, Claxton and Lewis (60) have carried out an extensive review of the published data on heat and mass transfer from isolated spheres over the Reynolds number range 10 to  $10^4$ . From this review, in conjunction with further experimental data, they have concluded that an adequate description of the overall heat transfer between spheres and an air stream at Reynolds numbers below 2000 could be obtained from the following expression

$$Nu = 2 + 0.69 Pr^{0.33} Re^{0.5} \dots (12)$$



- ① PURE PLATINUM WIRE.
- ② SILICA COATED Pt/Rh.
- ③ QUADRUPLE BORE QUARTZ.
- ④ GROOVE
- ⑤ SILICA COATED PLATINUM
- ⑥ PLATINUM 90% RHODIUM 10%
- ⑦ PURE PLATINUM SPHERE

FIG. 28 HIGH TEMPERATURE PROBE

Modification of this relationship in the manner advocated for the stagnation point studies then leads to

$$St = 2/(\overline{Re} \overline{Pr}) + 0.69 (\overline{\mu}/\mu_s) \overline{Pr}^{-0.67} Re_s^{-0.5} \quad \dots (13)$$

The predictions of convective heat transfer coefficients to spheres derived from this expression may then be compared with experimental measurements in order to assess the feasibility of modifying other well known expressions for use at high temperatures, using similar averaging procedures.

## 6.2 Experimental Work

### 6.2.1 Heat transfer coefficient measurements

The probe used in the measurement of convective heat transfer coefficients consisted of a 2.94 mm diameter sphere of pure platinum, supported by two wires (Fig. 28). These formed a Pt/Pt 10% Rh thermocouple pair which effectively monitored the surface temperature of the sphere. Firstly, the pure platinum and the alloy wires were welded together such that a length of the pure metal extended from the join. This length was then cut to provide an equivalent volume to that of the required sphere and carefully fused in an oxy-hydrogen flame. Any distortion of the bead so formed was removed by rotating slowly as the probe was gradually withdrawn from the outer edges of the flame. Finally the leads were threaded through two holes of a quadruple bore quartz tube fixed in a brass mounting block and screwed onto a double-acting pneumatic cylinder. The latter was actuated by means of a set of solenoid valves controlled by suitable timing circuits, enabling the probe to be exposed to a flame for a short period and then removed. A fixed height 12.7 mm above the burner on the axis of the flame was again chosen for all measurements. A UV recorder operated by the same circuits and capable of chart speeds of 3 m/s was used to obtain the temperature-time history of the bead during the exposure. Initially the deflection of the galvanometer

trace on the UV recorder was calibrated in terms of temperature. A variable millivolt source was connected to the input in place of the thermocouple and the deflections at given applied voltages noted. These were then converted into temperatures using standard reference tables for the particular thermocouple materials used. Details of the calculation of heat transfer coefficients and corrections for radiation losses and conduction effects are included in subsequent sections of this thesis.

### 6.2.2. Fuels and Burners

Studies of the heat transfer to the beads were undertaken in the same series of fuel-oxygen flames over a wide range of thermal throughputs. Natural gas, hydrogen, ethylene, propane and carbon monoxide were all burned with a stoichiometric supply of oxygen on the Carlisle glassworking torch employed in the stagnation point work. The multiport burner taking premixed stoichiometric natural gas-air was again included to provide a combustion product stream at a somewhat lower temperature.

### 6.2.3. Temperature and Velocity Measurements

The majority of the values of flame temperature required had already been determined for the work described earlier. Additional information, where necessary, was obtained using the method of D-line reversal against the black body radiation standard lamp.

Velocity measurement on the axes of the flames was carried out using a small water cooled total head probe, 3.6 mm in diameter.

## 6.3 Evaluation of Data

Convective heat transfer constitutes the predominant mechanism of heat input to the probe. However, minor contributions accrue from the direct radiation of the flame and from conduction along the support wires which, being of a smaller diameter, attract higher heat transfer coefficients and consequently lead the temperature of the main sphere. The convective coefficient may be deduced from the overall sensible heat gain of the bead,

making appropriate allowances for the secondary heating effects mentioned above and for radiative losses from the surface. Taking a heat balance on the spherical bead at a time  $t$  from the initial exposure:

$$\begin{aligned} \text{Net heat flow} &= \text{convected heat} && \text{conductive gain} && \text{conductive gain} \\ \text{into bead (J)} &= \text{to surface (J)} && + \text{from Pt wire (J)} && + \text{from alloy wire (J)} \\ & && - \text{radiated heat} && + \text{radiated heat} \\ & && \text{from surface (J)} && + \text{from flame (J)} \end{aligned}$$

or

$$q_{s \text{ ens}} = q_{c \text{ onv}} + q_{c2} + q_{c2} - q_r + q_r' \quad \dots\dots (14)$$

The net heat flux into the bead may be ascertained from the sensible heat gained in the course of a known temperature rise from  $(T_w - \Delta T_w/2)$  to  $(T_w + \Delta T_w/2)$  and the corresponding time interval  $\Delta t$ . This flux may then be converted into the form of an average heat transfer coefficient based on the surface area of the bead ( $A_b$ ) and the free stream and wall temperatures.

$$\text{i.e. } h_{s \text{ ens}} = \frac{q_{s \text{ ens}}}{A_b \Delta t (T_s - T_w)}$$

The other terms in Eq. (14) may similarly be converted into the form of transfer coefficients referred to the bead surface area and the free stream and wall temperatures,

$$\text{e.g. } h_{c1} = \frac{q_{c1}}{A_b \Delta t (T_s - T_w)}$$

$$\text{Then } h_{s \text{ ens}} = h_{c \text{ onv}} + h_{c1} + h_{c2} - h_r + h_r'$$

$$\text{or } \underline{h_{c \text{ onv}} = h_{s \text{ ens}} + h_r - h_{c1} - h_{c2} - h_r'} \quad \dots\dots (15)$$

### 6.3.1. Sensible Heat Gain

From the known temperature rise of the platinum surface, together with specific heat and density information supplied by the National Physical Laboratory, an initial estimate of a transfer coefficient associated with

the sensible heat gain was made. Initially temperature uniformity within the sphere was assumed, a first approximation to the prevailing heat transfer coefficient to the surface,  $h$ , being determined from

$$h = \frac{\pi D^3 \rho_b C_{pb} \Delta T_w}{6 (T_s - T_w) \Delta t}$$

By considering the original sphere to consist of a series of isothermal concentric shells, a transient heat balance equation was then set up. The temperature of each successive layer was computed as a function of the time from initial exposure and the time required for the surface temperature to achieve the measured rise from  $(T_w - 100)$  to  $(T_w + 100)$  determined for the particular value of  $h$  and the relevant flame temperature.

Repeating the procedure at slightly differing values of  $h$  (e.g.  $h + 20$ ,  $h - 20$  etc.) enabled a plot of the time for the given temperature rise to be made for the various  $h$ . The value of the sensible heat term  $h_{sens}$  was then read from this graph at the experimentally determined time interval. It is important to note that the mathematical analysis of the thermocouple response was carried out with the assumption of a uniform heat transfer coefficient over the whole of the exposed surface. In practice considerable variations in the magnitude of the local heat transfer coefficients are found. The existence of such variations is unlikely to have any significant effect on the accuracy of the calculations since only very small temperature gradients were predicted within the sphere, even at the highest heat transfer rates. Thus heat dissipation through the solid appears to be very rapid.

### 6.3.2. Conduction Gain from the Support Wires

A set of experimental measurements was carried out to estimate the magnitude of the heat flow to the sphere from the support leads.

Supplementary fine thermocouple leads were attached at known distances from the bead as shown in Fig. 28. These additional wires were led through the remaining bores of the quartz sheath and formed Pt/Pt 10% Rh

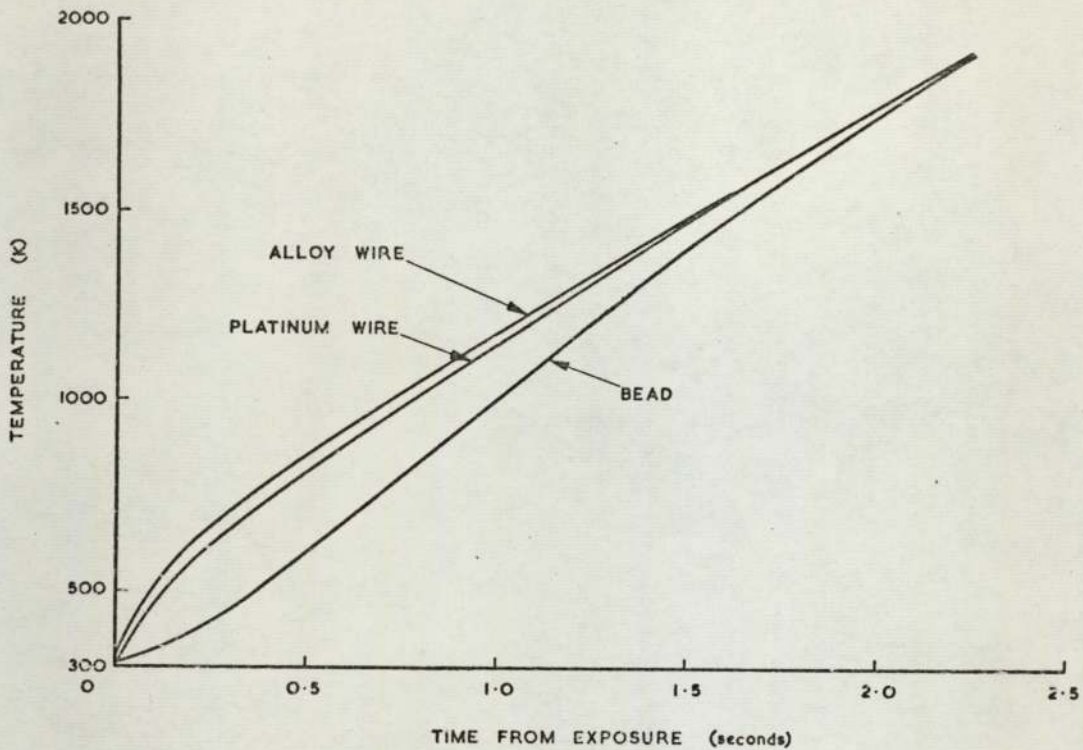


FIG. 29 TYPICAL RESPONSE OF BEAD THERMOCOUPLE PROBE.

thermocouple pairs with the main wires.

The temperature versus time curves for each junction were obtained at a series of heating rates covering the entire experimental range of heat transfer coefficients. Typified by Fig. 29, both these curves and that corresponding to the surface temperature of the bead remain substantially linear over temperature intervals of about 200 K in the required sink temperature range of 500 - 1600 K. Thus the conduction heat gains corresponding to the various measured time intervals were determined from the known dimensions of the main wires, their mean thermal conductivities over the temperature range in question and the average temperature differentials. The estimated total heat gain over the period  $\Delta t$  was then converted to an appropriate heat transfer coefficient from the knowledge of the bead surface area and the temperature of the flame and sink. These coefficients are designated  $h_{c1}$  and  $h_{c2}$  for the platinum and alloy wires respectively.

### 6.3.3. Direct Flame Radiation

Contributions to heat transfer from this source are small and have been ignored throughout, i.e.  $h_r' = 0$

### 6.3.4. Radiation Losses

For a surface at a temperature  $T$  radiating to an enclosure at  $T_R$ , the net rate of energy output is given by the expression

$$\frac{dq}{dt} = FA\epsilon\sigma (T^4 - T_R^4)$$

In the experimental work, however, the value of  $T$  is permitted to rise through 200 K so that due allowance for the progressively increasing rate of heat loss by radiation during the time interval  $\Delta t$  must be made. An effective value of  $\epsilon (T^4 - T_R^4)$  may be defined by

$$[\epsilon (T^4 - T_R^4)]_{av} = \frac{1}{\Delta t} \int_{t_1}^{t_2} (\alpha + \beta T)(T^4 - T_R^4) dt$$

since  $\epsilon = \alpha + \beta T$  where  $\alpha, \beta$  are constants over the temperature range considered. However, the rate of temperature rise remains virtually constant over the relevant time interval so that

$$[\epsilon (T^4 - T_R^4)]_{av} = \frac{1}{T_2 - T_1} \int_{T_1}^{T_2} (\alpha + \beta T)(T^4 - T_R^4) dT$$

For an object radiating to a room  $F = 1$ , so that the averaged rate of heat output is given by

$$\frac{dq}{dt} = A\sigma \frac{1}{T_2 - T_1} \int_{T_1}^{T_2} (\alpha + \beta T)(T^4 - T_R^4) dT$$

which leads to the expression for the effective correction, due to radiation, to the coefficient calculated from the sensible heat gain being

$$h_r = \frac{5.71 \times 10^{-3}}{(T_s - T_w)(T_2 - T_1)} \int_{T_1}^{T_2} (\alpha + \beta T)(T^4 - T_R^4) dT \dots (16)$$

Expression (16) has been evaluated for each of the measured temperature rises using emissivity data for platinum supplied by the National Physical Laboratory.

### 6.3.5. Convective Heat Transfer Coefficient

As described above, the convective heat transfer coefficient is derived from that referring to the sensible heat gain of the bead in conjunction with allowances for radiation and conduction effects.

$$h_{conv} = h_{sens} + h_r - h_{c1} - h_{c2}$$

In the majority of cases the total adjustment to the sensible heat term proves to be quite small. In the case of heat transfer from a typical stoichiometric hydrogen-oxygen flame burning 1.5 cubic metres of fuel per hour to a surface at 1200 K the values of the respective terms are

$$h_{sens} = 1095 \quad \text{W/m}^2 \text{K}$$

$$h_r = 7.4 \quad \text{W/m}^2 \text{K}$$

$$h_{c1} = 21.6 \quad \text{W/m}^2 \text{K}$$

$$h_{c2} = 10.8 \quad \text{W/m}^2 \text{K}$$

giving  $h_{conv}$  to be 1070 W/m<sup>2</sup>K at  $T_w = 1200$  K and  $Re_s = 24.0$ .

Although the contribution of each term depends on the sink temperatures involved the corrections always remain a small proportion (invariably less than 10% and usually only 2 - 3%) of the convective heat transfer coefficient.

### 6.4 Verification of the experimental method used

The expression derived by Rowe, Claxton and Lewis is strictly applicable to the heat transfer between isolated spheres and an extensive flowing medium. The experimental arrangement used in the studies on flames clearly represents but a crude approximation to this ideal. As a result it was considered essential to check whether or not the support wires had any appreciable effects on the flow pattern around the sphere and whether the corrections for the subsidiary heating effects were reasonable.

The first of these questions was resolved satisfactorily by the use

of flow visualisation techniques. The hydrogen bubble method was chosen for convenience since the necessary equipment was already available on the premises. A sheet of minute bubbles of hydrogen was generated by the application of an electrical potential between a wire and a second electrode immersed in a dilute solution of sodium hydroxide. The wire was made the cathode and stretched above a flat table over which a steady flow of the conducting fluid was pumped. Scaled up models of the probe and an isolated sphere were suspended in the fluid and the flow pattern observed using the bubbles as tracers. Virtually no differences in the flow over the bead surfaces were detected.

The validity of the established heat transfer relationship when applied to the experimental configuration was established by a check on the performance of the probe when exposed to an air stream having a particularly uniform velocity profile. This was generated by a specially contoured nozzle fitted to the end of a long cylinder. The cylinder was packed with material designed to reduce turbulence to the negligible proportions demanded for the calibration of hot wire anemometers. It was found that the heat transfer from a cooling probe corresponded to that predicted from the modified expression. (In practice the temperature differences were sufficiently small that the modifications had virtually no effect on the predictions derived <sup>from</sup> the original expression).

## 7. RESULTS OF STUDIES AT ELEVATED SURFACE TEMPERATURES

### 7.1 Comparison with the empirical prediction method

Experimental data have been obtained for heat transfer from the range of flames produced by the stoichiometric combustion of each of the available fuels with pure oxygen. In addition a premixed natural gas-air flame was included. Sink temperatures of 500, 800, 1200 and 1600K have been covered for each of the fuel-oxygen combinations, although the highest of these was omitted in the studies with the natural gas-air flame. In this case very low rates of temperature rise were encountered and large percentage corrections for radiative losses were necessary, thereby reducing the reliability of the measurements. The results are collected in Figs. 30 to 36, where the net convective coefficients to the probe are plotted over the full experimental range of free stream Reynolds numbers.

Predicted convective heat transfer coefficients have been evaluated from Eq. (13), the modified version of the expression recommended by Rowe, Claxton and Lewis. Measured flame temperatures have been used in the calculation of the requisite data on thermophysical properties and the resulting predictions have been included on the plots of the experimental data. It can be seen that tolerably good agreement is obtained for all fuels and surface temperature levels.

HEAT TRANSFER COEFFICIENT ( $W/m^2 K$ )

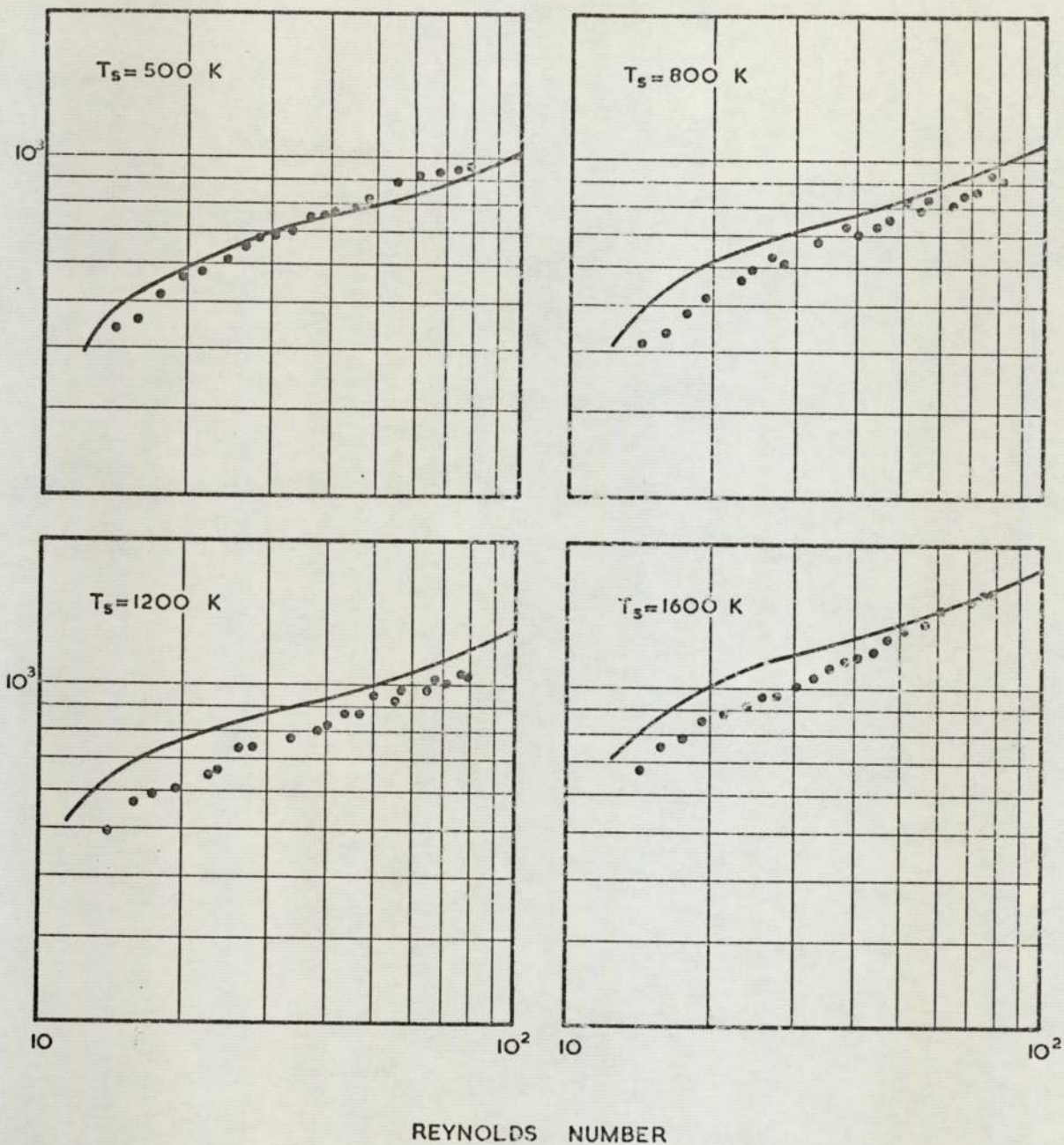
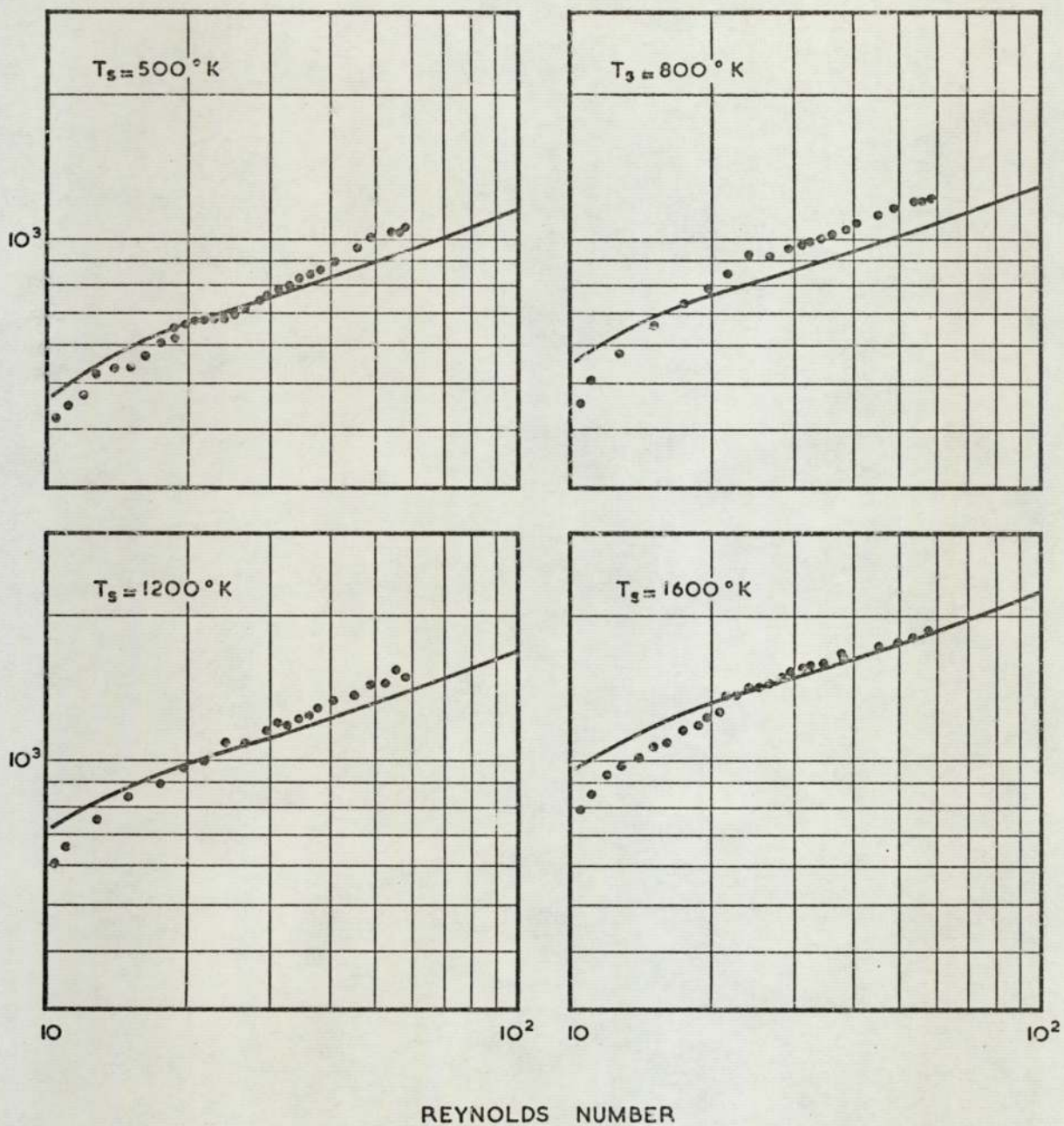


FIG.30 CONVECTIVE HEAT TRANSFER FROM A STOICHIOMETRIC NATURAL GAS OXYGEN FLAME AT A RANGE OF SINK TEMPERATURES.



REYNOLDS NUMBER

FIG. 31 CONVECTIVE HEAT TRANSFER FROM A STOICHIOMETRIC HYDROGEN OXYGEN FLAME AT A RANGE OF SINK TEMPERATURES.

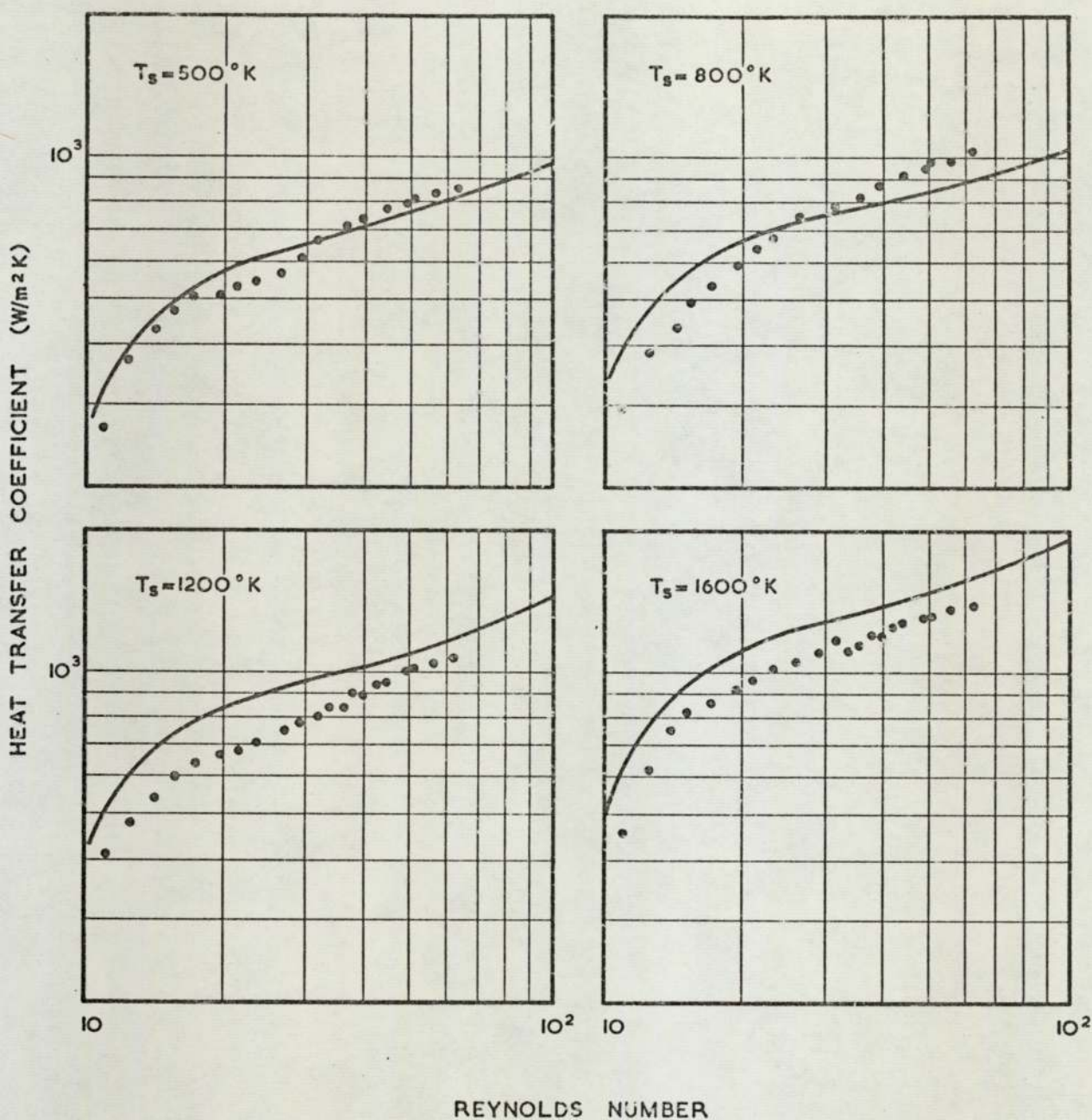


FIG. 32 CONVECTIVE HEAT TRANSFER FROM A STOICHIOMETRIC ETHYLENE OXYGEN FLAME AT A RANGE OF SINK TEMPERATURES.

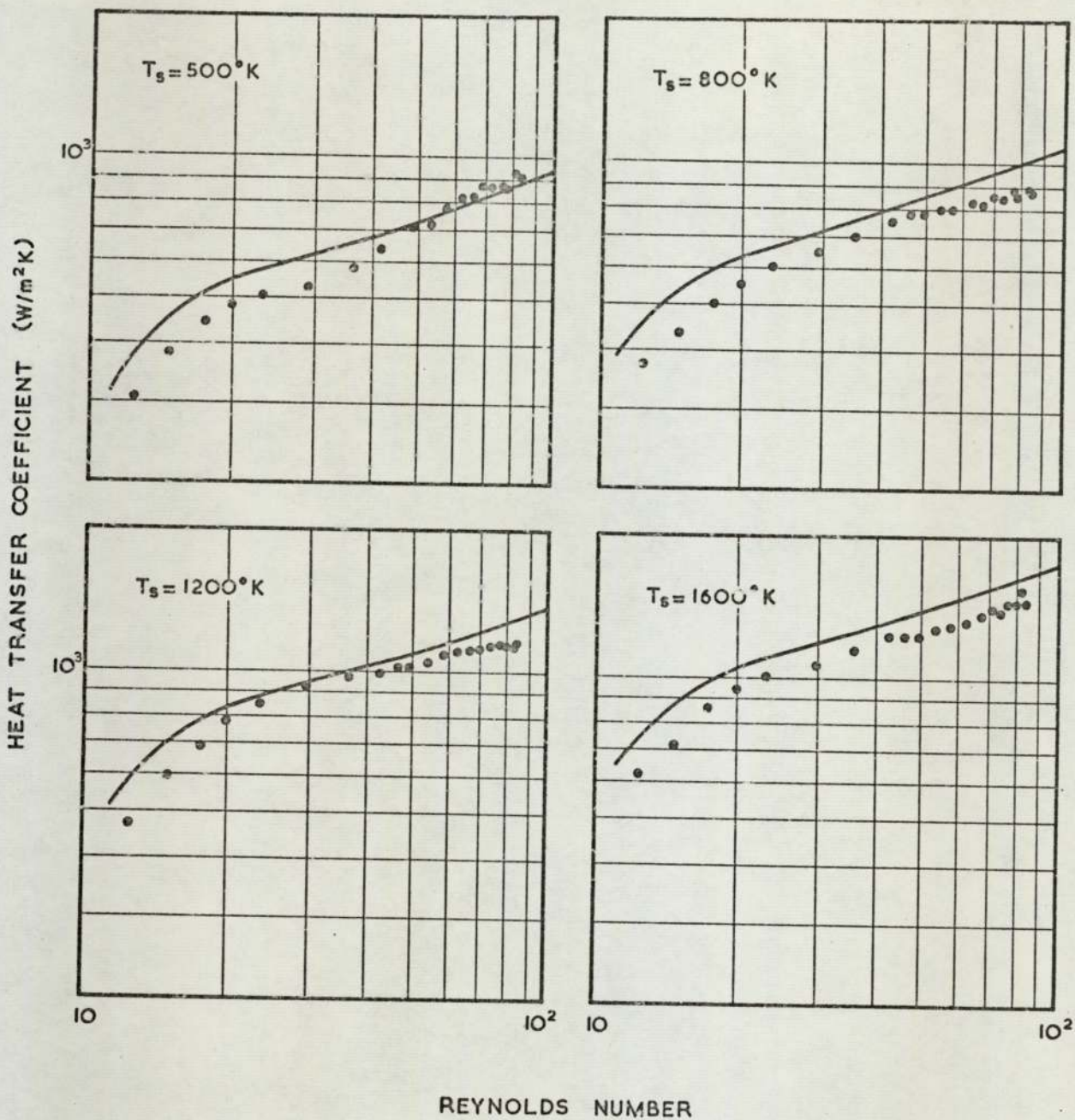


FIG. 33 CONVECTIVE HEAT TRANSFER FROM A STOICHIOMETRIC PROPANE OXYGEN FLAME AT A RANGE OF SINK TEMPERATURES.

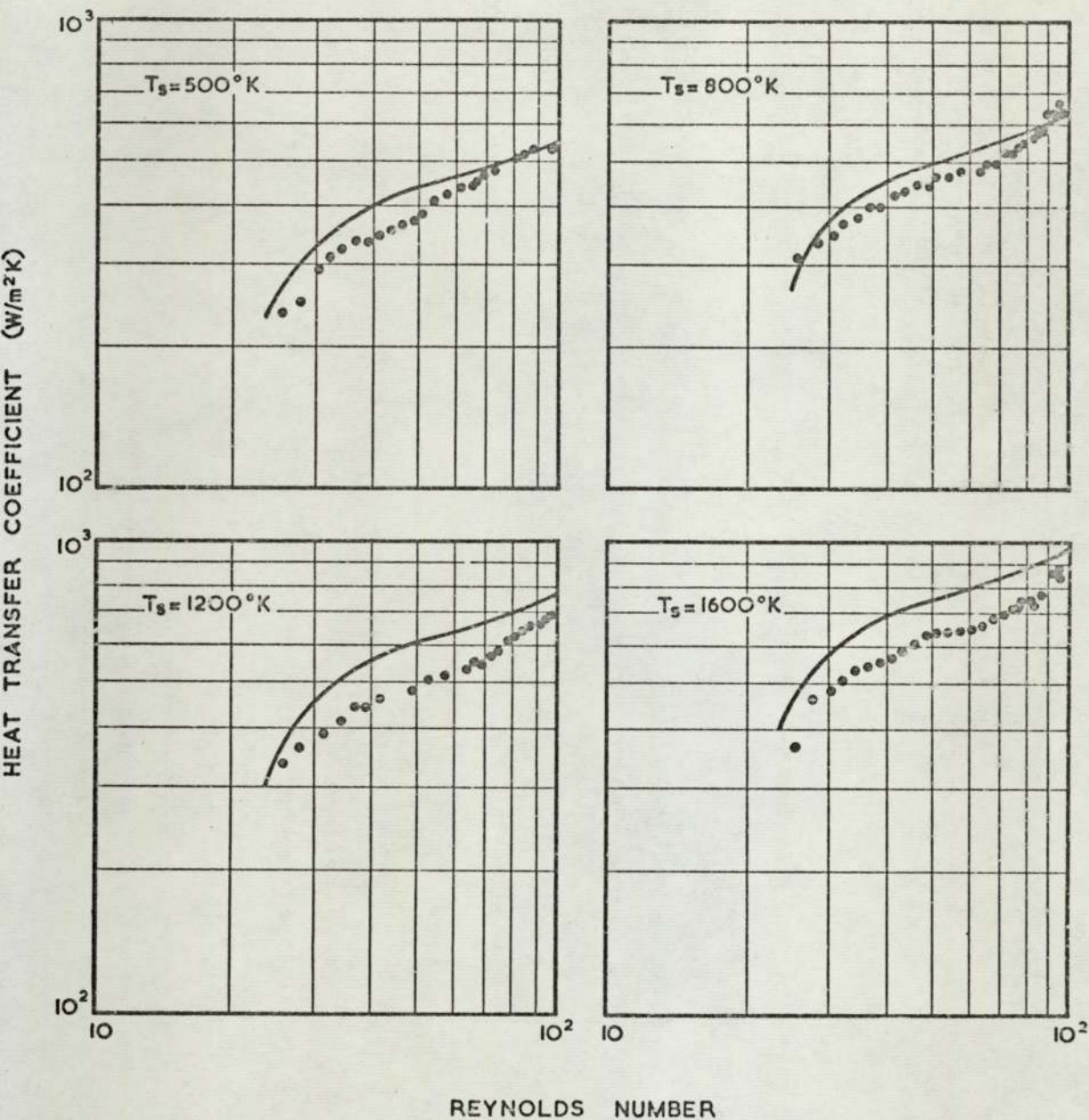


FIG. 34 CONVECTIVE HEAT TRANSFER FROM A STOICHIOMETRIC CARBON MONOXIDE -  $\text{O}_2$  FLAME AT A RANGE OF SINK TEMPERATURES.

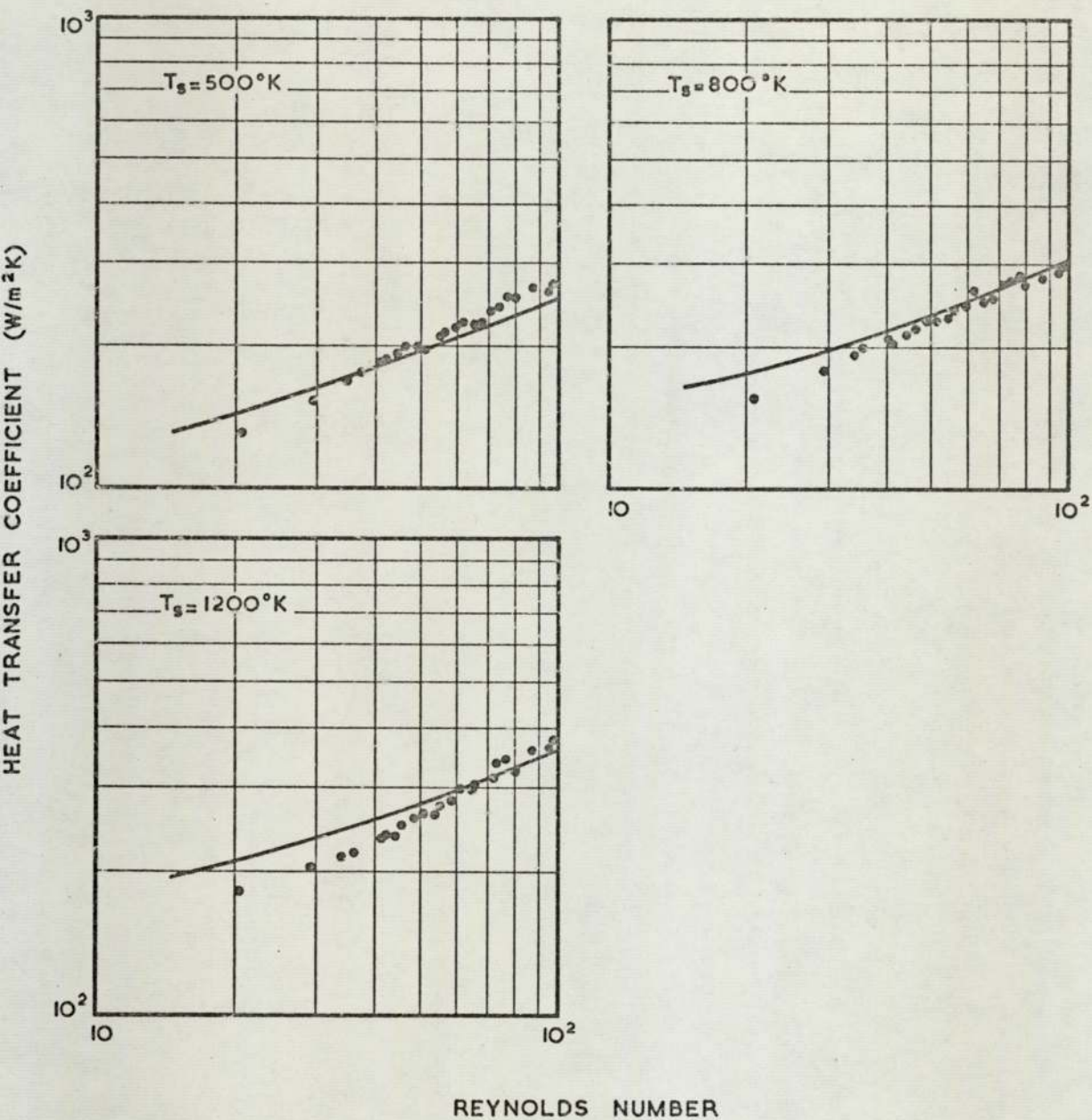


FIG. 35 CONVECTIVE HEAT TRANSFER FROM A STOICHIOMETRIC NATURAL GAS AIR FLAME AT A RANGE OF SINK TEMPERATURES.

HEAT TRANSFER COEFFICIENT ( $W/m^2K$ )

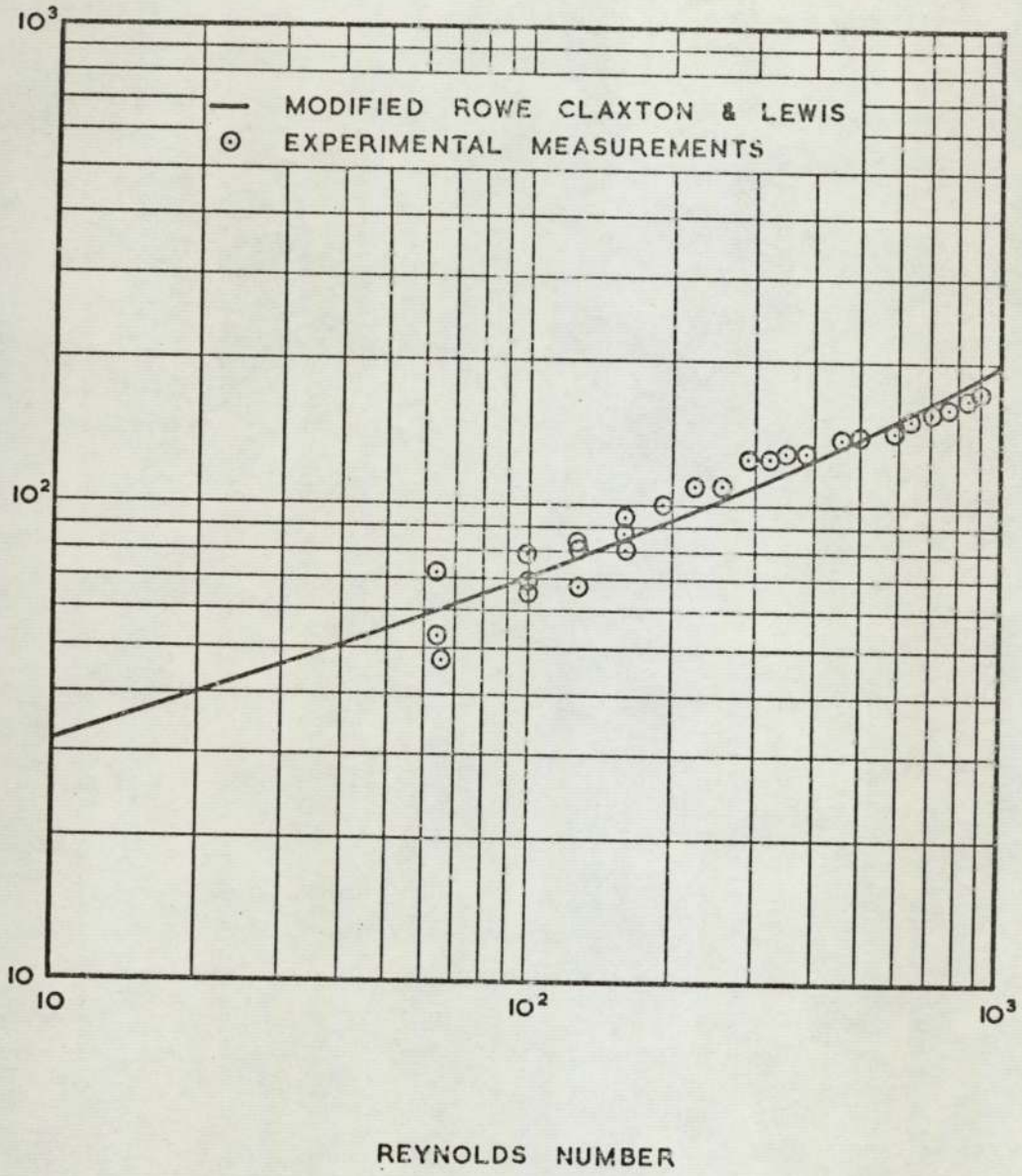


FIG. 36 MEASURED AND PREDICTED HEAT TRANSFER FROM THE BEAD THERMOCOUPLE PROBE AT  $400^{\circ}K$  TO A COLD AIR STREAM.

## 8. ALTERNATIVE CORRELATION PROCEDURES

Although it has already been shown that many of the simple methods for the prediction of heat transfer are likely to break down if applied to combustion systems, it is essential to verify that this is the case. It is abundantly clear that the straightforward methods of correlation using bulk, wall or mean film conditions fail completely when applied to heat transfer data obtained in flames. However, there is no justification for rejecting the remainder out of hand. These have been examined for two reasons. The first of these has been to estimate the degree of error associated with the use of traditional methods and the second to assess the feasibility of introducing further improvements.

### 8.1 Methods used for dissociated air - Fay and Riddell

The early work by Fay and Riddell forms the backbone of the theory of heat transfer from dissociated air. In view of the similarities with the problem encountered in combustion product mixtures it seems worthwhile to compare the relationships proposed for the two cases. The expressions are respectively

$$\dot{q} = 1.32 Pr_f^{-0.6} \left[ 1 + (Le^{0.52} - 1) \frac{\Delta H_{chem}}{H_g} \right] \left( \frac{\rho_w \mu_w}{\rho_s \mu_s} \right)^{0.1} Re_s^{-0.5} G \Delta H \quad \dots (17)$$

and

$$\dot{q} = 1.32 Pr_{eq}^{-0.6} \left( \frac{\bar{\mu}}{\mu_s} \right) Re_s^{-0.5} G \Delta H \quad \dots (18)$$

Apart from the fact that the use of equilibrium Prandtl numbers is probably more realistic a second point arises with the two terms represented by  $(\rho_w \mu_w / \rho_s \mu_s)^{0.1}$  and  $(\bar{\mu} / \mu_s)$ . The first of these carries a low valued exponent and lies close to but greater than unity over a wide range of wall and free stream conditions. This stems from the fact that the variations of density and viscosity with temperature are

in opposite directions for gases. With combustion products the correction factor  $(\rho_w \mu_w / \rho_s \mu_s)^{0.1}$  appears to act in the opposite direction to that expected for a stagnation point situation but is so close to unity that its effect on predictions is marginal. On the other hand the assumption of constant Lewis and Prandtl numbers is a more serious limitation since this renders the heat transfer coefficients derived from Eq. (17) less sensitive to temperature than those obtained from Eq. (18). The effect of this is shown by Fig. 37 which shows how a correlation based on the general form of Fay and Riddell's recommendations would be inadequate for heat transfer at elevated surface temperatures. The data used in this figure are those obtained for heat transfer to the bead thermocouple probe. Although this is not strictly comparable with stagnation point heat transfer the dependence on Reynolds number is the same in both cases so that similar trends are likely.

It can be seen from Eq. (17) that the quantity  $\dot{q} / (\rho_w \mu_w / \rho_s \mu_s)^{0.1} \Delta H$

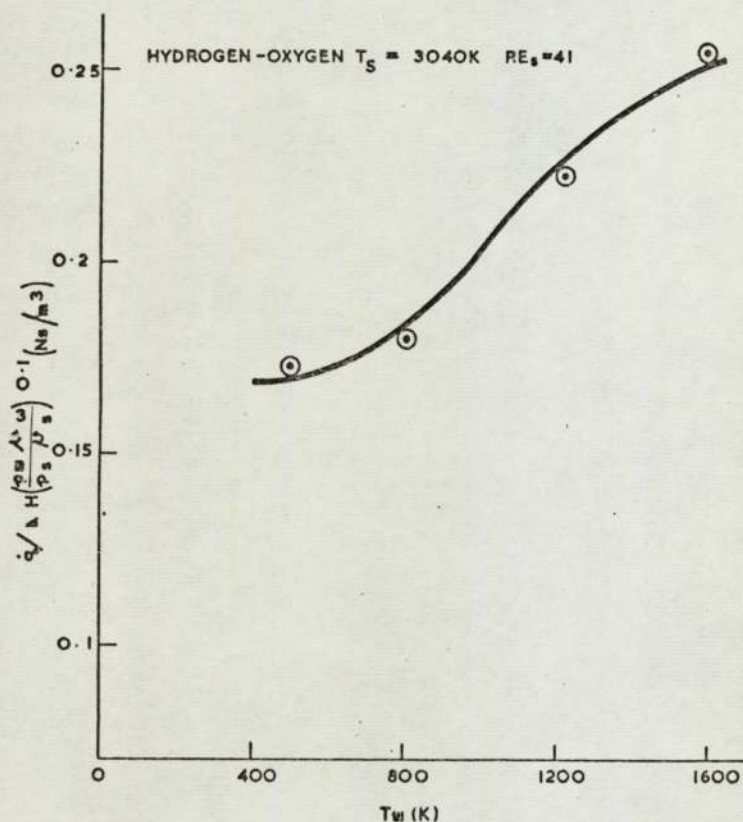


FIGURE 37 COMPARISON OF DATA FOR HIGH SINK TEMPERATURES WITH THE FORM OF PREDICTION RECOMMENDED BY FAY AND RIDDELL

should be largely independent of surface temperature for prescribed free stream conditions but this is not borne out by the data presented above.

Furthermore, an examination of the results for stagnation point heat transfer has shown that a satisfactory fit to the experimental data could only be achieved by providing for the exponent of the density-viscosity term to be specific to particular fuels. This fact, in conjunction with the observed dependence on sink temperature, leads to the conclusion that the semi-empirical prediction methods available for dissociated air cannot readily be adapted to combustion systems.

### 8.2 Methods used for Hydrogen and Helium - Taylor

The method shown to be successful for the prediction of heat transfer to precooled gases demands the use of gas properties evaluated at the mean film temperature and the attachment of a temperature ratio term directly to the Reynolds Number

Applying these methods to Sibulkin's stagnation point equation we have  $Nu^* = 1.32 (Re^*)^{0.5} (T_s/T^*)^{0.5} (Pr^*)^{0.4}$

giving

$$h = (1.32/D) C_p^* \mu^* Pr^{*-0.6} (T_s/T^*)^{0.5} (Re^*)^{0.5}$$

or

$$St^* = 1.32 (Pr^*)^{-0.6} (\mu^*/\mu_s)^{0.5} (T_s/T^*)^{0.5} Re_s^{-0.5} \dots (19)$$

The experimental values of  $St^*$  have been evaluated from Eq. (19) and are plotted against the above expression in Fig. 38. While reasonably good agreement is obtained with the results for the five fuel-oxygen flames, it is clear that the correlation procedure is unsuitable with the lower temperature natural gas-air results. This again contrasts with the weighted average form which successfully describes the heat transfer process for the whole range of fuel-oxidant combinations.

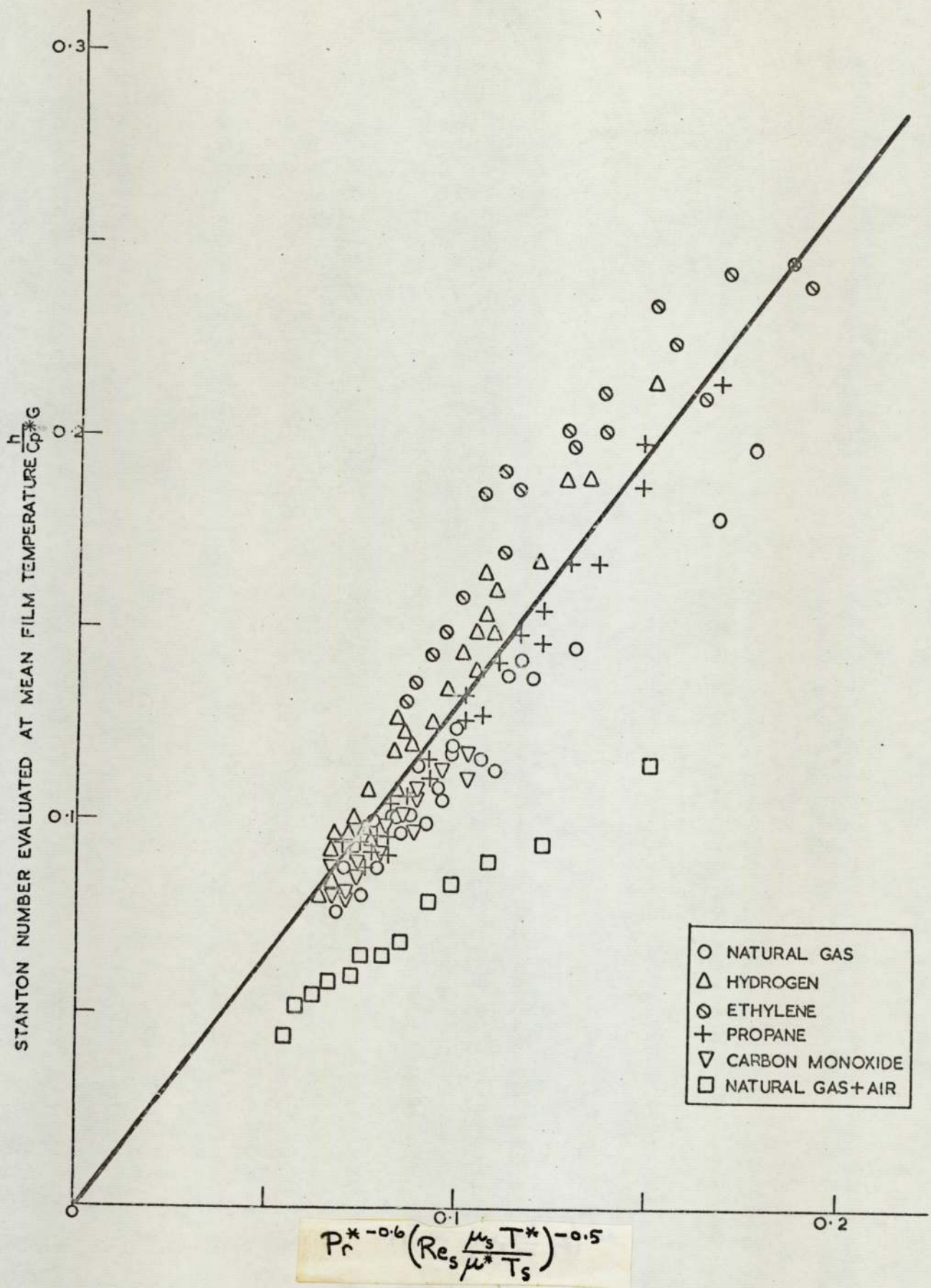


FIGURE 38. GENERALISED PLOT OF STAGNATION POINT HEAT TRANSFER DATA. THE CONTINUOUS LINE REPRESENTS M.F. TAYLOR'S FORM OF CORRELATION EQUATION.

Similarly it can be shown that Taylor's prediction method does not adequately represent the heat transfer coefficients measured with platinum beads at elevated surface temperatures.

In view of the uncertain nature of the dependence on temperature ratio further comparisons were made for heat transfer from combustion products in the stagnation point case. Because of the excellent agreement between the numerical solutions and the experimental work with stoichiometric methane-oxygen combustion products it was considered expedient to extend the range of wall and free stream temperatures for this combination. Numerical solutions were obtained for temperatures ranging from 400 to 2000 and 2200 to 3000K respectively, a constant value of free stream Reynolds number being used for all of the calculations. Nusselt numbers were then obtained by reference to the appropriate body dimension and the free stream thermal conductivity. The values produced were normalised against the corresponding constant property solutions and are plotted for various temperature ratios in Fig. 39.

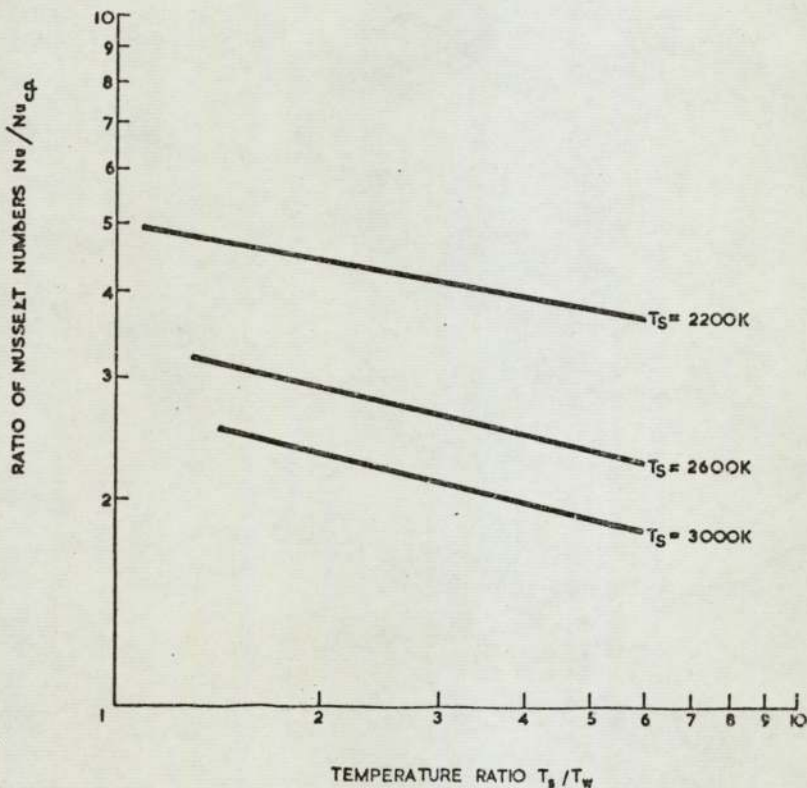


FIGURE 39 A COMPARISON OF NUSSELT NUMBERS DERIVED FROM NUMERICAL SOLUTION WITH THOSE FROM A CONSTANT PROPERTY RELATIONSHIP FOR STAGNATION POINT HEAT TRANSFER

Although it is evident that the relationship between the Nusselt numbers and the temperature levels is rather complex certain conclusions may be drawn. Firstly it appears that some influence of the actual flame temperature is superimposed on the effects of temperature ratio. For given free stream conditions the Nusselt numbers are related to the latter in the form of a dependence on  $(T_w/T_s)^{0.2}$ , this holding over a wide range of wall temperatures. However, the influence of the actual free stream temperature is quite marked so that the use of a simple temperature correction term does not seem to be very profitable.

### 8.3. The Use of Approximations Involving Hydrogen Atom Lewis Numbers

It has been suggested that, in certain circumstances, considerable simplifications to the methods of predicting heat transfer from dissociated gas streams can be made. By considering that hydrogen atoms are solely responsible for the additional heat transfer resulting from diffusion and recombination effects equilibrium Prandtl numbers can be calculated very simply from

$$Pr_{eqH} = Pr_f [1 + (Le_H - 1) \Delta H_{chem H} / \Delta H]^{-1}$$

In hydrogen combustion products such an assumption is not altogether unreasonable and at least for preliminary estimates of heat flux can be quite useful. This is shown by Table 6 which compares the values of Prandtl numbers based on hydrogen atom diffusion with those taking full account of the contributions to heat transfer arising from the recombination of other dissociated species.

Table 6 : A Comparison of Equilibrium Prandtl Numbers Calculated Using  
H - Atom Lewis Numbers with Those Obtained from Equilibrium  
Thermal Conductivity Data

Stoichiometric Hydrogen Oxygen Combustion Products

Temperature (K)	$Pr_{eqH}$	$Pr_{eq}$	$Pr_{eq}/Pr_{eqH}$
1800	0.738	0.7010	0.950
2000	0.710	0.6655	0.938
2200	0.677	0.6165	0.911
2400	0.628	0.5615	0.894
2600	0.562	0.5106	0.909
2800	0.487	0.4711	0.967
3000	0.438	0.4466	1.020

Stoichiometric Methane Oxygen Combustion Products

Temperature (K)	$Pr_{eqH}$	$Pr_{eq}$	$Pr_{eq}/Pr_{eqH}$
1800	0.6833	0.6648	0.972
2000	0.6626	0.6315	0.953
2200	0.6476	0.5999	0.926
2400	0.6183	0.5606	0.907
2600	0.5529	0.5156	0.932
2800	0.4749	0.4693	0.988
3000	0.4223	0.4328	1.025

However, it can be seen that the use of approximate Lewis numbers restricted solely to hydrogen atom diffusion leads to differences in the value of the equilibrium Prandtl number when compared to the best available method of calculation. These differences can amount to over

10% for some temperature levels although the average error over the normal range between flame and sink temperatures will be rather less than this figure.

Fortunately, it is frequently the case that the heat transfer rate predicted from semi empirical equations is dependent on the Prandtl number raised to some power. In most cases an exponent between -0.6 and -0.7 is quoted so that the influence of the Prandtl number term is much reduced. As a result the use of H-atom Lewis numbers has certain advantages especially when rapid practical estimates of heat flux are required for a system where thermophysical properties have not already been calculated. However, when attempting theoretical comparisons it is always advisable to make use of the best available information even though its acquisition may be rather more tedious.

From the table above it would appear that the use of Rosner's prediction method for stagnation point heat transfer

$$\dot{q} = 1.32 Pr_f^{-0.6} Re^{-0.5} G \Delta H [1 + (Le_H - 1) \Delta H_{chem} / \Delta H]^{0.6} \dots (2)$$

would give quite satisfactory estimates in combustion systems provided that the Prandtl and Lewis numbers be averaged over the requisite temperature range and the Reynolds number term be defined as  $Re_s^{-0.5} (\bar{\mu} / \mu_s)$ . The expression then closely resembles that of the 'weighted average' method and naturally provides for very similar estimates of heat flux.

## 9. HEAT TRANSFER FROM NON-STOICHIOMETRIC FLAMES

Following the success of the numerical solution and weighted average methods in predicting the heat transfer from stoichiometric combustion products, a similar comparison was undertaken using flames to which an excess of fuel or oxygen was supplied. This was felt to be of practical significance since in many industrial heating operations it is customary to run burners somewhat fuel-rich.

Theoretical studies were carried out in the case of heat transfer from both hydrogen-oxygen and methane-oxygen flames with direct comparisons with experimental measurements being possible for the latter. Similar experimental work was attempted using the hydrogen-oxygen system but it was found that the burner design available could not be operated satisfactorily over sufficiently wide ranges of mixture compositions. This appeared to be connected in some way with the mixing process at the burner head which became progressively less efficient as the ratio of hydrogen to oxygen departed from stoichiometric. The poor mixing was shown up by the addition of sodium carbonate used in temperature measurement with the line reversal equipment. Dark regions were apparent which became of significant proportions with both fuel-rich and oxygen-rich mixtures. These regions did not appear to be nearly so extensive with methane combustion.

### 9.1. Hydrogen-Oxygen System

The availability of Svehla's calculated thermodynamic and transport property data for hydrogen-oxygen combustion products prompted the numerical solution of the boundary layer equations for a range of mixture compositions. Both fuel-rich and oxygen-rich flames were covered, taking unburnt compositions of 5, 8.5, 11.19, 12.5 and 15% hydrogen by weight. These correspond to values of the equivalence

ratio, E, lying between 0.4177 and 1.4006. This quantity gives a measure of the departure from stoichiometric combustion and is defined by the ratio

$$E = \frac{(H_2/O_2)}{(H_2/O_2)_{stoich}}$$

It therefore takes a value greater than unity where an excess of fuel is present but remains less than unity for oxygen-rich mixtures.

An arbitrary figure for the free stream Reynolds number was selected and numerical solutions obtained using both frozen and equilibrium values for the Prandtl number. The free stream conditions were referred to the adiabatic flame temperature, with heat transfer to a sink at 600K. This provided an opportunity for a direct comparison to be made with the semi-empirical approach suggested by Rosner (61). The two numerical solutions incorporate the assumptions of unit Lewis number and the

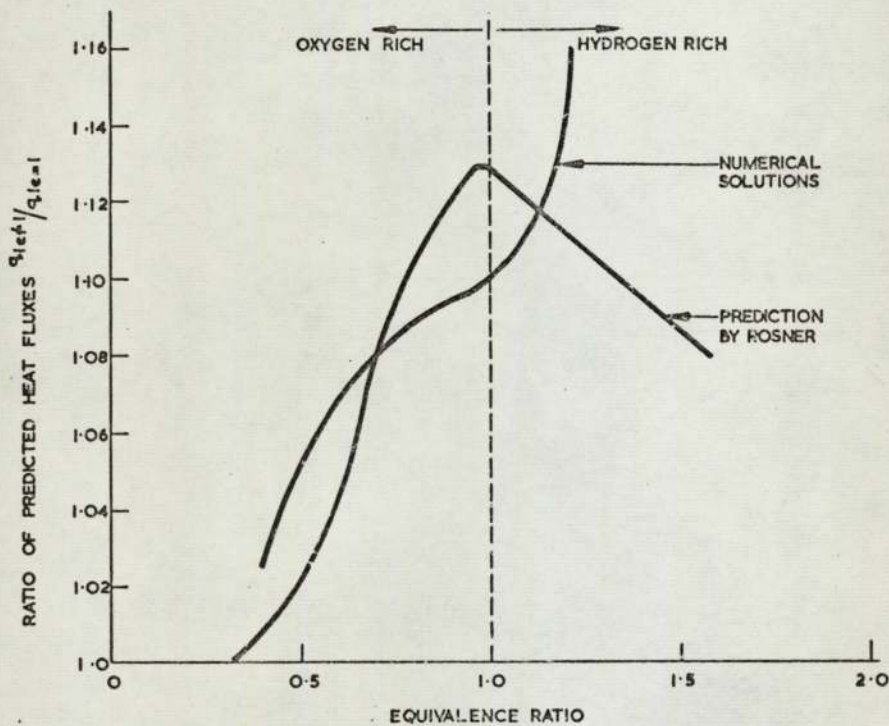


FIGURE 40 A COMPARISON OF PREDICTED NON-UNITY LEWIS NUMBER EFFECTS FOR THE HYDROGEN OXYGEN SYSTEM AT A WALL TEMPERATURE OF 600 K

variable non-unity case respectively. Rosner has estimated that the level of convective heat transfer from hydrogen oxygen flames would be significantly higher for predictions employing true Lewis numbers than for those where this quantity is restricted to unity. Figure 40 compares the data obtained by Rosner with the corresponding information derived from the numerical solutions. It is important to confirm that the same sources of property data were used in both cases since it can be seen that little similarity exists between the two methods of calculation. Of the numerical solutions, however, the version employing equilibrium values of fluid properties throughout is probably the more realistic and an indication of the predicted variation of heat flux with composition is furnished by Fig. 41.

## 9.2. Methane-oxygen system

In view of the uncertainties introduced by the numerical solutions for the non-stoichiometric hydrogen flames an experimental study of the problem was proposed. The methane-oxygen system was chosen for this purpose since this was clearly the most important combination in practical applications.

Experimental measurements of heat flux were obtained using the stagnation point heat transfer probe. Initially a series of mixtures containing from 28.57 to 50% methane by volume were covered, each over a range of thermal inputs. The Carlisle glassworking torch was found to provide satisfactory combustion quality between these limits with neither excessive air entrainment under oxygen-rich conditions nor 'yellow tipping' when running gas-rich.

The corresponding thermophysical physical property data was obtained and numerical solutions for the heat transfer rates were produced

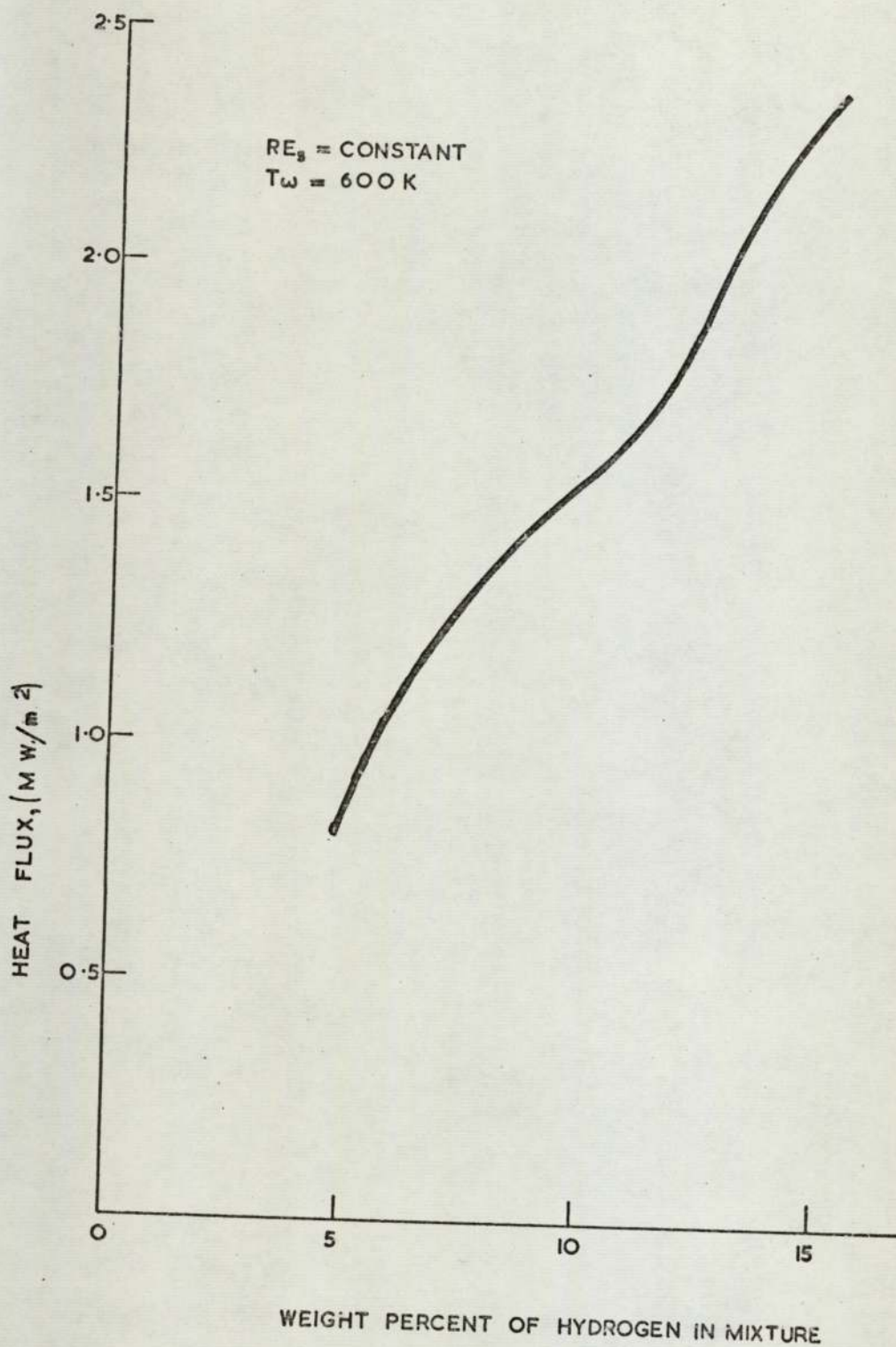


FIGURE 41 NUMERICAL PREDICTION OF STAGNATION POINT HEAT TRANSFER  
HYDROGEN-OXYGEN COMBUSTION PRODUCTS

together with parallel empirical predictions from the weighted average method. In general it can be seen (Fig. 42) that the agreement with experiment is quite satisfactory for mixtures near to stoichiometric but progressively deteriorates with increasing proportions of methane in the unburnt gas. From the rather limited data for oxygen-rich combustion it appeared that a similar trend might exist for such mixtures.

As a result it was decided to include a study of the heat transfer from the exceptionally lean system produced by the combustion of 10% CH<sub>4</sub> and 90% O<sub>2</sub>. (This has a calculated adiabatic flame temperature of 2270K.) When such a mixture was supplied to the Carlisle burner it was clear that the high velocity of the oxygen streams caused an unacceptable level of atmospheric air entrainment. This problem was overcome by the construction of a close fitting tunnel through which the burner was fired. Although rather noisy the arrangement appeared to be satisfactory.

The series of experimental measurements of flame temperature and heat transfer rate was commenced but only three readings were completed before the burner failed as a result of heat radiated from the tunnel walls. These are summarised in Table 7 together with theoretical predictions.

Table 7 : Measured and Predicted Heat Transfer from the Combustion Products of a 10% CH<sub>4</sub> 90% O<sub>2</sub> Mixture, T<sub>w</sub> = 400K

Reynolds number (Re <sub>s</sub> )	Flame Temp (K)	Heat Transfer Coefficient, (W/m <sup>2</sup> K)		
		Experiment	Numerical	Weighted average
102	2092	106	91.3	89.9
237	2133	157	143	138
304	2137	181	162	156

From these restricted values it can be seen that the trend anticipated

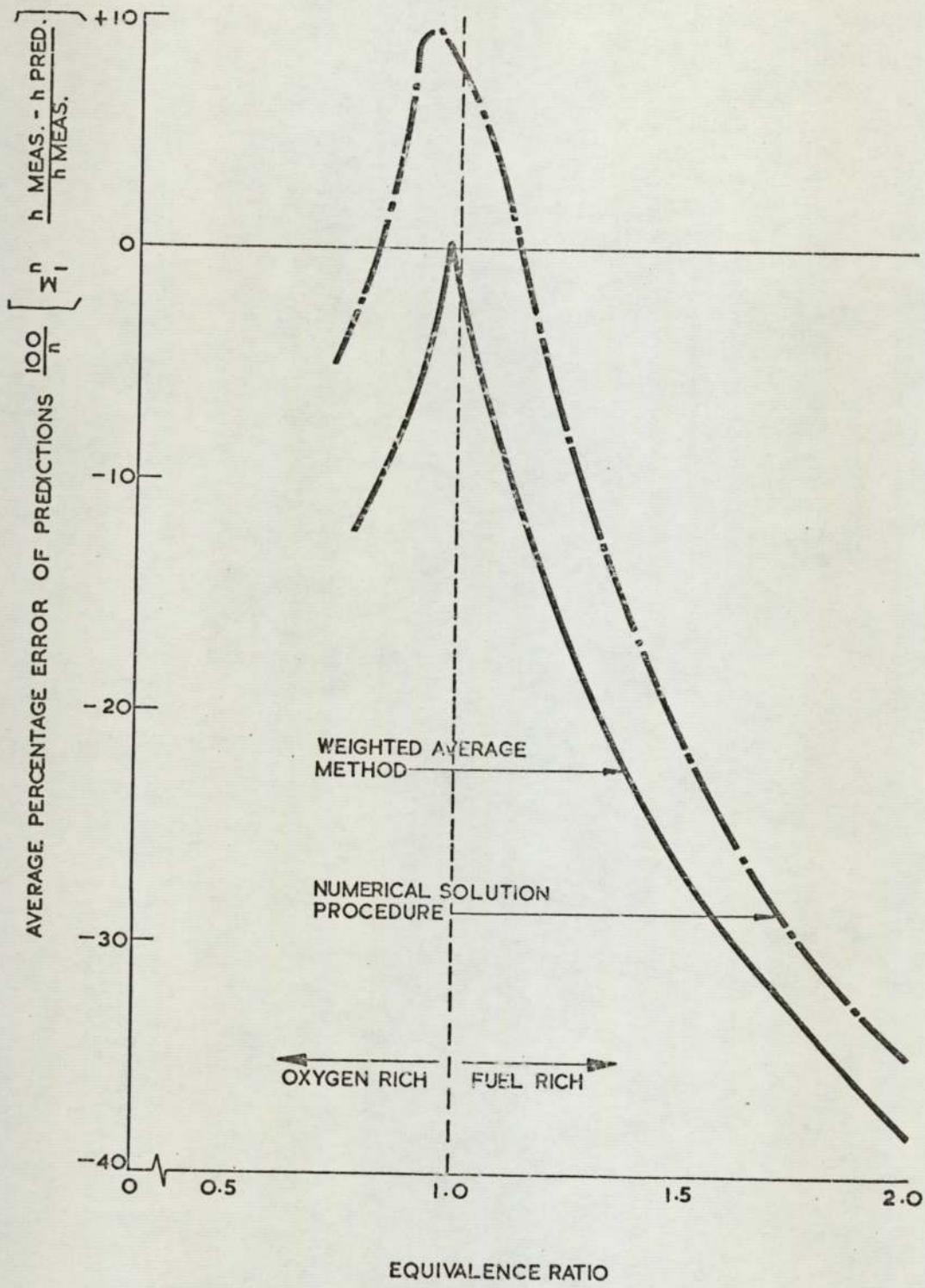


FIGURE 42 A COMPARISON OF MEASURED AND PREDICTED HEAT TRANSFER FROM METHANE-OXYGEN FLAMES TO A FORWARD STAGNATION POINT.

does not in fact materialise and the experimental measurements and theoretical predictions are in tolerably good agreement with each other. As a result it can be assumed that an adequate assessment of heat transfer rates may be obtained with either of the prediction methods, provided that the mixture contains rather less than 38% methane by volume. This corresponds to an equivalence ratio of 1.2 and any errors will then be less than 15%.

An interesting point arises from an examination of the experimental data for the various mixture compositions. It appears that minima exist in the curves relating running cost to heat flux for any specified heat flux. The precise positions of these minima are naturally dependent on the relative costs of fuel and oxygen, but for realistic prices are always associated by a gas rich mixture. This is demonstrated in Fig. 43

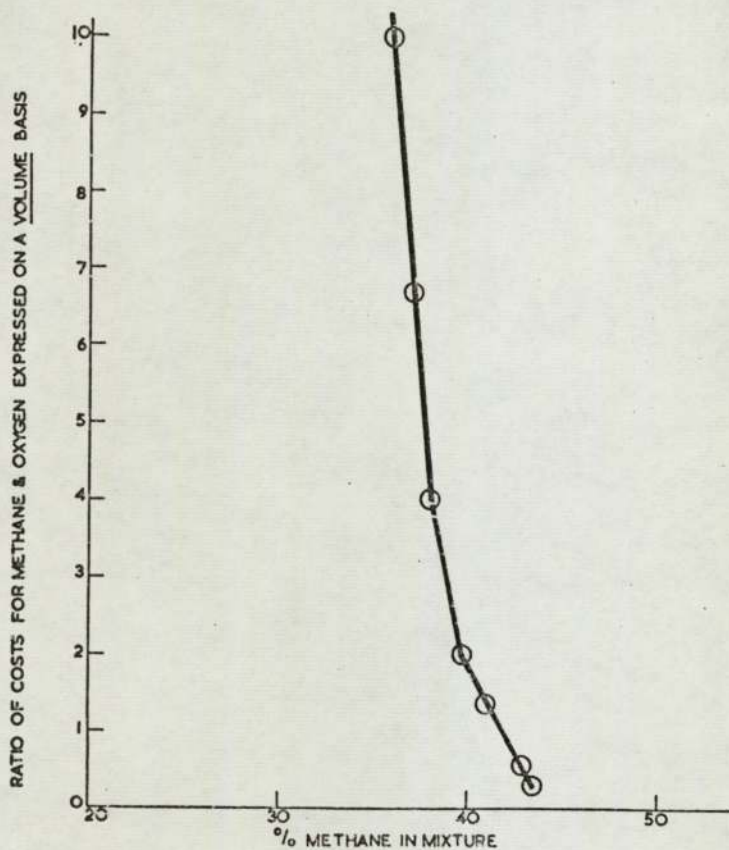


FIGURE 43. OPTIMUM MIXTURE COMPOSITION FOR OPERATION WITH PREDETERMINED FUEL AND OXYGEN TARIFFS.

which shows the optimum mixture composition for supplying a specified heat flux of  $1.1 \text{ MW/m}^2$  to a surface at  $400\text{K}$ . It should be noted that the preferred mixture composition will be independent of heat flux for given fuel and oxygen prices provided that the general equation describing the heat transfer process remains the same.

Tabulated Data for Heat Transfer from Methane - Oxygen Flames to the  
Forward Stagnation Point of a Hemisphere - Cylinder 12.7 mm in Diameter

Methane 28.57% Equivalence Ratio 0.800

Re <sub>s</sub>	Flame Temp (K)	Measured Flux(MW/m <sup>2</sup> )	Heat Transfer Coefficient (W/m <sup>2</sup> K)		
			Measured	Numerical	Wtd.Average
374	2968	1.44	561	538	472
334	-	1.32	514	515	446
292	-	1.13	444	469	418
249	-	1.12	440	440	385
215	2968	1.02	398	411	358
184	2951	0.960	375	374	335
143	2931	0.770	304	324	284

Methane 30.78% Equivalence Ratio 0.889

Re <sub>s</sub>	Flame Temp (K)	Measured Flux(MW/m <sup>2</sup> )	Heat Transfer Coefficient (W/m <sup>2</sup> K)		
			Measured	Numerical	Wtd.Average
335	2994	1.43	551	562	492
289	-	1.33	512	523	458
254	-	1.15	441	488	428
221	-	1.12	431	456	401
189	-	1.04	400	422	371
160	2983	0.913	352	383	330
135	2971	0.785	303	345	292

Methane 36.38% Equivalence Ratio 1.146

Re <sub>s</sub>	Flame Temp (K)	Measured Flux(MW/m <sup>2</sup> )	Heat Transfer Coefficient (W/m <sup>2</sup> K)		
			Measured	Numerical	Wtd.Average
255	3020	1.39	530	505	444
233	-	1.29	494	487	425
208	-	1.18	451	460	402
178	-	1.11	424	423	372
158	-	1.04	397	402	347
130	-	0.972	371	363	329
103	3002	0.840	323	314	309

Methane 33.33% Equivalence Ratio 1.000

Re <sub>s</sub>	Flame Temp (K)	Measured Flux (MW/m <sup>2</sup> )	Heat Transfer Coefficient (W/m <sup>2</sup> K)		
			Measured	Numerical	Wtd.Average
395	3023	1.45	553	628	603
390	-	1.51	576	622	597
366	-	1.49	568	601	580
344	-	1.49	568	585	563
335	-	1.41	535	578	558
332	-	1.37	521	574	553
315	-	1.42	542	560	535
293	-	1.35	515	544	520
270	-	1.29	490	518	493
261	-	1.24	470	510	490
240	-	1.24	469	488	469
235	-	1.16	440	482	464
216	-	1.12	426	460	441
203	-	1.11	424	448	429
180	-	1.02	388	422	405
179	-	1.07	409	421	405
149	3007	0.945	364	383	380
118	2974	0.845	328	340	317
97.5	2958	0.710	278	311	284
92.6	2946	0.637	250	304	279
78.8	2928	0.586	232	269	243
59.5	2924	0.414	164	195	179

Methane 40.0% Equivalence Ratio 1.333

Re <sub>s</sub>	Flame Temp (K)	Measured Flux (MW/m <sup>2</sup> )	Heat Transfer Coefficient (W/m <sup>2</sup> K)		
			Measured	Numerical	Wtd.Average
243	2951	1.26	495	458	404
217	-	1.22	478	425	382
192	-	1.14	446	402	358
162	-	1.07	420	370	328
140	-	1.00	393	341	308
120	2945	0.919	361	293	264
98.2	2936	0.879	347	266	251

Methane 44.44% Equivalence Ratio 1.600

Re <sub>g</sub>	Flame Temp (K)	Measured Flux (MW/m <sup>2</sup> )	Heat Transfer Coefficient (W/m <sup>2</sup> K)		
			Measured	Numerical	Wtd.Average
212	2855	1.19	482	352	356
197	-	1.15	468	340	344
173	-	1.13	458	318	322
146	-	0.925	376	293	295
121	-	0.900	366	266	269
111	2848	0.855	349	253	256
90	2843	0.840	344	228	234

Methane 50.0% Equivalence Ratio 2.000

Re <sub>g</sub>	Flame Temp (K)	Measured Flux (MW/m <sup>2</sup> )	Heat Transfer Coefficient (W/m <sup>2</sup> K)		
			Measured	Numerical	Wtd.Average
198	2577	1.08	465	320	300
184	-	1.01	461	308	285
159	-	0.980	444	285	265
151	-	0.907	416	268	260
127	2560	0.790	362	242	236
113	2551	0.770	358	227	219
78	2543	0.710	331	188	179

## 10. DISCUSSION

### 10.1 Hydrogen Atom Concentrations

The experimental data which demand immediate explanation are those referring to the hydrogen atom concentrations in the flame gases. Examination of the concentration profiles along the flame axes indicates that the measured values pass through an equilibrium position. This situation is normally inadmissible since it constitutes a contravention of the second law of thermodynamics.

Two possible explanations can be offered. The first of these, the entrainment of atmospheric air into the flowing gases, does not appear to be sufficiently serious to cause the required departure from the nominal composition. This follows from the slow decay of flame temperature from the maximum value with increasing distance from the burner. Thus the entrainment of diluents must occur at a low rate - at least for the first 30 mm or so above the burner. This contention is supported by measurements of nitrogen oxide concentrations carried out by Waters (62) on the same burner. Waters investigated the variation of the total concentration of nitric oxides with distance from the burner; the measurements indicating a steady rate of formation for the first 20-30 mm at the base of the flame. This remained below the equilibrium value based on the total nitrogen contained in the natural gas supplied. However, an increased rate of formation appeared to take place at greater heights indicating that entrainment from the surrounding atmosphere may then be appreciable. This should not invalidate the measurements of H-atom levels since these were only taken in the base regions of the flames.

The second and most probable explanation of the low hydrogen atom populations stems from the high diffusion coefficients applicable to that species. The severe temperature gradients in the outer edges of the

flame lead to correspondingly large changes in gas composition which may result in significant diffusion of hydrogen atoms from the flame. This effect has been reported by Hayhurst and Telford (65) in their work on fuel rich hydrogen flames. The experimental results in the methane-oxygen and hydrogen-oxygen flames indicate that this may be the reason since the depopulation appears to be somewhat larger in the latter case than in the former where equilibrium concentrations are appreciably lower.

## 10.2. Stagnation Point Studies

### 10.2.1. Experimental Measurements

The experimental heat transfer data for stagnation point conditions, having been obtained from the analysis of transient heat flows within the beryllium copper element, are particularly susceptible to uncertainties in the metal properties. Enquiries of the manufacturers revealed that the accuracy of their published data should ensure measured heat fluxes within  $\pm 5\%$  of the true values. In addition it was clear that probable variations between batches were likely to introduce only marginal errors in the experimental results. Heat transfer through the pins supporting the beryllium copper plug and across the annular gap between the plug and the stainless steel case have been estimated to be negligible. It was deemed necessary, however, to check whether or not metallurgical changes could have resulted from the many hundreds of heating cycles involved in the experimental programme. A metallographic examination of the material showed that no alteration of crystalline structure had occurred. In addition, the repetition of some of the runs carried out early in the work indicated that no change in response had been produced.

Possible interactions between free and forced convection mechanisms have been considered. It is evident that the denser boundary layer

associated with the cooler surface has an inherent tendency to fall in the hotter gases. The effect is to oppose the flow of the approaching fluid thereby reducing the forced convection component of heat transfer and is, therefore, greatest at low gas velocities. Pei (64) has indicated that the effects of natural convection may be completely ignored for  $GrRe^{-2} < 0.05$  and are less than 10 per cent of the total for  $GrRe^{-2} < 0.3$ . Calculation shows that little or no interaction should occur under the experimental conditions.

The flame temperatures measured at the set position above the burner generally fall below the calculated adiabatic flame temperatures. This is to be expected since several mechanisms for energy loss are in evidence. Slight losses occur by radiation from the flame gases to the surrounding medium. Snelleman (65) has estimated losses from this effect to be of the order of 20 K in a slightly rich  $C_2H_2/O_2$  flame at the position of maximum temperature. Other minor losses include the effects of incomplete reaction, the temperature of the fuel gases supplied and the difference between the flame and the measured excitation temperatures. The presence of water vapour in the air supply also has an influence on the temperature of the premixed natural gas-air flame, which could amount to a reduction of 15 K compared with the dry air value. The decline in the measured fuel-oxygen flame temperatures as the thermal input is reduced appears to result from conductive heat losses through the burner, only partially regained by the incoming supplies. It is significant that such effects were absent with the premixed burner which, being of considerably lighter construction, presented less opportunity for irrecoverable heat losses.

The accuracy of the temperature measurements, (estimated at  $\pm 50K$ ) has a greater influence on the predicted values of heat transfer coefficient than on those derived from the experimental data. An

overestimation of flame temperature by this amount leads to an increase in the former of some 7.5% while reducing the latter by approximately 2.5%.

#### 10.2.2. Comparison with numerical solutions

It is evident that the numerical solution procedure used in this work provides an adequate method for the prediction of stagnation point heat transfer from stoichiometric combustion products. This is especially satisfying since it is clear that the conditions prevailing in fuel oxygen flames provide a more severe test of the theory than the system of dissociated air for which it was originally developed. The presence of significant concentrations of hydrogen atoms in most fuel-oxygen combustion products results in the diffusion-recombination mechanism carrying a proportionally greater part of the overall heat transfer than would be the case for dissociated air. This stems from the low mass of the hydrogen atom compared with the effective molecular weight of the combustion product mixture, a situation which gives rise to high diffusion coefficients. In the case of heat transfer from dissociated air streams the difference between the masses of the various species is very much less so that the allowances for diffusion and recombination becomes rather less complicated. The situation is further eased by the fact that the assumption of a simple binary mixture can be made where air is concerned.

It was found that the closest agreement of the numerical solutions with experiment was obtained for the methane systems and in particular with methane-air. This is not unexpected since the smallest property variations occur for combustion with air and, as a result of the lower flame temperature, diffusion - recombination effects will be slight. The slight underestimation of the heat transfer from the hydrogen oxygen flame which is shown in Fig. 19 can probably be attributed to the effects of diffusional separation. The use of reacting thermal

conductivity data in the solution of the boundary layer equations introduces the assumption that a constant elemental composition is preserved throughout. Nachtsheim (66) has recently shown that this may not be the case. He has pointed out that, as a result of the large differences in the molecular weights and hence in the diffusion coefficients of the species present in hydrogen-oxygen combustion products, some diffusional separation may be expected in systems having severe temperature gradients. Nachtsheim has shown this diffusional separation to be significant in the nominally stoichiometric hydrogen-oxygen system at wall and free stream temperatures of 2400K and 4000K respectively. Under these conditions a 30% deviation exists in the elemental mass fraction of hydrogen at the wall compared with that at the outer edge of the boundary layer. The effect is strongly temperature dependent and at more modest temperature levels rapidly diminishes. With the same ratio of wall to free stream temperatures as before, but with values of 1824K and 3040K the deviation in elemental composition across the boundary layer results in an increase in the elemental mass fraction of hydrogen near the wall by about 8%. This corresponds to a mixture containing 12.04% of hydrogen by weight instead of the 11.19% which constitutes a stoichiometric mixture with oxygen.

An increase in concentration of this magnitude may not appear to be very significant but certain features of the series of numerical solutions carried out so far would indicate otherwise. It has been found that the present solutions of the conservation equations for stoichiometric combustion products show small differences between predictions which use equilibrium values of fluid properties and those employing frozen values. Provided that the equations and the method used in their solution are sufficiently reliable in their present forms, then it is implied that the thermophysical properties of the fluid remote from the wall have but a minor influence on the heat flux received by the surface.

Should this effect be real then the increased hydrogen concentration near to the wall could have an important influence on heat transfer from dissociated systems. In support of this view it has also been shown that, using the numerical prediction procedure, appreciably higher heat transfer rates result when using fuel rich hydrogen-oxygen mixtures at corresponding values of the Reynolds number. It follows that compositional changes resulting from diffusional separation may well be the cause of the measured heat fluxes for the hydrogen-oxygen system being marginally higher than those predicted, although extensive investigations would be necessary before this could be either confirmed or denied.

In spite of the possible interferences from diffusional separation effects it is nevertheless preferable to use the numerical solution when drawing comparisons between various fuels - at least where stoichiometric combustion with oxygen is concerned. This is because the uncertainties in the data gathered from experimental work tend to be greater than the apparent differences in heat transfer rates. The exception to this is found with the carbon monoxide flame which provides very much lower heat transfer rates than the remainder as a result of the reduced concentrations of dissociated species and the lower flame temperature.

It is, however, quite informative to study the predicted heat transfer rates from the range of fuels taking a theoretical standpoint. Table 8 below indicates the magnitude of the heat fluxes to the forward stagnation point of a 12.7 mm diameter sphere where the Reynolds number based on this dimension and free stream gas properties is 300. Adiabatic flame temperature is taken to apply to the free stream.

Table 8 : A Comparison of the Predicted Rates of Heat Transfer from Stoichiometric Fuel-Oxygen Combustion Products to the Forward Stagnation Point of a Sphere

Fuel Gas	C/H Ratio	Relative heat transfer rate to a sink at			
		400K	800K	1200K	1600K
H <sub>2</sub>	0	1.00	1.03	0.995	0.940
CH <sub>4</sub>	0.25	0.835	0.835	0.760	0.670
C <sub>3</sub> H <sub>8</sub>	0.375	0.791	0.765	0.724	0.665
CO	∞	0.492	0.448	0.408	0.359
C <sub>2</sub> H <sub>4</sub>	0.5	1.01	0.99	0.95	0.92

It can be seen that the available heat transfer rates from the combustion products of the saturated compounds H<sub>2</sub>, CH<sub>4</sub>, C<sub>3</sub>H<sub>8</sub> and CO are in sequence with their carbon to hydrogen ratios. This might be expected since the thermal conductivity of steam is rather higher than that of carbon dioxide. In addition the presence of larger proportions of hydrogen may be assumed to result in correspondingly higher concentrations of hydrogen atoms in the burned gases and provide greater heat transfer by diffusion and exothermic recombination processes.

It is important to emphasise that this line of reasoning is only strictly applicable to fuels in a true homologous series. This is shown by the results for ethylene where the situation is complicated by the higher flame temperature consequent on the large bond energy of the molecule. Similarly acetylene would be expected to provide still higher heat transfer rates than either of the related gases ethane or ethylene.

### 10.2.3. Comparison with empirical prediction

The three modifications to both the Stanton and Nusselt number forms of Sibulkin's original relationship have been listed in Table 5. The convective heat transfer coefficients have been evaluated for each case at a free stream Reynolds number of 300. Corresponding experimental values interpolated from plots such as Fig. 19 have also been included.

The relevant Nusselt and Stanton numbers,  $\bar{Nu}$  and  $\bar{St}$ , have been defined to be  $hD/\bar{\lambda}$  and  $h/G \bar{C}_p$  respectively. In effect the latter incorporates an assumption of uniform mass velocity which, in turn, enables the free stream and weighted Reynolds numbers to be related through the viscosity ratio  $\mu_s/\bar{\mu}$ . The three forms listed differ in the choice of the Reynolds number. In equations A and B the value obtained from free stream properties  $D_b G/\mu_s$  has been used while in C and D the weighted values  $D_b G/\bar{\mu}$  has been taken. It is clear from the table that the use of expressions A to D results in considerable overestimation of the convective heat transfer from the fuel-oxygen flames. Even in the lower temperature natural gas-air system it can be seen that the predictions are generally unsatisfactory with the possible exception of Eq. (A). It is worth noting that the use of the free stream Reynolds number and an averaged Stanton number in Eq. (B) is similar to the correlation procedure proposed by Rosner (36). In the present case, however, the Lewis number correction is incorporated in the equilibrium Prandtl number.

An empirical modification of the free stream Reynolds number by the factor  $\bar{\mu}/\mu_s$  as in equations (E) and (F) results in much closer agreement between the predicted and measured coefficients for all the fuel oxygen flames. The use of such a factor has little theoretical justification and it may well be that improved definitions of the averaged transport properties for the boundary layer could render it unnecessary.

For the natural gas-air flame the modified Stanton number form, Eq. (F), gives an acceptably good fit to the experimental data whereas the Nusselt form (E) significantly underestimates the coefficients. This effect is puzzling since it might be supposed that the coefficients obtained in the lower temperature flame should be more readily predictable because of the smaller variations in physical properties and a lower degree of dissociation. It is of course possible, but not readily verifiable, that the calculated values of mean thermal conductivity over the temperature range 400 - 3000K are more realistic than those for the range 400 - 2200K. Use of Fay and Riddell's term  $(\rho_w \mu_w / \rho_s \mu_s)^{0.1}$  for modifying the free stream Reynolds number results in calculated coefficients well in excess of the experimental values.

The present comparison of empirical prediction and experiment apparently reinforces the proposition that heat flux from high temperature gas streams is best correlated on a Stanton number basis in which enthalpy difference rather than temperature difference may be regarded as the driving force for heat transfer (67). Such a procedure is likely to reduce the inaccuracies resulting from the employment of theoretical values for high temperature transport properties, the most uncertain of which is thermal conductivity.

The ability of Eq. (F) to correlate the experimental results is gratifying but it must be emphasized that the range of experimental conditions over which it has been tested to date is limited. In this respect scrutiny of the thermophysical property data of Table 4 is instructive. From the table it can be seen that the range of Prandtl numbers, viscosity ratios  $(\bar{\mu}/\mu_s)$  and temperature differences is comparatively small. Significant variations in heat transfer coefficient are thus attributed to differences in either mean equilibrium specific heat or mean equilibrium thermal conductivity and the comparisons of Table 5 support this contention. The agreement between

predicted and experimental coefficients is strongly dependent on the term  $(\bar{\mu}/\mu_s)$  by which the Reynolds number is modified.

It should be emphasised that the proposed empirical correlation has little theoretical backing and quite probably an improved version could be obtained with the use of other forms of property averaging. However, it is clear that the method suggested provides the basis for making relatively simple estimates of heat transfer from flames under stagnation point conditions.

#### 10.2.4. Comparison with the results of Kilham and Purvis

Perhaps the most interesting of previously published work is that of Kilham and Purvis which has been mentioned earlier. This considers the heat transfer from methane and propane oxygen flames to a forward stagnation point.

Comparisons between the sets of data are limited to the results for methane combustion, since the mixtures used in the two programmes do not overlap in the studies on propane. An immediate difference is noted between the values quoted for the flame temperatures. These appear to be significantly lower for the flames dealt with in the paper than for those measured on the Carlisle burner. (Table 9). The reason for this difference cannot be firmly established but some variations in experimental techniques are apparent. Firstly the flame used by Kilham and Purvis was totally coloured with sodium, whereas the Carlisle burner used in the present studies had provision for a small premixed flame on the axis, and this was used for seed addition. The former method, total colouration, can result in an underestimation of temperature where the flame is not homogeneous in character. This is generally the case with open flames because of the cooling effect of the surrounding atmosphere.

The second difference between the two sets of measurements concerns the method of seed addition. In the work on the Carlisle glassworking torch used in the majority of the experimental programme, this was

accomplished by carrying forward traces of the salt in the fuel stream. Kilham and Purvis, on the other hand used nitrogen as the carrier gas and this must act as a diluent to reduce the flame temperature, however small the effect might be.

The influence of the diffusion or entrainment of atmospheric air into the system is less well defined, but this would intuitively seem to be greater in the smaller flames than with those produced by the Carlisle glassworking burner. This contention is borne out to some extent if the experimental results for the rich flames and for the ones near to stoichiometric are compared. The discrepancies between the measured temperatures are by no means the same but are in the order of 80 to 120K respectively. This may be explained by the energy release which would accompany the introduction of oxygen into the fuel-rich flame partially off-setting the reduction in temperature attributed to the nitrogen. Whether this would account for the whole of the difference represented by the figures of 80 to 120K is debatable.

In view of these differences a glassworking torch of the same design as that used in the cited work was purchased. (This was J.7 burner manufactured by Jencons Ltd., Hemel Hempstead.) Measurements of flame temperature were then carried out using a similar method to that described by these authors. An absolute minimum of nitrogen was used for seeding and the results obtained are listed below. It can be seen that very similar values are obtained with the two experimental rigs. At face value this tends to confirm the accuracy of the apparatus used for the work reported in this thesis. However, this could not be assumed since, when questioned, Kilham and Purvis were of the opinion that edge effects could be ignored. Since it was impractical to modify the relevant burner for axial colouration no firm conclusions can be reached concerning the validity of this statement.

It was found however, that total colouration of the Carlisle burner flame resulted in a reduction in the measured temperature of some 40K.

The values recorded for the stoichiometric combustion of methane with oxygen were 3023K and 2984K respectively. The inference to be drawn here is that total colouration of the flames should be avoided wherever possible. This is especially the case with flames containing dissociated material since it is known that the concentrations of the various species and consequently the heat transfer rates, exhibit a strong dependence on the free stream temperature. Thus errors in temperature measurement will have a pronounced effect on the heat transfer predicted for fuel-oxygen systems.

Although a difference of 40K is insufficient to account for the whole of the discrepancies between the two sets of measurements, it is reasonable to expect that the reduction in measured temperature would be still greater with the smaller J7 flames than with those produced on the Carlisle burner. This stems from a greater proportion of the optical path then passing through the cooler parts of the flame so that the measured temperature becomes more dependent on the temperature of those regions. Thus it is quite conceivable that the differences between the quoted flame temperatures can be attributed to this cause particularly when it has been shown that measurements on the J7 burner using the same method of seed addition are in such close agreement.

#### Comparison of Temperatures Measured on a Jencons J7 Torch

Fuel Oxygen Mixture	Mass Velocity (kg/m <sup>2</sup> s)	Measured Temperature (K)	
		Kilham and Purvis	Present Work
33% CH <sub>4</sub> 67% O <sub>2</sub>	3.659	2900	2918
40% CH <sub>4</sub> 60% O <sub>2</sub>	2.908	2873	2885

A final comment concerns the manner in which heat flux data was obtained from the responses of the probes used in the two series of measurements. The method employed at Solihull was based on a knowledge of the thermal properties and dimensions of the calorimetric insert. Consequently a separate calibration experiment was not strictly necessary although a check on the response was in fact carried out for heat transfer under conditions of low temperature differentials. In the work reported by Kilham and Purvis the information was gathered by way of a calibration experiment in an air stream of 1021K using Sibulkin's expression to describe the heat transfer process. This is strictly a constant property relationship so that the validity of its application over temperature differences of 650K needs independent confirmation.

However, if the differences between the measured flame temperatures can be attributed to the techniques used then it is found that the measured heat fluxes are in quite close agreement after the differences in probe size are taken into account. This has been accomplished by assuming that the heat flux is proportional to the square root of the free stream velocity and inversely proportional to the square root of the probe diameter. The values obtained are listed in the table overleaf.

Table 9: A comparison of heat fluxes extrapolated from the present data with those measured by Kilham and Purvis

Present Work			Kilham and Purvis		
Measured Temp (K)	Equivalence Ratio $\phi$	Heat Flux (MW/m <sup>2</sup> )	Measured Temp (K)	Equivalence Ratio $\phi$	Heat Flux (MW/m <sup>2</sup> )
3023	1.00	2.26	2900	1.03	2.53
2951	1.33	2.06	2873	1.31	2.02

It is unfortunate that further comparisons cannot be made since the paper represents virtually the only published work on systems similar to those used here. There is however sufficient to suggest that the present results are not unreasonable.

### 10.3 Measurements at High Surface Temperatures

It is evident that the excellent agreement of the empirical prediction method with experiment extends to the higher surface temperature levels studied with the bead thermocouple probes. This is indeed a most valuable finding since it begins to put the use of such extrapolation procedures onto a more sound basis.

#### 10.3.1 Experimental measurements

Little needs to be said regarding the actual measurements or the method whereby the heat transfer coefficients were calculated from the recorded temperature history of the probe. This has been covered in detail and all of the possible mechanisms for heat transfer have been examined and appropriate allowances have been made. The interaction of natural and forced convection has again been considered and found to be absolutely negligible.

The chief cause for concern which arose in the course of the

measurements was associated with the insertion of the probe into the flame. In the first place it was questioned whether the piston rod was actually at rest when the measurements were commenced. This point was resolved by arranging for an electrical contact to be made when the probe reached the limit of its travel. This completed a circuit to the marker channel of the recording oscillograph and enabled the time for insertion to be obtained. This was invariably within the limits demanded by the response of the probe and the pneumatic assembly was considered to be satisfactory in this respect.

The second point was concerned with the vibration induced in the thermocouple bead and wires by the sudden movements of the insertion mechanism. Ciné photography indicated that small amplitude oscillations persisted throughout the measuring period and it was thought that these might have some effect on the heat transfer process. This arises from the known effects of vibration on boundary layer phenomena and, although usually more important in natural convection studies, it was considered to be worthy of investigation in the present work.

The thermocouple probe was attached to a lever pivoted near one end. At the end remote from the pivot the lever was held onto an eccentric cam by means of powerful springs. This cam was driven by a 100W electric motor, the speed of which could be varied using a rheostat. The thermocouple was located at the appropriate point above the unlit burner and vibrated over a range of frequencies for each flame condition. The flow rates of fuel and oxygen were set to the required values and the flame ignited. The response of the thermocouple was determined in the same way as before but no increase in heat transfer rates could be detected.

As a result one can reasonably expect the data obtained experimentally to be quite reliable and reflect the true heat transfer characteristics of the various flames to within 15%. This figure is composed of the contributions to the overall errors from both measurement and calculation

listed below.

Flame temperature measurement	$\pm 2\frac{1}{2} \%$
Metal properties	$\pm 5 \%$
Calculation method	$\pm 1\frac{1}{2} \%$
Calibration and reading of oscillograph	$\pm 5 \%$

The errors on bead size, radiation from the surface, conduction gains from the leads and flame radiation effects are all insignificant and probably affect the measured coefficients by rather less than 1%.

### 10.3.2. Comparison with empirical prediction

The agreement with the modified version of Rowe, Claxton and Lewis' expression for heat transfer to isolated spheres is reasonably satisfactory. Although not quite as good as the results for the stagnation point case the accuracy is certainly adequate for most calculations on combustion systems.

It must be pointed out that certain of the experimental data points appear to fall marginally outside the quoted range of the correlation put forward by Rowe, Claxton and Lewis. However, although the representation of the flow characteristics by a Reynolds number based on free stream conditions provides for the accurate assessment of heat transfer, this does not necessarily carry the same meaning as the Reynolds number for a constant property problem. A more reasonable choice for this purpose would require the thermophysical properties of the combustion products to be taken at a temperature representative of the boundary layer as a whole. In such a case the criteria set by the original authors would be met comfortably for the whole of the experimental range. It does not therefore appear necessary to exclude the few measurements taken at the lowest thermal inputs from the graphs illustrating the agreement of the modified relationship with the experimental data. Even if this were done the general conclusions would remain the same since only a small number of data points are involved.

#### 10.4 Heat Transfer from Non-Stoichiometric Flames

The results obtained for heat transfer from the combustion products of non-stoichiometric mixtures of fuel and oxygen are of considerable interest from both practical and theoretical points of view. Especially important with regard to the former are the calculations carried out on the economics of working flame operation. Based on experimental observation these indicate that some financial advantage may be gained with the use of fuel rich flames, even where oxygen is available at particularly attractive rates. It seems that the provision of excess fuel tends to produce an increase in heat flux which more than compensates for the reduction in mass velocity associated with the lower proportions of oxygen. For tariffs applicable to many industrial users the limited data available suggests an optimum mixture composition containing between 40 and 45% methane by volume. This is significantly greater than the  $33\frac{1}{3}\%$  which constitutes a stoichiometric mixture. However, it must always be borne in mind that the possibility of soot and carbon monoxide formation is correspondingly higher and this may need to be taken into account where the heating operation is carried out in a confined space or where large scale usage is contemplated.

On the theoretical side, the numerical solutions for both hydrogen and methane flames have predicted a progressively increasing heat flux for a specified free stream Reynolds number as the mixture burned becomes richer in fuel. This is not altogether surprising since the larger concentrations of free radicals would result in parallel increases in the amount of heat transfer occurring by the diffusion and recombination of these species. Unfortunately the increase predicted is insufficient when compared with experimental measurements of heat transfer rates and large errors appear with the richest of the mixtures studied.

The discrepancies are rather puzzling since it seems reasonable to expect that the inclusion of true equilibrium thermal conductivities

in the numerical calculations would be sufficient to allow accurate predictions to be made, bearing in mind that the method was quite successful for stoichiometric mixtures. It is possible that the poor performance of the numerical method, and incidentally the semi-empirical expression, lies with an escalation of the effect of diffusional separation. This has been mentioned before in connection with the underestimation of heat transfer from the hydrogen-oxygen flame and may be the cause of the observed behaviour. Because of the complexity of the problem no attempt has been made to ascertain whether or not this hypothesis is valid although it clearly becomes a useful topic for further investigation at a later date. Consequently the main value of this part of the work must be seen as defining the limitations of the simpler techniques for heat transfer calculation and in providing experimental information previously unavailable.

## 11. CONCLUSIONS

Some measure of success has been achieved in relating the forced convective heat transfer from high temperature flames to the thermo-physical properties of their combustion products. For stoichiometric combustion it has been shown that the numerical solution of the boundary layer conservation equations can provide an accurate assessment of the stagnation point heat fluxes. However, in view of the expensive and time consuming nature of such methods an empirical modification to the corresponding relationship for low temperature conditions has been made. This enables more rapid estimates of heat flux to be obtained and appears to be adequate for most practical purposes.

Parallel modifications have also been made to an accepted relationship describing convective heat transfer to an isolated sphere under conditions of small temperature differences. It has been found that the resulting expression provides satisfactory agreement with measurements of heat transfer from fuel-oxygen flames for surface temperatures ranging to 1600K.

The limited amount of work carried out on non-stoichiometric mixtures has indicated a progressive deterioration in the accuracy of both numerical and empirical prediction methods when the mixture burned becomes richer in fuel. Possible reasons for this inadequacy have been suggested although these have not been substantiated. As a result it seems advisable to confine the use of the suggested prediction methods to stoichiometric or oxygen-rich mixtures.

## ACKNOWLEDGEMENTS

The author wishes to express his sincere thanks to Dr.R.M.Davies of the Gas Council, Midlands Research Station for the advice and encouragement offered during the course of this work. The numerous and most helpful discussions with Professor F.M.Page and Dr.R.G.Temple of the University of Aston in Birmingham are also gratefully acknowledged. In addition thanks are due to Mrs. H.E. Toth, again of the Gas Council, for programming many of the more tedious calculations and to R.Newman for providing equipment for the spectroscopic examination of radical concentrations.

APPENDIX 1

CALCULATION OF THERMODYNAMIC AND TRANSPORT PROPERTIES

Table 10 : Force Constants used in Transport Property Calculations\*

Species	$\sigma$	$\epsilon/k$
H	2.708	37.0
H <sub>2</sub>	2.827	59.7
H <sub>2</sub> O	2.710	506.0
O	3.050	106.7
OH	3.147	79.8
O <sub>2</sub>	3.467	106.7
CO	3.690	91.2
CO <sub>2</sub>	3.941	195.2
Ne	3.798	71.4
N	3.298	71.4
NO	3.492	116.7

\*Taken mainly from NASA TR-R 132. Values for H<sub>2</sub>O from Monchick, L.

J.Chem Phys. 35 1676 (1961).

Table 11 : Enthalpy of Pure Components at Temperatures up to 4000K

(J/kg - mole)

Temp (K)	N <sub>2</sub>	H <sub>2</sub> O	O <sub>2</sub>	CO <sub>2</sub>	H <sub>2</sub>	O	OH	H	NO	N	CO	CH <sub>4</sub>
288	0	0	0	0	241.716	249.230	159.892	338.936	90.405	473.060	283.053	802.803
300	0.352	0.402	0.352	0.444	242.185	249.494	160.253	339.187	90.769	473.311	283.405	803.231
400	3.269	3.793	3.324	4.378	245.094	251.662	163.225	341.268	93.754	475.387	286.327	807.027
600	9.192	10.842	9.544	13.290	250.950	255.919	169.131	345.428	99.861	479.548	292.296	816.316
800	15.350	18.343	16.141	23.195	256.840	260.131	175.067	349.585	106.270	483.709	298.533	827.924
1000	21.767	26.342	23.015	33.789	262.826	265.158	181.124	353.746	112.955	487.865	305.051	841.562
1200	28.419	34.844	30.076	44.870	268.946	268.503	187.349	357.907	119.849	492.027	311.790	856.870
1400	35.250	43.836	37.821	56.298	275.234	272.676	193.761	362.064	126.894	496.188	318.705	873.526
1600	42.220	53.254	44.593	67.981	281.697	276.849	200.346	366.225	134.057	500.344	325.750	891.249
1800	49.294	63.054	52.011	79.848	288.323	281.019	207.086	370.381	141.298	504.505	332.896	909.827
2000	56.457	73.175	59.520	91.858	295.113	285.184	213.963	374.542	148.607	508.666	340.113	929.091
2200	63.682	83.573	67.127	103.984	302.041	289.353	220.954	378.703	155.962	512.827	347.392	948.916
2400	70.961	94.210	74.825	116.199	309.098	293.522	228.045	382.860	163.363	516.988	354.717	969.214
2600	78.282	105.048	82.611	128.493	316.269	297.696	235.224	387.021	170.797	521.157	362.081	989.901
2800	85.641	116.069	90.485	140.851	323.540	301.873	242.474	391.182	178.257	525.330	369.481	1010.93
3000	93.034	127.246	98.438	153.262	330.911	306.055	249.795	395.338	185.745	529.516	376.907	1032.25
3200	100.447	138.569	106.475	165.720	338.379	310.253	257.171	399.474	193.255	533.723	384.359	1053.83
3400	107.886	150.014	114.579	178.223	345.927	314.457	264.597	403.656	200.786	537.951	391.831	1075.65
3600	115.345	161.575	122.759	190.760	353.566	318.680	272.073	407.817	208.333	542.208	399.319	1097.67
3800	122.821	173.246	130.997	203.335	361.281	332.916	279.587	411.978	215.893	546.503	406.829	1119.88
4000	130.314	185.017	139.293	215.943	369.067	327.169	287.143	416.134	223.474	550.844	414.351	1142.28

# EQUILIBRIUM COMPOSITION & THERMOPHYSICAL PROPERTIES OF STOICHIOMETRIC COMBUSTION PRODUCTS

TABLE 12a. METHANE OXYGEN

TEMP (K)	COMPOSITION							MOL	
	H <sub>2</sub> O	H <sub>2</sub>	O <sub>2</sub>	O	OH	H	CO	CO <sub>2</sub>	WT.
4000	0.01901	0.05695	0.03630	0.28162	0.07598	0.37853	0.14600	0.00561	12.14
3800	0.04913	0.08009	0.05495	0.23060	0.10519	0.31130	0.15735	0.01138	13.51
3600	0.10884	0.09786	0.07407	0.17029	0.12727	0.22921	0.16960	0.02287	15.41
3400	0.20047	0.10105	0.08727	0.11151	0.13118	0.14798	0.17660	0.04395	17.65
3200	0.31069	0.08836	0.08953	0.06400	0.11518	0.08314	0.17071	0.07839	19.94
3000	0.41908	0.06689	0.07995	0.03179	0.08679	0.04065	0.14787	0.12697	22.00
2800	0.51010	0.04496	0.06180	0.01341	0.05649	0.01727	0.11166	0.18431	23.69
2600	0.57740	0.02715	0.04092	0.00468	0.03176	0.00630	0.07210	0.23969	24.96
2400	0.62139	0.01473	0.02301	0.00131	0.01528	0.00192	0.03928	0.28308	25.80
2200	0.64662	0.00707	0.01088	0.00028	0.00617	0.00047	0.01781	0.31069	26.29
2000	0.65914	0.00292	0.00423	0.00004	0.00203	0.00009	0.00656	0.32500	26.54
1800	0.66437	0.00099	0.00130	0.00000	0.00051	0.00001	0.00187	0.33094	26.64
1600	0.66614	0.00026	0.00030	0.00000	0.00009	0.00000	0.00038	0.33284	26.67
1400	0.66658	0.00005	0.00004	0.00000	0.00001	0.00000	0.00005	0.33327	26.68
1200	0.66666	0.00000	0.00001	0.00000	0.00000	0.00000	0.00000	0.33333	26.68
1000	0.66666	0.00000	0.00001	0.00000	0.00000	0.00000	0.00000	0.33333	26.68
800	0.66666	0.00000	0.00001	0.00000	0.00000	0.00000	0.00000	0.33333	26.68
600	0.66666	0.00000	0.00001	0.00000	0.00000	0.00000	0.00000	0.33333	26.68
400	0.66666	0.00000	0.00001	0.00000	0.00000	0.00000	0.00000	0.33333	26.68
300	0.66666	0.00000	0.00001	0.00000	0.00000	0.00000	0.00000	0.33333	26.68

TEMP (K)	MIXTURE ENTHALPY (MJ/kE)	FROZEN SP. HEAT (J/kgK)	EQUIL'M SP. HEAT (J/kgK)	FROZEN COND <sup>y</sup> W/°K	EQUIL'M COND <sup>y</sup> W/mK	MIXTURE DENSITY (kg/m <sup>3</sup> )	MIXTURE VISCOS <sup>y</sup> (μNs/m <sup>2</sup> )	EQUIL'M FRANDTL NUMBER
3800	25.408169	2238	-	0.4810	4.9799	0.0433	95.15	-
3600	20.498669	2211	-	0.4348	5.2195	0.0521	94.07	-
3400	15.952709	2187	20871	0.3872	4.6284	0.0633	92.61	0.4176
3200	12.228589	2168	16390	0.3439	3.5728	0.0759	90.37	0.4146
3000	9.365950	2153	12375	0.3087	2.4980	0.0893	87.35	0.4328
2800	7.222149	2139	9187	0.2808	1.6372	0.1031	83.62	0.4693
2600	5.644012	2123	6690	0.2581	1.0315	0.1169	79.49	0.5156
2400	4.506114	2100	4787	0.2377	0.6407	0.1310	75.03	0.5606
2200	3.690660	2072	3463	0.2186	0.4066	0.1456	70.44	0.5999
2000	3.085958	2036	2650	0.2000	0.2760	0.1617	65.79	0.6315
1800	2.605807	1992	2212	0.1772	0.2026	0.1803	60.90	0.6648
1600	2.187337	1938	1998	0.1542	0.1606	0.2031	55.83	0.6943
1400	1.799984	1874	1835	0.1308	0.1308	0.2322	50.46	0.7274
1200	1.431537	1798	1798	0.1092	0.1092	0.2709	44.79	0.7376
1000	1.080611	1710	1710	0.0882	0.0882	0.3250	38.76	0.7512
800	0.748395	1611	1611	0.0667	0.0667	0.4063	32.17	0.7769
600	0.437080	1499	1499	0.0474	0.0474	0.5417	24.97	0.7900
400	0.149549	1373	1373	0.0281	0.0281	0.8126	17.06	0.8326
300	0.015644	1305	1305	0.0187	0.0187	1.0834	12.82	0.8963

TEMP (K)	COMPOSITION										MOL WT
	H <sub>2</sub> O	H <sub>2</sub>	O <sub>2</sub>	O	OH	H	CO	CO <sub>2</sub>			
4000	0.02969	0.10030	0.02854	0.24971	0.08941	0.50236	-	-	-	7.67	
3800	0.07636	0.14172	0.04239	0.20253	0.12290	0.41410	-	-	-	8.77	
3600	0.16841	0.17597	0.05485	0.14653	0.14686	0.30737	-	-	-	10.30	
3400	0.30930	0.18731	0.06045	0.09282	0.14865	0.20147	-	-	-	12.10	
3200	0.47832	0.17070	0.05685	0.05100	0.12758	0.11556	-	-	-	13.88	
3000	0.64311	0.13486	0.04632	0.02420	0.09380	0.05773	-	-	-	15.38	
2800	0.77866	0.09363	0.03320	0.00983	0.05975	0.02493	-	-	-	16.48	
2600	0.87587	0.05743	0.02105	0.00335	0.03313	0.00916	-	-	-	17.20	
2400	0.93755	0.03105	0.01179	0.00093	0.01588	0.00279	-	-	-	17.62	
2200	0.97228	0.01462	0.00576	0.00020	0.00646	0.00068	-	-	-	17.84	
2000	0.98947	0.00583	0.00239	0.00003	0.00216	0.00012	-	-	-	17.95	
1800	0.99673	0.00189	0.00081	0.00000	0.00056	0.00002	-	-	-	18.00	
1600	0.99925	0.00046	0.00021	0.00000	0.00010	0.00000	-	-	-	18.01	
1400	0.99988	0.00008	0.00004	0.00000	0.00001	0.00000	-	-	-	18.02	
1200	0.99999	0.00001	0.00000	0.00000	0.00000	0.00000	-	-	-	18.02	
1000	0.99999	0.00001	0.00000	0.00000	0.00000	0.00000	-	-	-	18.02	
800	0.99999	0.00001	0.00000	0.00000	0.00000	0.00000	-	-	-	18.02	
600	0.99999	0.00001	0.00000	0.00000	0.00000	0.00000	-	-	-	18.02	
400	0.99999	0.00001	0.00000	0.00000	0.00000	0.00000	-	-	-	18.02	
300	0.99999	0.00001	0.00000	0.00000	0.00000	0.00000	-	-	-	18.02	

TEMP (K)	MIXTURE ENTHALPY (MJ/kg)	FROZEN SP. HEAT (J/kgK)	EQUIL'M SP. HEAT (J/kgK)	FROZEN CONDY (W/mK)	EQUIL'M CONDY (W/mK)	MIXTURE DENSITY (kg/m <sup>3</sup> )	MIXTURE VISCOSY (μNs/m <sup>2</sup> )	EQUIL'M PRANDTL NUMBER		
									CO	CO <sub>2</sub>
4000	47.294093	3391	75705	0.7350	-	0.0240	88.46	-	-	-
3800	38.821405	3338	59319	0.6906	-	0.0288	88.96	-	-	-
3600	29.925618	3282	45450	0.6348	-	0.0352	89.87	-	-	-
3400	22.139566	3228	33952	0.5710	-	0.0432	90.32	-	-	-
3200	16.194077	3179	24659	0.5062	5.2984	0.0529	89.62	0.4466	0.4466	-
3000	12.004971	3133	17581	0.4482	3.4481	0.0625	87.59	0.4711	0.4711	-
2800	9.154206	3087	11787	0.3989	2.1109	0.0721	84.37	0.5106	0.5106	-
2600	7.223858	3038	7995	0.3583	1.2596	0.0801	80.44	0.5615	0.5615	-
2400	5.835478	2983	5460	0.3228	0.7620	0.0897	75.81	0.6655	0.6655	-
2200	4.930420	2922	4238	0.2911	0.4875	0.0992	70.81	0.7195	0.7195	-
2000	4.164238	2850	3440	0.2624	0.3406	0.1089	65.85	0.7678	0.7678	-
1800	3.527379	2767	2783	0.2262	0.2333	0.1217	60.35	0.8092	0.8092	-
1600	2.962161	2670	2683	0.1893	0.1905	0.1378	54.52	0.8444	0.8444	-
1400	2.434392	2558	2560	0.1530	0.1530	0.1570	48.40	0.8681	0.8681	-
1200	1.933836	2430	2450	0.1212	0.1212	0.1626	42.08	0.9095	0.9095	-
1000	1.462124	2291	2291	0.0938	0.0938	0.2194	35.55	0.9212	0.9212	-
800	1.018323	2149	2149	0.0673	0.0673	0.2739	28.52	0.9847	0.9847	-
600	0.601969	2017	2017	0.0466	0.0466	0.3652	21.25	1.0824	1.0824	-
400	0.210503	1902	1902	0.0268	0.0268	0.5494	13.89	-	-	-
300	0.022330	1866	1866	0.0176	0.0176	0.7320	10.21	-	-	-

TEMP (K)	COMPOSITION							MOL WT.	
	H <sub>2</sub> O	H <sub>2</sub>	O <sub>2</sub>	O	OH	H	CO		CO <sub>2</sub>
4000	0.01325	0.03713	0.04145	0.30096	0.06556	0.30566	0.22668	0.00931	14.64
3800	0.02458	0.05259	0.06312	0.24714	0.09136	0.25225	0.24074	0.01863	16.06
3600	0.07740	0.06455	0.08609	0.18359	0.11144	0.18617	0.25386	0.03690	18.03
3400	0.14394	0.06672	0.10318	0.12126	0.11591	0.12025	0.25873	0.07001	20.39
3200	0.22501	0.05832	0.10777	0.07022	0.10268	0.06755	0.24501	0.12744	22.85
3000	0.30617	0.04425	0.09752	0.03511	0.07796	0.03307	0.20835	0.19758	25.18
2800	0.37592	0.02992	0.07580	0.01485	0.05103	0.01409	0.15501	0.28338	27.19
2600	0.42866	0.01821	0.05016	0.00518	0.02880	0.00516	0.09910	0.36474	28.77
2400	0.46371	0.00996	0.02806	0.00144	0.01387	0.00158	0.05374	0.42764	29.86
2200	0.48397	0.00482	0.01315	0.00031	0.00560	0.00039	0.02438	0.46739	30.50
2000	0.49402	0.00200	0.00504	0.00005	0.00184	0.00046	0.00901	0.48796	30.83
1800	0.49820	0.00068	0.00153	0.00000	0.00046	0.00001	0.00260	0.49652	30.96
1600	0.49959	0.00018	0.00034	0.00000	0.00008	0.00000	0.00054	0.49927	31.00
1400	0.49994	0.00003	0.00005	0.00000	0.00001	0.00000	0.00007	0.49990	31.01
1200	0.50000	0.00000	0.00001	0.00000	0.00000	0.00000	0.00000	0.49999	31.01
1000	0.50000	0.00000	0.00001	0.00000	0.00000	0.00000	0.00000	0.49999	31.01
800	0.50000	0.00000	0.00001	0.00000	0.00000	0.00000	0.00000	0.49999	31.01
600	0.50000	0.00000	0.00001	0.00000	0.00000	0.00000	0.00000	0.49999	31.01
400	0.50000	0.00000	0.00001	0.00000	0.00000	0.00000	0.00000	0.49999	31.01
300	0.50000	0.00000	0.00001	0.00000	0.00000	0.00000	0.00000	0.49999	31.01

TEMP (K)	MIXTURE ENTHALPY (MJ/kg)	EQUIL'M SP. HEAT (J/kgK)	FROZEN SP. HEAT (J/kgK)	FROZEN COND. (W/mK)	EQUIL'M COND. (W/mK)	MIXTURE DENSITY (kg/m <sup>3</sup> )	MIXTURE VISCOSITY (N·s/m <sup>2</sup> )	EQUIL'M FRANDTL NUMBER
3800	21.425483	21214	1918	0.3979	-	0.0512	97.14	-
3600	17.694347	19230	1901	0.3603	-	0.0608	95.28	-
3400	14.111376	16673	1886	0.3224	-	0.0737	93.09	-
3200	11.037102	13861	1877	0.2887	2.9536	0.0669	90.28	0.4237
3000	8.552702	11059	1871	0.2616	2.1240	0.1021	86.85	0.4237
2800	6.610724	8470	1866	0.2400	1.4429	0.1183	82.88	0.4865
2600	5.144879	6245	1858	0.2220	0.9296	0.1348	78.58	0.5279
2400	4.080269	4474	1845	0.2058	0.5971	0.1515	74.16	0.5557
2200	3.322458	3199	1826	0.1902	0.3898	0.1682	69.70	0.5720
2000	2.769800	2388	1800	0.1750	0.2477	0.1874	65.19	0.6285
1800	2.335769	1971	1766	0.1568	0.1810	0.2098	60.56	0.6595
1600	1.961748	1781	1725	0.1384	0.1404	0.2355	55.72	0.7067
1400	1.615639	1681	1676	0.1195	0.1196	0.2691	50.64	0.7120
1200	1.285347	1616	1615	0.1020	0.1020	0.3156	45.22	0.7164
1000	0.969709	1542	1542	0.0836	0.0836	0.3780	39.44	0.7273
800	0.669888	1454	1454	0.0642	0.0642	0.4725	33.07	0.7489
600	0.389139	1349	1349	0.0460	0.0460	0.6295	26.00	0.7619
400	0.131884	1219	1219	0.0275	0.0275	0.9451	18.06	0.8003
300	0.013723	1142	1142	0.0183	0.0183	1.2530	13.72	0.8507

TEMP (K)	COMPOSITION										MOL WT.
	H <sub>2</sub> O	H <sub>2</sub>	O <sub>2</sub>	O	OH	H	CO	CO <sub>2</sub>			
4000	0.01573	0.04540	0.03911	0.29233	0.07042	0.33799	0.19137	0.00763			13.54
3800	0.04085	0.06403	0.05942	0.23980	0.09782	0.27835	0.20435	0.01537			14.95
3600	0.09092	0.07832	0.08071	0.17775	0.11885	0.20506	0.23980	0.03065			16.90
3400	0.16818	0.08076	0.09614	0.11705	0.12309	0.13229	0.23980	0.05850			19.22
3200	0.26163	0.07047	0.09982	0.06758	0.10861	0.07425	0.21392	0.10372			21.61
3000	0.35434	0.05332	0.08996	0.03372	0.08219	0.06330	0.18326	0.16692			23.82
2800	0.43317	0.03591	0.06983	0.01426	0.05367	0.01544	0.13712	0.24061			25.70
2600	0.49220	0.02177	0.04624	0.00497	0.03024	0.00564	0.08799	0.31095			27.14
2400	0.53117	0.01186	0.02593	0.00139	0.01456	0.00173	0.04779	0.36558			28.12
2200	0.55362	0.00572	0.01219	0.00030	0.00588	0.00042	0.02168	0.40019			28.70
2000	0.56477	0.00237	0.00470	0.00005	0.00193	0.00000	0.00800	0.41811			28.99
1800	0.56941	0.00081	0.00143	0.00000	0.00049	0.00001	0.00230	0.42555			29.11
1600	0.57097	0.00021	0.00032	0.00000	0.00009	0.00000	0.00047	0.42794			29.15
1400	0.57136	0.00004	0.00005	0.00000	0.00001	0.00000	0.00006	0.42849			29.16
1200	0.57142	0.00000	0.00001	0.00000	0.00000	0.00000	0.00000	0.42857			29.16
1000	0.57142	0.00000	0.00001	0.00000	0.00000	0.00000	0.00000	0.42857			29.16
800	0.57142	0.00000	0.00001	0.00000	0.00000	0.00000	0.00000	0.42857			29.16
600	0.57142	0.00000	0.00001	0.00000	0.00000	0.00000	0.00000	0.42857			29.16
400	0.57142	0.00000	0.00001	0.00000	0.00000	0.00000	0.00000	0.42857			29.16
300	0.57142	0.00000	0.00001	0.00000	0.00000	0.00000	0.00000	0.42857			29.16

TEMP (K)	MIXTURE ENTHALPY (KJ/kg)	FROZEN SP. HEAT (J/kgK)	EQUIL'M SP. HEAT (J/kgK)	FROZEN COND'Y W/mk	EQUIL'M COND'Y W/mk	MIXTURE DENSITY (kg/m <sup>3</sup> )	MIXTURE VISCOSY (μNs/m <sup>2</sup> )	EQUIL'M FRANDTL NUMBER		
4000	26.785286	2065	27342	0.4679	-	0.0416	97.97	-		
3800	22.997860	2044	24764	0.4321	-	0.0481	96.36	-		
3600	18.803384	2022	21619	0.3907	-	0.0577	94.83	-		
3400	14.840578	2004	18216	0.3485	-	0.0689	92.93	-		
3200	11.510444	1990	14812	0.3108	3.2136	0.0823	90.32	0.4163		
3000	8.771799	1981	11616	0.2806	2.2873	0.0968	87.10	0.4423		
2800	6.854955	1972	8784	0.2564	1.5254	0.1118	83.21	0.4792		
2600	5.343520	1961	6424	0.2366	0.9727	0.1271	79.00	0.5218		
2400	4.248904	1946	4591	0.2188	0.6077	0.1427	74.57	0.5635		
2200	3.167601	1922	3293	0.2018	0.3847	0.1589	70.07	0.5998		
2000	2.894474	1892	2484	0.1851	0.2596	0.1762	65.48	0.6266		
1800	2.441835	1855	2070	0.1651	0.1898	0.1970	60.73	0.6622		
1600	2.050136	1809	1906	0.1450	0.1520	0.2226	55.80	0.7001		
1400	1.687978	1753	1797	0.1242	0.1242	0.2530	50.60	0.7315		
1200	1.342860	1687	1687	0.1050	0.1050	0.2963	45.10	0.7242		
1000	1.013206	1608	1608	0.0857	0.0957	0.3556	29.19	0.7354		
800	0.700591	1516	1516	0.0654	0.0654	0.4437	32.74	0.7585		
600	0.407980	1408	1408	0.0467	0.0467	0.5927	17.69	0.7722		
400	0.138862	1279	1279	0.0279	0.0279	0.8874	13.35	0.8124		
300	0.014421	1206	1206	0.0185	0.0185	1.1838	18.94	0.8681		

TABLE 12e CARBON MONOXIDE OXYGEN

TEMP (K)	COMPOSITION								MOL WT.
	H <sub>2</sub> O	H <sub>2</sub>	O <sub>2</sub>	O	OH	H	CO	CO <sub>2</sub>	
4000	0.00000	0.00000	0.03898	0.29184	0.00000	0.00000	0.50935	0.02029	21.08
3800	0.00000	0.00000	0.10584	0.32003	0.00000	0.00000	0.52649	0.05285	25.58
3600	0.00000	0.00000	0.18363	0.26812	0.00000	0.00000	0.53502	0.11358	30.15
3400	0.00000	0.00000	0.22132	0.17759	0.00000	0.00000	0.50967	0.20198	33.09
3200	0.00000	0.00000	0.21339	0.09881	0.00000	0.00000	0.44792	0.31725	34.93
3000	0.00000	0.00000	0.17690	0.04729	0.00000	0.00000	0.35911	0.45867	36.66
2800	0.00000	0.00000	0.12832	0.01932	0.00000	0.00000	0.25769	0.61255	38.61
2600	0.00000	0.00000	0.08090	0.00658	0.00000	0.00000	0.16195	0.75700	40.55
2400	0.00000	0.00000	0.04372	0.00180	0.00000	0.00000	0.08746	0.86880	42.11
2200	0.00000	0.00000	0.01992	0.00038	0.00000	0.00000	0.03984	0.9403	43.14
2000	0.00000	0.00000	0.00744	0.00006	0.00000	0.00000	0.01487	0.97769	43.68
1800	0.00000	0.00000	0.00218	0.00001	0.00000	0.00000	0.00435	0.99347	43.92
1600	0.00000	0.00000	0.00046	0.00000	0.00000	0.00000	0.00092	0.99862	43.99
1400	0.00000	0.00000	0.00006	0.00000	0.00000	0.00000	0.00012	0.99981	44.01
1200	0.00000	0.00000	0.00000	0.00000	0.00000	0.00000	0.00001	0.99999	44.01
1000	0.00000	0.00000	0.00000	0.00000	0.00000	0.00000	0.00001	0.99999	44.01
800	0.00000	0.00000	0.00000	0.00000	0.00000	0.00000	0.00001	0.99999	44.01
600	0.00000	0.00000	0.00000	0.00000	0.00000	0.00000	0.00001	0.99999	44.01
400	0.00000	0.00000	0.00000	0.00000	0.00000	0.00000	0.00001	0.99999	44.01
300	0.00000	0.00000	0.00000	0.00000	0.00000	0.00000	0.00001	0.99999	44.01

TEMP (K)	MIXTURE ENTHALPY (MJ/kg)	FROZEN SP. HEAT (J/kgK)	EQUIL'M SP. HEAT (J/kgK)	FROZEN COND <sup>y</sup> W/mK	EQUIL'M COND <sup>y</sup> W/mK	MIXTURE DENSITY (kg/m <sup>3</sup> )	MIXTURE VISCOS <sup>y</sup> (μNs/m <sup>2</sup> )	EQUIL'M FRAUDTL NUMBER	
3800	13.377756	1340	-	0.1953	-	0.0817	100.69	-	
3600	11.388096	1340	8754.	0.1883	-	0.1025	97.68	-	
3400	9.579165	1344	8633	0.1802	-	0.1185	93.96	-	
3200	7.964456	1352	8002	0.1713	1.0912	0.1330	89.62	0.5572	
3000	6.480003	1362	7042	0.1625	0.9488	0.1489	85.03	0.6311	
2800	5.154881	1373	5908	0.1535	0.7693	0.1682	80.24	0.6162	
2600	4.059102	1380	4734	0.1445	0.5714	0.1906	75.48	0.6253	
2400	3.224533	1382	3629	0.1357	0.3913	0.2130	70.98	0.6582	
2200	2.621169	1379	2679	0.1270	0.2577	0.2387	66.72	0.6937	
2000	2.182485	1370	1947	0.1183	0.1739	0.2659	62.58	0.7006	
1800	1.842192	1357	1471	0.1094	0.1282	0.2972	58.41	0.6701	
1600	1.550744	1339	1350	0.1007	0.1054	0.3348	54.03	0.6223	
1400	1.280230	1314	1326	0.0914	0.0914	0.3628	49.44	0.7176	
1200	1.019713	1281	1281	0.0817	0.0817	0.4169	44.52	0.6982	
1000	0.768045	1235	1235	0.0690	0.0690	0.5766	39.31	0.7029	
800	0.527071	1169	1169	0.0549	0.0549	0.6696	33.60	0.7163	
600	0.302147	1076	1076	0.0398	0.0398	0.8938	27.15	0.7341	
400	0.099552	939	939	0.0242	0.0242	1.3407	19.59	0.7587	
300	0.010234	846	846	0.0164	0.0164	1.7877	15.21		

COMPOSITION

TEMP (K)	COMPOSITION											MOL WT.
	N <sub>2</sub>	H <sub>2</sub> O	H <sub>2</sub>	O <sub>2</sub>	O	OH	H	NO	N	CO	CO <sub>2</sub>	
4000	0.50545	0.00298	0.01779	0.00917	0.14156	0.02134	0.21155	0.02039	0.00125	0.06731	0.00130	20.03
3800	0.52352	0.00859	0.02718	0.01459	0.11883	0.03158	0.18136	0.02265	0.00059	0.06857	0.00256	20.77
3600	0.54979	0.02169	0.03673	0.02088	0.09042	0.04140	0.14043	0.02372	0.00026	0.06968	0.00499	21.80
3400	0.58251	0.04536	0.04185	0.02605	0.06092	0.04612	0.09524	0.02289	0.00010	0.06951	0.00945	23.05
3200	0.61678	0.07776	0.03950	0.02806	0.03583	0.04312	0.05559	0.02005	0.00000	0.06628	0.01704	24.32
3000	0.64867	0.11319	0.03169	0.02598	0.01812	0.03405	0.02523	0.01579	0.00000	0.05859	0.02868	25.48
2800	0.67210	0.14154	0.02128	0.02125	0.00786	0.02278	0.01188	0.01123	0.00000	0.04578	0.04431	26.30
2600	0.69018	0.16292	0.01279	0.01470	0.00280	0.01306	0.00432	0.00702	0.00000	0.03087	0.06139	26.97
2400	0.70224	0.17648	0.00687	0.00854	0.00080	0.00536	0.00131	0.00381	0.00000	0.01736	0.07623	27.33
2200	0.70931	0.18406	0.00327	0.00412	0.00017	0.00258	0.00032	0.00176	0.00000	0.00805	0.08635	27.56
2000	0.71285	0.18778	0.00135	0.00162	0.00003	0.00085	0.00006	0.00067	0.00000	0.00300	0.09180	27.68
1900	0.71432	0.18934	0.00046	0.00030	0.00000	0.00021	0.00001	0.00020	0.00000	0.00086	0.09410	27.73
1600	0.71480	0.1888	0.00012	0.00011	0.00000	0.00004	0.00000	0.00005	0.00000	0.00018	0.09483	27.74
1400	0.71492	0.19003	0.00001	0.00007	0.00000	0.00001	0.00000	0.00001	0.00000	0.00001	0.09502	27.75
1200	0.71493	0.19004	0.00000	0.00000	0.00000	0.00000	0.00000	0.00000	0.00000	0.00000	0.09503	27.75
1000	0.71493	0.19004	0.00000	0.00000	0.00000	0.00000	0.00000	0.00000	0.00000	0.00000	0.09503	27.75
800	0.71493	0.19004	0.00000	0.00000	0.00000	0.00000	0.00000	0.00000	0.00000	0.00000	0.09503	27.75
600	0.71493	0.19004	0.00000	0.00000	0.00000	0.00000	0.00000	0.00000	0.00000	0.00000	0.09503	27.75
400	0.71493	0.19004	0.00000	0.00000	0.00000	0.00000	0.00000	0.00000	0.00000	0.00000	0.09503	27.75
300	0.71493	0.19004	0.00000	0.00000	0.00000	0.00000	0.00000	0.00000	0.00000	0.00000	0.09503	27.75

TEMP (K)	MIXTURE ENTHALPY (MJ/kg)	FROZEN SP. HEAT (J/kgK)	EQUILM SP. HEAT (J/kgK)	FROZEN CONDY (W/mK)	EQUILM CONDY (W/mK)	MIXTURE DENSITY (kg/m <sup>3</sup> )	MIXTURE VISCOSY (μNs/m <sup>2</sup> )	EQUILM PRANDTL NUMBER
4000	12.386880	1590	-	0.3146	1.2029	0.0610	97.55	-
3800	11.223415	1582	-	0.2944	1.5685	0.0566	94.70	-
3600	9.801764	1572	-	0.2710	1.8499	0.0738	91.94	-
3400	8.263813	1561	7632	0.2461	1.8639	0.0826	89.08	0.3648
3200	6.810993	1552	6785	0.2222	1.5921	0.0926	86.02	0.3666
3000	5.543091	1542	5563	0.2009	1.4886	0.1033	82.72	0.3872
2800	4.581290	1534	4415	0.1850	1.4099	0.1144	79.16	0.4226
2600	3.797195	1527	3459	0.1715	0.9277	0.1261	75.48	0.4947
2400	3.185457	1516	2692	0.1597	0.3435	0.1387	71.63	0.5615
2200	2.707999	1502	2127	0.1485	0.2333	0.1526	67.58	0.6165
2000	2.321115	1485	1764	0.1376	0.1715	0.1686	63.53	0.6537
1800	1.990358	1463	1564	0.1255	0.1366	0.1876	59.28	0.6792
1600	1.688676	1437	1462	0.1128	0.1154	0.2112	54.85	0.6953
1400	1.401648	1403	1406	0.0999	0.0999	0.2414	50.23	0.7072
1200	1.124621	1362	1362	0.0870	0.0871	0.2816	45.43	0.7103
1000	0.857131	1312	1312	0.0739	0.0738	0.3380	40.18	0.7137
800	0.600573	1251	1251	0.0600	0.0600	0.4225	34.56	0.7207
600	0.358161	1187	1187	0.0465	0.0465	0.5633	28.28	0.7223
400	0.12662	1130	1130	0.0326	0.0326	0.8449	21.04	0.7301
300	0.013228	1106	1106	0.0243	0.0243	1.1735	16.82	0.7391

TEMP (K)	COMPOSITION											MOL WT
	H <sub>2</sub>	H <sub>2</sub> O	H <sub>2</sub>	O <sub>2</sub>	O	OH	H	HO	N	CO	CO <sub>2</sub>	
4000	0.51068	0.00279	0.01565	0.00913	0.14125	0.02061	0.20468	0.02035	0.00125	0.07124	0.00137	
3800	0.52831	0.00806	0.02353	0.01456	0.11871	0.03058	0.17576	0.02271	0.00059	0.07249	0.00270	
3600	0.55432	0.02046	0.03462	0.02032	0.09049	0.04023	0.17634	0.02503	0.00026	0.07355	0.00527	
3400	0.58615	0.04302	0.05957	0.02621	0.06111	0.04498	0.09250	0.02303	0.00010	0.07324	0.00999	
3200	0.61934	0.07404	0.07740	0.02837	0.03603	0.04219	0.05409	0.02021	0.00000	0.06971	0.01802	
3000	0.65038	0.10700	0.02958	0.02665	0.01835	0.03332	0.02704	0.01601	0.00000	0.06129	0.03036	
2800	0.67493	0.15227	0.02014	0.02165	0.00794	0.02238	0.01156	0.01136	0.00000	0.04794	0.04683	
2600	0.69310	0.15582	0.01211	0.01499	0.00283	0.01284	0.00421	0.00711	0.00000	0.02221	0.06480	
2400	0.70528	0.16885	0.00651	0.00870	0.00080	0.00325	0.00128	0.00386	0.00000	0.01813	0.08034	
2200	0.71244	0.17614	0.00311	0.00017	0.00000	0.00000	0.00031	0.00178	0.00000	0.00841	0.09092	
2000	0.71603	0.17971	0.00128	0.00163	0.00003	0.00083	0.00006	0.00068	0.00000	0.00314	0.09660	
1800	0.71752	0.18121	0.00044	0.00049	0.00000	0.00021	0.00001	0.00020	0.00000	0.00092	0.09300	
1600	0.71801	0.18172	0.00012	0.00009	0.00000	0.00004	0.00000	0.00004	0.00000	0.00020	0.09377	
1400	0.71812	0.18184	0.00004	0.00000	0.00000	0.00000	0.00000	0.00000	0.00000	0.00005	0.09934	
1200	0.71812	0.18184	0.00000	0.00000	0.00000	0.00000	0.00000	0.00000	0.00000	0.00000	0.09996	
1000	0.71812	0.18184	0.00000	0.00000	0.00000	0.00000	0.00000	0.00000	0.00000	0.00000	0.09996	
800	0.71812	0.18184	0.00000	0.00000	0.00000	0.00000	0.00000	0.00000	0.00000	0.00000	0.09996	
600	0.71812	0.18184	0.00000	0.00000	0.00000	0.00000	0.00000	0.00000	0.00000	0.00000	0.09996	
400	0.71812	0.18184	0.00000	0.00000	0.00000	0.00000	0.00000	0.00000	0.00000	0.00000	0.09996	
288	0.71812	0.18184	0.00000	0.00000	0.00000	0.00000	0.00000	0.00000	0.00000	0.00000	0.09996	

TEMP (K)	MIXTURE ENTHALPY (MJ/kg)	FROZEN SP. HEAT (J/kgK)	EQUILM SP. HEAT (J/kgK)	FROZEN COND. (W/mK)	EQUILM COND. (W/mK)	MIXTURE DENSITY (kg/m <sup>3</sup> )	MIXTURE VISCOSITY (μNs/m <sup>2</sup> )	EQUILM FRANZL NUMBER
4000	12.18405	1580	-	0.3094	1.1531	0.0617	97.64	-
3800	11.05846	1571	-	0.2899	1.5051	0.0573	94.80	-
3600	9.68066	1561	-	0.2671	1.7826	0.0744	91.98	-
3400	8.18400	1550	7444	0.2428	1.8063	0.0832	89.11	0.3672
3200	6.76266	1540	6655	0.2196	1.5516	0.0932	86.03	0.3690
3000	5.54741	1531	5490	0.1995	1.1644	0.1039	82.71	0.3500
2800	4.56303	1523	4382	0.1833	0.7971	0.1151	79.15	0.4351
2600	3.78279	1515	3446	0.1700	0.5216	0.1268	75.44	0.4585
2400	3.17234	1505	2686	0.1584	0.3406	0.1395	71.59	0.5647
2200	2.69504	1492	2121	0.1474	0.2317	0.1535	67.56	0.6186
2000	2.31035	1475	1757	0.1366	0.1704	0.1696	63.48	0.6548
1800	1.98108	1454	1556	0.1246	0.1358	0.1887	59.26	0.6793
1600	1.68094	1428	1456	0.1122	0.1149	0.2124	54.83	0.6947
1400	1.39570	1396	1400	0.0994	0.004	0.2428	50.21	0.7092
1200	1.12015	1355	1355	0.0868	0.0868	0.2833	45.42	0.7093
1000	0.85382	1305	1305	0.0736	0.0736	0.3400	40.17	0.7126
800	0.59854	1246	1246	0.0598	0.0598	0.4249	34.54	0.7194
600	0.35567	1181	1181	0.0464	0.0464	0.5666	28.30	0.7210
400	0.12532	1124	1124	0.0325	0.0325	0.8499	21.07	0.7286
288	0.00076	1100	1100	0.0243	0.0243	1.1804	16.28	0.7370

APPENDIX 2

DERIVATION OF TRANSFORMATION EQUATIONS FOR THE NUMERICAL SOLUTION PROCEDURE

The equation of state for a perfect gas is

$$P_1 = \rho_1 R_1 T$$

where the total pressure P is given by

$$P = \sum_1 P_1 = \bar{c} \bar{R} T$$

and  $\bar{R}$  is the gas constant for the mixture.

The continuity equation is

$$\frac{\partial(ru\rho)}{\partial x} + \frac{\partial(rv\rho)}{\partial y} = 0$$

$$\text{or } \frac{\partial}{\partial x} \left( \frac{ruP_e}{RT} \right) + \frac{\partial}{\partial y} \left( \frac{rvP_e}{RT} \right) = 0$$

This may be expanded to give

$$rP_e \frac{\partial}{\partial x} \left( \frac{u}{RT} \right) + \frac{u}{RT} \frac{\partial}{\partial x} (rP_e) + rP_e \frac{\partial}{\partial y} \left( \frac{v}{RT} \right) + \frac{v}{RT} \frac{\partial}{\partial y} (rP_e) = 0$$

$$\text{or } \frac{\partial}{\partial x} \left( \frac{u}{RT} \right) + \frac{\partial}{\partial y} \left( \frac{v}{RT} \right) = - \frac{u}{RT r P_e} \frac{\partial}{\partial x} (rP_e) \text{ since } P_e r \neq f(y) \quad \dots (1)$$

$$\text{Now let } \Psi(x, y) = \int_0^y \frac{u}{RT} dy + \Psi(x, 0)$$

$$\text{so that } \frac{\partial \Psi}{\partial y} = \frac{u}{RT} \quad \dots (2)$$

substituting 2 into 1

$$\frac{\partial}{\partial x} \frac{\partial \Psi}{\partial y} + \frac{\partial}{\partial y} \left( \frac{v}{RT} \right) = - \frac{1}{rP_e} \frac{\partial \Psi}{\partial y} \frac{\partial}{\partial x} (rP_e)$$

integrating with respect to y

$$\frac{v}{RT} = - \frac{\partial \Psi}{\partial x} - \frac{\Psi}{rP_e} \frac{\partial}{\partial x} (rP_e) \quad \dots (3)$$

Taking the momentum equations 4 and 5 in conjunction with 2 and 3

$$\rho u \frac{\partial u}{\partial x} + \rho u \frac{\partial u}{\partial y} = - \frac{\partial P}{\partial x} + \frac{\partial}{\partial y} \left( \mu \frac{\partial u}{\partial y} \right) \quad \dots (4)$$

$$\frac{\partial P}{\partial y} = 0 \quad \dots (5)$$

$$u \frac{P_e}{RT} \frac{\partial u}{\partial x} + v \frac{P_e}{RT} \frac{\partial u}{\partial y} = - \frac{dP_e}{dx} + \frac{\partial}{\partial y} \left( \mu \frac{\partial u}{\partial y} \right)$$

$$\frac{\partial \Psi}{\partial y} \frac{\partial u}{\partial x} - \frac{\partial u}{\partial y} \left[ \frac{\partial \Psi}{\partial x} - \frac{\Psi}{rP_e} \frac{\partial}{\partial x} (P_e r) \right] = - \frac{1}{P_e} \frac{dP_e}{dx} + \frac{1}{P_e} \frac{\partial}{\partial y} \left( \mu \frac{\partial u}{\partial y} \right) \dots (6)$$

It is now necessary to obtain a 'similar' solution to the above equation so that  $\Psi$  and  $v$  are given by

$$\Psi(x, \eta) = N(x) f(\eta) \dots (7)$$

$$u(x, \eta) = U_e(x) f'(\eta) \dots (8)$$

From 2 and 7

$$\frac{\partial \Psi}{\partial y} = \frac{u}{RT} = \frac{\partial \Psi \partial \eta}{\partial \eta \partial y} = N(x) f'(\eta) \frac{\partial \eta}{\partial y}$$

From 8

$$\frac{u}{RT} = \frac{u_e(x) f'(\eta)}{RT}$$

so that 
$$\frac{u_e(x) f'(\eta)}{RT} = N(x) f'(\eta) \frac{\partial \eta}{\partial y}$$

or 
$$N(x) \frac{\partial \eta}{\partial y} = \frac{u_e(x)}{RT}$$

thus 
$$\eta = \frac{u_e(x)}{N(x)} \int_0^y \frac{dy}{RT}$$

$$= \frac{\rho_e u_e(x)}{P_e N(x)} \int_0^y \frac{\rho}{\rho_e} dy$$

From the similarity criteria 7 and 8 it is clear that

(a) 
$$\frac{\partial \Psi}{\partial y} = \frac{\partial \Psi}{\partial \eta} \frac{\partial \eta}{\partial y} = \frac{\partial \Psi}{\partial \eta} \frac{\rho u_e(x)}{P_e N(x)} = \frac{\rho u_e}{P_e} f'$$

(b) 
$$\frac{\partial u}{\partial x} = f' \frac{\partial u_e(x)}{\partial x} + u_e(x) \frac{\partial f'}{\partial x}$$

$$= f' \frac{\partial u_e(x)}{\partial x} + u_e(x) f'' \frac{\partial \eta}{\partial x} \text{ since } \frac{\partial f'}{\partial x} = \frac{\partial f'}{\partial \eta} \frac{\partial \eta}{\partial x}$$

(c) 
$$\frac{\partial \Psi}{\partial x} = f \frac{\partial N(x)}{\partial x} + N(x) \frac{\partial f}{\partial x}$$

$$= f \frac{\partial N(x)}{\partial x} + N(x) f' \frac{\partial \eta}{\partial x} \text{ since } \frac{\partial f}{\partial x} = \frac{\partial f}{\partial \eta} \frac{\partial \eta}{\partial x}$$

$$\begin{aligned}
 (d) \quad \mu \frac{\partial u}{\partial y} &= \mu \frac{\partial u}{\partial \eta} \frac{\partial \eta}{\partial y} = \mu \left[ \frac{\partial u_e(x)}{\partial \eta} f' + \frac{\partial f'}{\partial \eta} u_e(x) \right] \frac{\partial \eta}{\partial y} \\
 &= \frac{\rho \mu u_e^2}{P_e N(x)} f'' \quad \text{since} \quad \frac{\partial u_e(x)}{\partial \eta} = 0 \\
 &= \frac{\rho_e \mu_e u_e^2}{P_e N(x)} C f'' \quad \text{where} \quad C = \frac{\rho \mu}{\rho_e \mu_e}
 \end{aligned}$$

Substitute into momentum equation 6

$$\begin{aligned}
 \frac{\rho u_e}{P_e} f' \left[ f' \frac{du_e}{dx} + u_e f'' \frac{d\eta}{dx} \right] - \left[ \frac{\partial \Psi}{\partial x} + \frac{N(x)f}{P_e r} \frac{d(P_e r)}{dx} \right] \frac{\mu u_e^2}{P_e N(x)} f'' \\
 = + \frac{1}{P_e} \rho_e u_e \frac{du_e}{dx} + \frac{1}{P_e} \frac{\partial}{\partial y} \left[ \frac{\rho_e \mu_e u_e^2}{P_e N(x)} C f'' \right] \\
 \left[ \frac{\rho u_e}{P_e} (f')^2 + u_e f'' \frac{d\eta}{dx} \frac{dx}{du_e} \right] \frac{du_e}{dx} - \left[ \frac{\partial \Psi}{\partial x} + \frac{f N(x)}{P_e r} \frac{d(P_e r)}{dx} \right] \frac{\rho u_e^2 f''}{P_e N(x)} \\
 - \frac{\rho_e u_e}{P_e} \frac{du_e}{dx} \\
 = \frac{1}{P_e} \frac{\partial \eta}{\partial y} \frac{\partial}{\partial \eta} \left[ \frac{\rho_e \mu_e u_e^2}{P_e N(x)} C f'' \right] \\
 = \frac{1}{P_e} \frac{\rho u_e}{P_e N(x)} \frac{\rho_e \mu_e u_e^2}{P_e N(x)} (C f'')'
 \end{aligned}$$

but  $\frac{\partial \eta}{\partial x} = 0$  so that

$$\begin{aligned}
 \left[ \frac{\rho u_e}{P_e} (f')^2 - \frac{\rho_e u_e}{P_e} \right] \frac{du_e}{dx} - \left[ f \frac{dN(x)}{dx} + \frac{f N(x)}{P_e r} \frac{d(P_e r)}{dx} \right] \frac{\rho u_e^2}{P_e N(x)} f'' \\
 = \frac{1}{P_e} \frac{\rho u_e}{P_e N(x)} \frac{\rho_e \mu_e u_e^2}{P_e N(x)} (C f'')'
 \end{aligned}$$

$$\text{Now} \quad \frac{f}{P_e r} \frac{d(NP_e r)}{dx} = \frac{f}{P_e r} P_e r \frac{dN(x)}{dx} + \frac{f}{P_e r} N(x) \frac{d(P_e r)}{dx}$$

So that

$$(Cf'')' \frac{1}{P_e} \frac{\rho_e u_e}{P_e N} \frac{\rho_e u_e u_e^2}{P_e N} + \left[ \frac{\rho_e u_e}{P_e} - \frac{\rho_e u_e (f')^2}{P_e} \right] \frac{du_e}{dx} + \frac{f}{P_e r} \frac{d(NP_e r)}{dx} \frac{\rho_e u_e^2 f''}{P_e N} = 0$$

or rearranging

$$(Cf'')' \frac{\rho_e \mu_e r u_e}{P_e N [d(NP_e r)/dx]} + \frac{r}{[d(NP_e r)/dx]} \frac{P_e^2 N}{\rho_e u_e^2} \left[ \frac{\rho_e u_e}{P_e} - \frac{\rho_e u_e (f')^2}{P_e} \right] \frac{du_e}{dx} + \frac{r P_e^2 N}{\rho_e u_e^2} \frac{f}{P_e r} \frac{\rho_e u_e^2 f''}{P_e N} = 0$$

$$(Cf'')' \frac{\rho_e \mu_e r u_e}{P_e N [d(NP_e r)/dx]} + ff'' + \frac{1}{u_e} \frac{du_e}{dx} \frac{P_e r N}{d(NP_e r)/dx} \left[ \frac{\rho_e}{\rho} - (f')^2 \right] = 0$$

Set  $\frac{\rho_e \mu_e r u_e}{P_e N [d(NP_e r)/dx]} = 1$  to obtain  $N(x)$

Now  $\frac{d(Q^2)}{dx} = \frac{d(Q^2)}{dQ} \frac{dQ}{dx} = 2Q \frac{dQ}{dx}$  (where  $Q$  is any dependent variable)

so that

$$\frac{d(NP_e r)^2}{dx} = \frac{2(NP_e r) P_e \mu_e r u_e}{P_e N} = 2 \rho_e \mu_e r u_e$$

But at  $x = 0$   $r = 0$

$$(NP_e r)^2 = 2 \int_0^x \rho_e \mu_e r^2 u_e dx$$

and so

$$N(x) = \left[ \frac{2 \int_0^x \rho_e \mu_e r^2 u_e dx}{P_e^2 r^2} \right]^{1/2}$$

thus the required transformations

$$\begin{aligned} \text{are } \eta &= \frac{u_e(x)}{N(x)} \frac{\rho_e}{P_e} \int_0^y \frac{\rho}{\rho_e} dy \\ &= \frac{\rho_e u_e r}{(2x)^{1/2}} \int_0^y \frac{\rho}{\rho_e} dy \end{aligned} \quad \dots (9)$$

where  $\bar{x} = \int_0^x \rho_e \mu_e r^2 u_e dx$  . . . (10)

Giving rise to the momentum equation in the form

$$(Cf'')' + ff'' + \frac{1}{u_e} \frac{du_e}{dx} \left\{ \frac{\rho_e}{\rho} - (f')^2 \right\} \frac{P_e P_e r}{\rho_e \mu_e r u_e} \frac{2\bar{x}}{P_e^2 r^2} = 0$$

$$(Cf'')' + ff'' + \frac{2\bar{x}}{u_e} \frac{du_e}{dx} \frac{d\bar{x}}{dx} \frac{1}{\rho_e \mu_e u_e r^2} \left\{ \frac{\rho_e}{\rho} - (f')^2 \right\} = 0$$

$$(Cf'')' + ff'' + \frac{2\bar{x}}{u_e} \frac{du_e}{dx} \left[ \frac{\rho_e}{\rho} - (f')^2 \right] = 0 \quad \dots (11)$$

Taking the energy equation

$$\rho u \frac{\partial H}{\partial x} + \rho v \frac{\partial H}{\partial y} = \frac{\partial}{\partial y} \left[ \frac{\mu}{Pr} \frac{\partial H}{\partial y} + \frac{\mu}{2} \left( 1 - \frac{1}{Pr} \right) \frac{\partial u^2}{\partial y} \right]$$

Now it can be shown that when the transformation equation are used

$$\rho u \frac{\partial Q}{\partial x} + \rho v \frac{\partial Q}{\partial y} = \rho u_e^2 \rho_e \mu_e r^2 \left( f' \frac{\partial Q}{\partial x} - f' \frac{\partial \eta}{\partial x} \frac{\partial Q}{\partial \eta} - \frac{f}{2x} \frac{\partial Q}{\partial \eta} \right)$$

so

$$\rho u \frac{\partial H}{\partial x} + \rho v \frac{\partial H}{\partial y} = \rho u_e^2 P_e \mu_e r^2 \left[ f' \frac{\partial H}{\partial x} - f' \frac{\partial \eta}{\partial x} \frac{\partial H}{\partial \eta} - \frac{f}{2x} \frac{\partial H}{\partial \eta} \right]$$

$$\therefore \left[ f' \frac{\partial H}{\partial x} - f' \frac{\partial \eta}{\partial x} \frac{\partial H}{\partial \eta} \right] = \frac{1}{\rho u_e^2 \rho_e \mu_e r^2} \frac{\partial}{\partial y} \left[ \frac{\mu}{Pr} \frac{\partial H}{\partial y} + \frac{\mu}{2} \left( 1 - \frac{1}{Pr} \right) \frac{\partial u^2}{\partial y} \right]$$

Assume  $H = H_e g(\eta)$  . . . (12)

$u = U_e f'(\eta)$  . . . (13)

$\psi = N(x) f(\eta) = \frac{(2\bar{x})^{1/2}}{P_e r} f(\eta)$

$\frac{\partial}{\partial y} = \frac{\rho u_e r}{(2\bar{x})^{1/2}} \frac{\partial}{\partial \eta}$

$$\left[ f' \frac{\partial H}{\partial x} - f' \frac{\partial \eta}{\partial x} \frac{\partial H}{\partial \eta} - \frac{f}{2x} \frac{\partial H}{\partial \eta} \right]$$

$$= \frac{1}{\rho u_e^2 \rho_e \mu_e r^2} \frac{\rho u_e r}{(2\bar{x})^{1/2}} \frac{\partial}{\partial \eta} \left[ \frac{\mu}{Pr} \frac{\rho u_e r}{(2\bar{x})^{1/2}} \frac{\partial H}{\partial \eta} + \frac{\mu}{2} \left( 1 - \frac{1}{Pr} \right) \frac{\rho u_e r}{(2\bar{x})^{1/2}} \frac{\partial u^2}{\partial \eta} \right]$$

$$= \frac{1}{2x} \frac{\partial}{\partial \eta} \left[ \frac{C}{Pr} \frac{\partial H}{\partial \eta} + \frac{C}{2} \left( 1 - \frac{1}{Pr} \right) \frac{\partial (u)^2}{\partial \eta} \right]$$

thus

$$f' \frac{\partial H}{\partial x} - f' \frac{\partial \eta}{\partial x} \frac{\partial H}{\partial \eta} - \frac{f}{2x} \frac{\partial H}{\partial \eta} = \frac{1}{2x} \left[ \frac{C}{Pr} \frac{\partial H}{\partial \eta} + \frac{C}{2} \left( 1 - \frac{1}{Pr} \right) \frac{\partial u^2}{\partial \eta} \right]$$

$$H = H_e g(\eta)$$

$$\frac{\partial H}{\partial \eta} = H_e g' + \epsilon \frac{\partial H_e}{\partial \eta} = H_e g'$$

$$f' \frac{\partial H}{\partial x} - f' \frac{\partial \eta}{\partial x} H_e g' - \frac{f}{2x} H_e g' = \frac{1}{2x} \frac{\partial}{\partial \eta} \left[ \frac{C}{2} \left( 1 - \frac{1}{Pr} \right) \frac{\partial u^2}{\partial \eta} \right] + \frac{1}{2x} \left[ \frac{C}{Pr} H_e g' \right]'$$

multiply by  $2x/H_e$  and rearrange

$$\left( \frac{C}{Pr} g' \right)' + fg' = \frac{2x f'}{H_e} \frac{dH}{dx} + \frac{u_e^2}{H_e} \left[ \frac{C}{2u_e^2} \left( \frac{1}{Pr} - 1 \right) \frac{\partial u^2}{\partial \eta} \right]'$$

$$\begin{aligned} \text{Now } \frac{C}{2u_e^2} \left( \frac{1}{Pr} - 1 \right) \frac{\partial u^2}{\partial \eta} &= \left[ \frac{C}{2u_e^2} \left( \frac{1}{Pr} - 1 \right) \frac{\partial u^2}{\partial u} \frac{\partial u}{\partial \eta} \right] \frac{u_e^2}{H_e} \\ &= \left[ \frac{C}{u_e^2} \left( \frac{1}{Pr} - 1 \right) u \frac{\partial u}{\partial \eta} \right] \frac{u_e^2}{H_e} \\ &= \left[ \frac{C}{u_e^2} \left( \frac{1}{Pr} - 1 \right) u_e f'(\eta) u_e f''(\eta) \right] \frac{u_e^2}{H_e} \\ &= Cf'f'' \left( \frac{1}{Pr} - 1 \right) \frac{u_e^2}{H_e} \end{aligned}$$

so that the energy equation becomes

$$\left( \frac{C}{Pr} g' \right)' + fg' = \left\{ cf'f'' \left( \frac{1}{Pr} - 1 \right) \frac{u_e^2}{H_e} \right\}' + \frac{2x f' g}{H_e} \frac{dH_e}{dx} \dots (14)$$

Equations 11 and 14 then constitute the set of equations to be solved in conjunction with the boundary conditions

$$\begin{aligned} f'(\infty) &= 1 & g'(\infty) &= 0 \\ f''(\infty) &= 0 & g(\infty) &= 1 \end{aligned}$$

### APPENDIX 3

#### AN APPLICATION OF THE RESULTS OBTAINED - THE RELATIVE ECONOMIC MERITS OF ELECTRICAL AUGMENTATION AND OXYGEN ENRICHMENT IN METHANE FLAMES

The use to which the reported work may be put is best illustrated by an example which arose during the course of study. Prompted by a recent publication, it was felt that the practical application of electrically augmented burners to industrial heating operations should be reconsidered. These can, in general, be divided into two main categories. The first group includes cases where the thermal efficiency of the system is secondary to a main requirement of high rates of energy transfer from the flame to the workpiece. A multitude of processes, usually employing open flames, falls within this classification, which includes glassworking and flame hardening together with welding, brazing and soldering operations. In many of these, oxygen enrichment is used to obtain high flame temperatures and consequently rapid heat transfer, although this necessarily increases the cost of the operation. The economic necessity for rapid heating in many processes thus dictates the use of extremely hot flames, even where the heated object remains at a relatively modest temperature level.

The second classification includes most industrial furnaces and one of the main considerations is that of fuel economy, although certain of these furnaces may also be designed to produce high heat transfer rates. However, many furnaces operate at high temperatures and as a result it is the cost per unit of heat delivered at the relevant sink temperature which becomes of prime importance when the performance of various fuels is to be evaluated. Direct comparisons based on their initial gross cost may therefore lead to quite erroneous conclusions particularly in cases where the fuels have widely different flame temperatures.

The publication by Allen and Harker (68) has attempted to provide an indication of the relative costs of heating with methane-oxygen and electrically augmented methane-air flames. It has been demonstrated by several authors that considerable enhancement of heat transfer rates can be achieved by the use of electrically boosted flames in place of ordinary unaugmented gas-air. As a result it has been suggested that potential applications of boosted burners may lie in the fields of automatic welding, metal working and other flame impingement processes.

Allen and Harker, in the paper cited, have made a theoretical comparison of the performance of both augmented and unaugmented methane flames based on the cost of the heat actually transferred to a workpiece, and on the cost of achieving a particular flame temperature. Both of these approaches appear to be rather misleading when applied to the majority of flame impingement situations. Very little significance can be attached to the flame temperature in these circumstances since it has no direct bearing on the heat transfer rates attained with different fuels. The same fundamental criticism also applies to the first basis of comparison chosen, namely that of the cost of heat transferred to the heated surface. In view of the low thermal efficiencies of open flame processes it is clear that only a small proportion of the total heat supplied is transferred to the object immersed in the flame. Consequently a more accurate assessment of performance would be afforded by the cost of attaining a specified heat flux, which in effect determines the rate at which the process may be carried out. The information presented in the paper would, however, be applicable to furnace operations were it not for the unfortunate choice of fuel and oxygen prices, which hampers the direct use of the published results. These appear to have been based on

purchases at cylinder rates rather than on the bulk deliveries normally taken by industrial users. As a result, grossly distorted cost differentials are introduced which cause unnecessary difficulty in the interpretation of the data. It was felt that the findings of the present studies could be profitably applied to this problem in an attempt to clarify the situation. Realistic fuel and oxygen prices have been taken and more suitable criteria selected for the comparisons between the respective flame systems.

### 1. Open Flame Applications

As mentioned above it is required to compare the costs incurred in the production of a specified heating rate when using the various augmented and unaugmented methane flames. In view of the wide range of temperatures met in industrial practice it has been decided to investigate the performance of each system over the range 400 to 2000K.

The work on heat transfer to surfaces at elevated temperatures has demonstrated that the inclusion of weighted average values of thermophysical properties and a correction factor  $(\bar{\mu}/\mu_s)$  to the free stream Reynolds number, provides a practical method for extending the range of established low temperature relationships. In the case of heat transfer to small spheres it has been shown that the energy exchange is governed by the expression

$$\bar{St} = 2/(\bar{Re} \bar{Pr}) + 0.69 (\bar{\mu}/\mu_s) \bar{Pr}_{eq}^{-0.67} Re_s^{-0.5} \quad \dots (1)$$

The first term on the right hand side of this equation arises from the existence of a lower limit to the Nusselt number as the Reynolds number is reduced. At sufficiently high flow velocities this term may be dropped which leads to a simplified equation

$$\bar{St} = 0.69 (\bar{\mu}/\mu_s) \bar{Pr}^{-0.67} Re_s^{-0.5} \quad \dots (2)$$

where  $Re_s$  is the Reynolds number based on free stream properties and the characteristic dimension of the heated object.

$$\text{Thus } Re = \frac{DF\rho_s}{A\mu_s}$$

$$\text{and } \frac{h_1}{h_2} = \frac{\overline{C_{p1}} \overline{\mu_1} (\overline{Pr_1})^{-0.67}}{\overline{C_{p2}} \overline{\mu_2} (\overline{Pr_2})^{-0.67}} \left[ \frac{F_1 \rho_{s1} \mu_{s2}}{F_2 \rho_{s2} \mu_{s1}} \right]^{0.5} \dots\dots(3)$$

However, the total combustion product flow rates,  $F_1$  and  $F_2$  are directly related to the appropriate supply of cold fuel gases and the volume of cold combustion products formed for each volume of fuel burned (p).

$$\text{i.e. } F = n F_g \dots\dots(4)$$

$$n = \frac{\rho_o p}{\rho_T} \dots\dots(5)$$

Consequently, by equating the heat fluxes, relative gas flow rates may be obtained for each system, since from (3) and (4)

$$\frac{F_{g2}}{F_{g1}} = \left[ \frac{\overline{C_{p1}} \overline{\mu_1} (\overline{Pr_1})^{-0.67} \Delta T_1}{\overline{C_{p2}} \overline{\mu_2} (\overline{Pr_2})^{-0.67} \Delta T_2} \right]^2 \frac{\rho_{s2} n_1 \mu_{s2}}{\rho_{s2} n_2 \mu_{s1}} \dots\dots(6)$$

Thus, by the choice of some arbitrary values for the gas input to the methane-oxygen flame, corresponding flow rates for the electrically augmented cases may then be compared as follows:

(a) Electrically boosted flames

$$\text{Gross calorific value of fuel gas} = 37 \times 10^6 \text{ J/m}^3$$

$$\text{Cost of gas supplied} = 37 \times 10^6 C_g \text{ pence/m}^3$$

$$\text{Cost of electricity supplied} = 37 \times 10^6 R_b C_e \text{ pence/m}^3$$

$$\text{or } \underline{\text{Total cost}} = 37 \times 10^6 F_{g2} (C_g + C_e R_b) \text{ pence} \dots\dots(7)$$

(b) Fuel-oxygen flames

$$\text{Cost of fuel gas} = 37 \times 10^6 C_g \text{ pence/m}^3$$

$$\text{Cost of oxygen} = 2 C_o \text{ pence}$$

$$\text{or } \underline{\text{Total cost}} = F_{g1} (37 \times 10^6 C_g + 2 C_o) \text{ pence} \dots\dots(8)$$

From equations (6) (7) and (8), the costs incurred in obtaining any specified heat transfer rate to a given object have been evaluated for augmented burners over a range of electrical energy additions corresponding to  $R_b$  from 0 to 2. The results of these calculations have been presented graphically in Fig.44 in terms of the percentage of the cost when using a methane-oxygen flame. The following data has been used.

Table 13 : Methane, electricity and oxygen costs

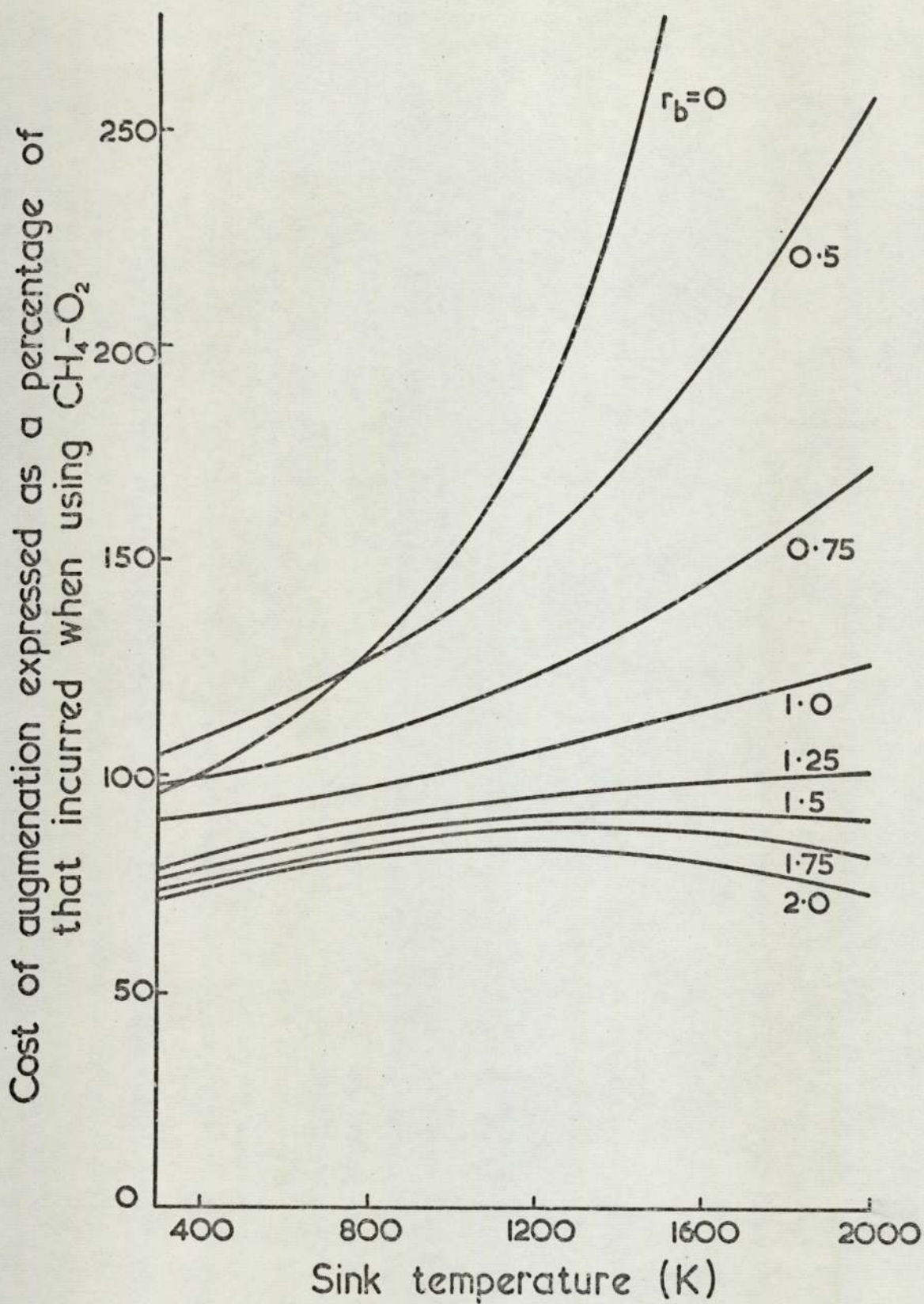
Methane	$C_G = 32 \times 10^{-9} \text{ p/J}$	(Corresponding to 8d per therm)
Electricity	$C_E = 173 \times 10^{-9} \text{ p/J}$	(Corresponding to $1\frac{1}{2}$ d per kWh)
Oxygen	$C_O = 2.65 \text{ p/m}^3$	(Corresponding to 15/- per 1000 s ft <sup>3</sup> )

## 2. Furnace Applications

The cost of heat available at a specific rejection temperature has been judged to be a major factor in the running costs of most furnaces. This quantity may readily be determined from a knowledge of the heat contents of the combustion products at the flame and sink temperatures, together with appropriate data for the fuel and oxygen prices. The results obtained have been presented graphically for the various flames (Fig.45) in terms of the relative cost of the available heat compared with that incurred with the use of an unaugmented methane-air flame. The calculations were carried out as follows:

### (a) Methane-air

The heat available above a reference temperature level  $T$  is  $(I_f - I_T) p$  Joules for every cubic metre of fuel burned, where  $p$  is the ratio of the volume of cold combustion products to the volume of cold fuel



0.44 Relative costs of achieving any specified heat flux using stoichiometric methane-oxygen or augmented methane-air flames (cost data of table 13)

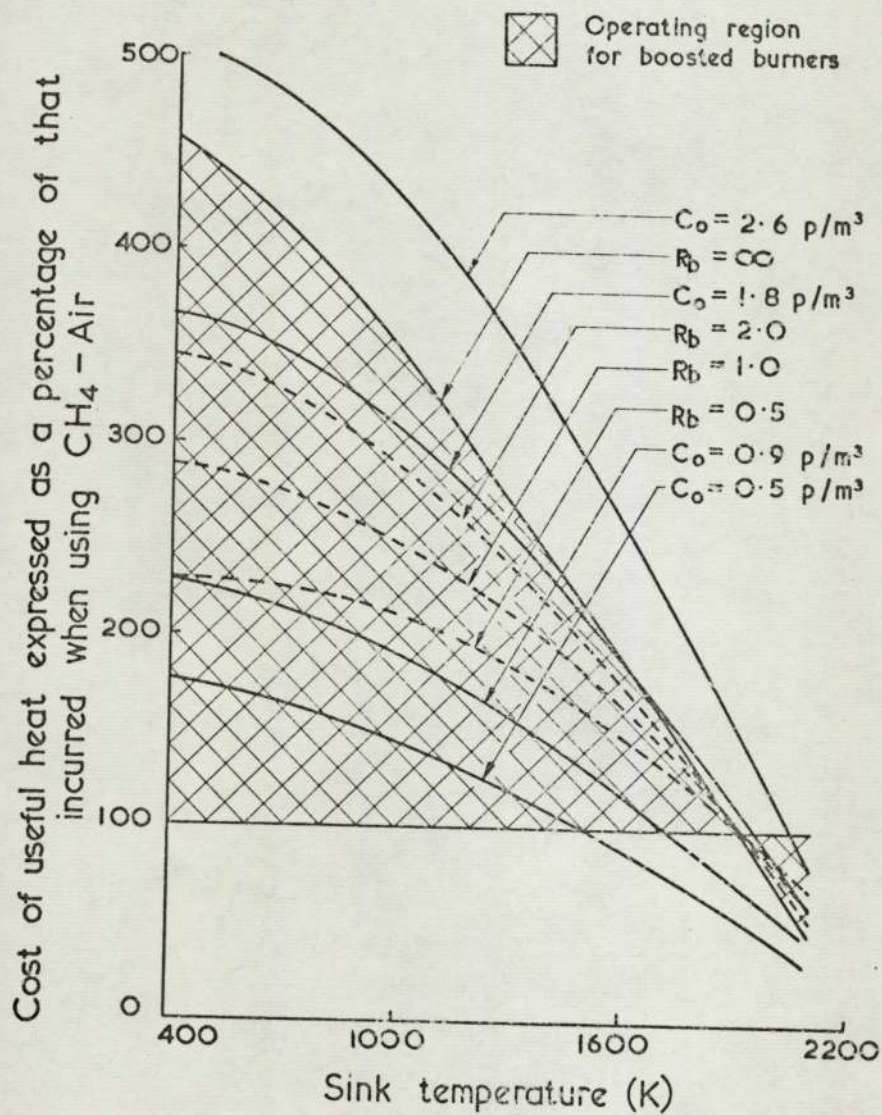


Fig.45 Relative costs of supplying useful heat with augmented and oxygen enriched flames as a function of the rejection temperature (electricity and gas costs as table 13)

supplied. Taking the gross calorific value of methane to be

$$37 \times 10^6 \text{ J/m}^3$$

$$\frac{\text{Gross heat supplied}}{\text{Useful heat}} = \frac{37 \times 10^6}{p (I_f - I_T)}$$

$$\text{The cost of each unit of heat at the temperature T} = \frac{37 \times 10^6 C_G}{p \Delta I} \text{ pence/available J}$$

### (b) Methane-oxygen

As above, the fuel cost may be determined as

$$\frac{37 \times 10^6 C_G}{p \Delta I} \text{ pence/available Joule}$$

$$\text{The oxygen cost for a stoichiometric mixture is } \frac{2 C_O}{p \Delta I}$$

Thus the overall cost for each available unit of heat is given by

$$\frac{1}{p \Delta I} (37 \times 10^6 C_G + 2C_O) \text{ pence/available Joule.}$$

### (c) Augmented methane-air

The methane cost may be determined in the same manner as before. The electrical energy input is directly proportional to the required boost ratio and to the gas flowrate.

$$\text{Electrical cost} = \frac{37 \times 10^6 C_F R_b}{p \Delta I} \text{ pence}$$

$$\text{Total cost} = \frac{37 \times 10^6}{p \Delta I} (C_G + C_E R_b) \text{ pence/available Joule.}$$

## 3. Discussion of Calculations

### 3.1 Open Flame Applications

While it is accepted that the particular prices for the gas and electricity supplies may not be universally applicable, it is felt that the values selected should provide a reasonable indication of the relative merits of the combustion systems studied. It would appear that, where rapid heat transfer is of primary importance, the use of augmented flames having boost ratios in excess of unity may introduce some savings on running costs. Calculations have been based

exclusively on data for the combustion products of methane but results should be equally valid for either Algerian or North Sea natural gases.

It can be seen from Fig.44 that, using a boost ratio of 2, fuel economies amounting to about 25% may be achieved. Clearly, differing fuel and oxygen prices would alter the form of Fig.44 but it can be seen from Eqs. 7 and 8 that the contribution of the gas cost to the overall running expenses is small. Thus other combinations of electricity and oxygen prices may be accommodated by the application of a multiplying factor  $1.53 \times 10^7 C_e/C_o$  to the information obtained from the figure. Similarly, other gas and oxygen tariffs may be included by the use of the corresponding factor  $5.54 C_g/(C_g + 5.4 \times 10^{-8} C_o)$ .

It is most unlikely that the ratio of electricity to oxygen costs could be significantly improved upon, even by a power user with a favourable load factor. Oxygen supplies at the cost quoted in Table 13 are available to consumers requiring relatively small deliveries. In fact larger consumers such as steelworks may obtain supplies at less than a third of this rate, while the relevant electrical costs may be only slightly less, thereby reducing or even eliminating the economic possibilities of augmentation.

Although fuel savings of up to 25% may be effected in certain circumstances it is most unlikely that they would prove to be sufficiently large to offset the investment cost incurred with the installation of the ancillary electrical equipment. This is a consequence of the small scale of most open flame operations and the complexity of the high voltage electrical system required. In addition, all aspects of safety and reliability have been discounted, both of which act to the detriment of augmented flame burners.

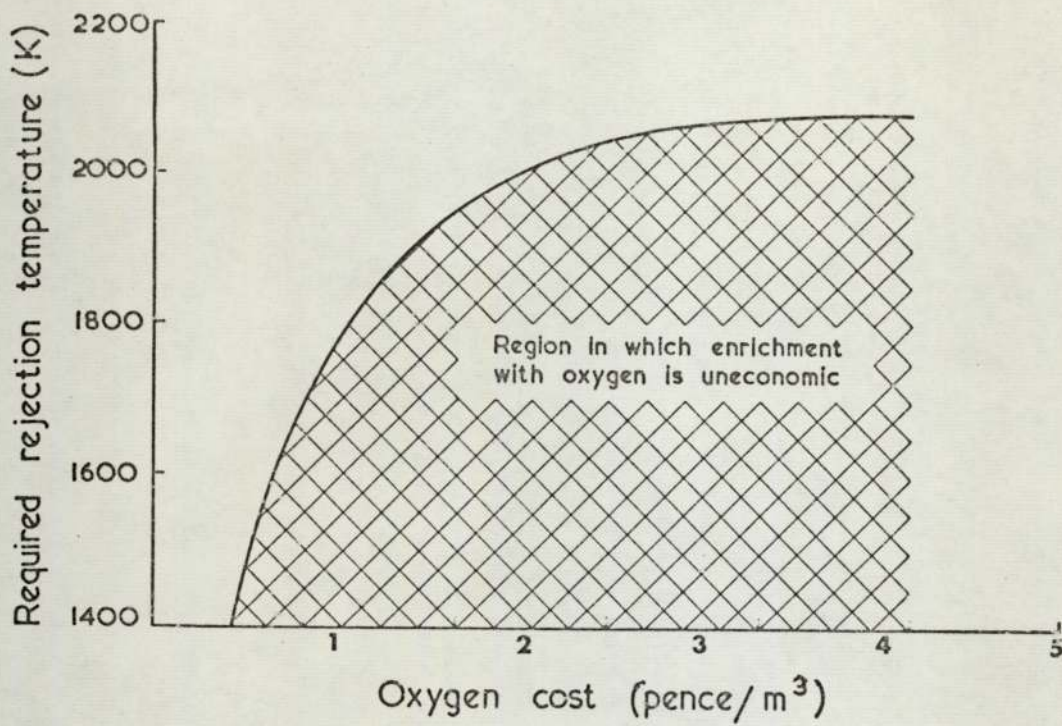


Fig. 46 Curve depicting the economics of methane-air and methane-oxygen flames based on the cost of available heat at a specified rejection temperature ( $C_e = 32 \times 10^{-9}$  pence/J)

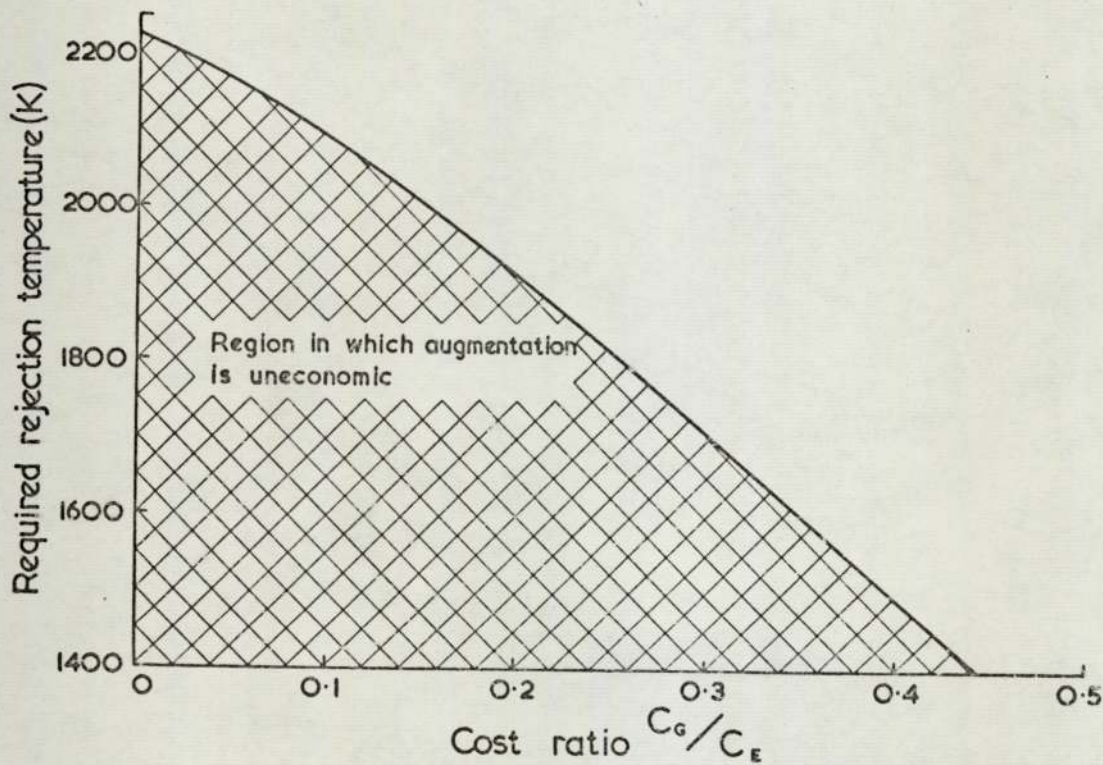


Fig. 47 Curve depicting the economics of augmented and unaugmented methane-air flames based on the cost of heat at a specified rejection temperature.

### 3.2 Furnace Applications

The cost of supplying heat to carry out a specified furnace operation has been calculated as a percentage of the cost applicable to the use of unaugmented gas-air flames. The results obtained are displayed in Fig.45 in terms of the relative costs for the various systems over a wide range of furnace conditions. A gas cost corresponding to 8d per therm has been employed throughout. It is clear from the figure that the use of oxygen enrichment is, in the majority of cases, an uneconomic venture. This is only to be expected since the oxygen introduced does not contribute to the total energy of the system, but merely raises the temperature by the exclusion of diluents. Economies resulting from the higher operating temperatures of oxygen enriched flames are only obtained when cheap oxygen is available. The 'break even' temperatures are presented for various oxygen costs in Fig.46. It is evident that only extremely large consumers maintaining furnaces in excess of 1500 K are likely to benefit from the use of oxygen enrichment.

It is abundantly clear that for the particular fuel costs chosen, the application of boosted burners to furnace projects are most unlikely in the foreseeable future since the use of unaugmented flames holds distinct financial advantages at temperatures below 1900 K. It is possible to estimate the 'break even' temperature for other tariffs from the conditions that the cost of available heat using the gas flame then must equal the cost of electricity. It follows that, for this condition, the economics of augmented flames must be independent of the boost ratio thereby explaining the intersection of the relevant curves on Fig.45 at 1920 K. The locus of this point may then be determined for other prices from

$$\frac{37 \times 10^6 C_G}{p \Delta I} = C_E$$

or 
$$\Delta I = 3.52 \times 10^6 \frac{C_G}{C_E} \text{ J/m}^3$$

$\Delta I$  has been calculated for a series of possible ratios for  $C_q/C_e$  and the corresponding temperatures deduced. The resulting curve of temperature against the cost ratio is depicted in Fig. 47. This shows that, even with terms most favourable to electricity, economies would only result with furnaces operating in excess of 1500 K. It is important to emphasize that amortization of the considerable capital expenditure and all questions of safety have once again been discounted in this comparison. In view of these factors it is therefore most unlikely that boosted burners will find any significant applications in the field of industrial heating, although possible uses as a form of high temperature reactor may emerge.

This cost comparison demonstrates one of the potential uses of the data produced in the course of this work. It can be seen that certain assumptions regarding flame size and velocity have had to be made, together with other minor approximations. However, the calculation does indicate that boosted burners are probably unsuitable for industrial use as a heat transfer tool - a useful conclusion and one which is borne out in practice.

## BIBLIOGRAPHY

1. HIRSCHFELDER, J.O., CURTISS, C.F., and BIRD, R.B.  
Molecular Theory of Gases and Liquids. Wiley, New York (1954).
2. JANAF Thermochemical Tables. Prepared by JANAF Thermochemical Panel, Dow Chemical Co., Midland, Michigan, U.S.A. Updated Frequently.
3. FRANCIS, W.E., and TOTH, H.E. Gas Council Special Report No.2 (1963).
4. KOTARI, M., Proc.Physico - Mathematical Soc.Japan. 24, 76, (1942).
5. MASON, E.A., J.Chem.Phys. 22, 169, (1954).
6. MONCHICK, L., and MASON, E.A. J.Chem.Phys. 35, 1676, (1961).
7. SUTHERLAND, W., Phil.Mag. 40, 421, (1895).
8. WASSILJEWA, A., Physik.Z. 5, 737, (1904).
9. WILKE, C.R., J.Chem.Phys. 18, 517, (1950).
10. BUDDENBURG, J.W., and WILKE, C.R., Ind.Eng.Chem.41, 1345, (1949).
11. FRANCIS, W.E., Trans Faraday Soc. 54, 1492, (1958).
12. BROKAW, R.S., J.Chem.Phys. 29, 391, (1958).
13. DAVIES, R.M., Private Communication (1970).
14. EUCKEN, A., Physik.Z. 14, 324, (1913).
15. CHAPMAN, S., and COWLING, T.G. The Mathematical Theory of Non-uniform Gases. Cambridge University Press (1952)
16. SCHAFAR, K., Z.Phys.Chem. B53, 149, (1943).
17. MEIXNER, J., Z.Naturf. 8A, 69, (1953).
18. MASON, E.A., and MONCHICK, L., J.Chem.Phys. 36. 1622, (1962).
19. LINDSAY, A.L., and BROMLEY, L.A., Ind.Eng.Chem. 42, 1508, (1950).
20. BROKAW, R.S., J.Chem.Phys. 32, 1005, (1960).

21. BROKAW, R.S., J.Chem.Phys. 35, 1569, (1961).
22. SVEHLA, R.A., NASA SP-3011 (1964).
23. PERKINS, H.C., and WORSOE SCHMIDT, P. Int.J.Heat Mass Transfer 8, 1011, (1965).
24. HUMBLE, L.V., LOWDERMILK, W.H., and DESMON, L.G., NACA Report No.1020 (1951).
25. McELIGOT, D.M., SMITH, S.B., and BANKSTON, C.A., ASME.J. Heat Transfer 642 (1970).
26. TAYLOR, M.F., NASA TN-D2280 (1964).
27. TAYLOR, M.F., NASA TN-D2595 (1965).
28. SLABY, J.G., and MATTSON, W.F., NASA TN-D4959 (1968).
29. McELIGOT, D.M., SMITH, S.B., and BANKSTON, C.A., ASME.J. Heat Transfer 642 (1970).
30. DEISSLER, R.G., and EIAN, C.S., NACA TN - 2629 (1952).
31. WORSOE - SCHMIDT, P., Technical Report 247-8 Department of Mechanical Engineering, Stanford Univ., California (1964).
32. KAYS, W.M., and NICOLL, W.B., TR No.43, Department of Mechanical Engineering, Stanford Univ., California (1963).
33. KAYS, W.M., Convective Heat and Mass Transfer, P266 McGraw-Hill Brook Co. (1966).
34. COHEN, C.B., and RESHOTKO, E., NACA TN-2479 (1951).
35. SIBULKIN, M., J.Aeron.Sci. 19, 570, (1952).
36. ROSNER, D.E., AeroChem Research Laboratories Report ARL 99 Part 1 (1961).
37. DAVIES, R.M., and TOTH, H.E., Fourth Symposium on Thermophysical Properties. ASME (1968) p.350.
38. LEES, L., Jet Propulsion 26, (4), 259, (1956).
39. FAY, J.A., and RIDDELL, R.F., J.Aeron.Sci. 25, 73, (1958).

40. ROSE, P.H., and STARK, W.I., *J.Aeron.Sci.* 25, 86, (1958).
41. GRONEGRESS, H.W., and ROSSER, H., *Gas Warne International*, 16, 193, (1967).
42. FAY, R.H., Paper Presented at the AWS 1966 National Meeting, St.Louis, Oct. 1966.
43. REED, T.B., *J.Appl.Phys.* 34, (8), 2266, (1963).
44. IVERNEL, A., *Silicates Industriels* 31 (9) 355 (1966).
45. DAVIES, R.M., Tenth Symposium (International) on Combustion The Combustion Institute (1965)
46. HARKER, J.H., and FELLIS, I., *Combustion and Flame* 12, 587 (1968).
47. KILHAM, J.K., and GARSIDE, J.E. Gas Research Board Publication No.47 (1949).
48. DUNHAM, P.G., Convective Heat Transfer from Carbon Monoxide Flames. PhD.Thesis. University of Leeds (1963).
49. GIEDT, W.H., COBB, L.L., and RUSS, E.J. Paper Presented at the Winter Annual Meeting of ASME (1960). Paper No.60-WA-256.
50. GIEDT, W.H., and WOODRUFF, L.W., *ASME J.Heat Transfer.* 415 (1966).
51. ANDERSON, J.E., and STRESINO, E.F., *ASME J. Heat Transfer* 49, (1963).
52. BRIM, L.H., and EUSTIS, R.H. Paper Presented at the Space Technology and Heat Transfer Conference, Los Angeles, June 1970.
53. KILHAM, J.K., and PURVIS, M.R.I., *Combustion and Flame* 16, 47, (1971).
54. DORRANCE, W.H., *Viscous Hypersonic Flow*. McGraw-Hill Book Co.(1962).
55. BAXENDALE, D.N., LIVESEY, J.B., ROBERTS, A.L., SMITH, D.B., and WILLIAMS, A., *Combustion Science and Technology.* 2, 287, (1971).
56. QUINN, T.J., and BARBER, C.R., *Metrologia* 3, (1), 19, (1967).
57. BRITISH STANDARD 1042 "Flow Measurement".
58. MITCHELL, A.C.G., and ZERMANSKY, M.W., *Resonance Radiation and Excited Atoms*. Cambridge University Press (1934).

59. SMITH, H., and SUGDEN, T.M., Proc.Roy.Soc.A. 219, 204, (1953).
60. ROWE, P.N., CLAXTON, K.T., and LEWIS, J.B., Trans.Inst.Chem. Eng. 43, T14, (1965).
61. ROSNER, D.E., Combustion and Flame 9 (2), 199, (1965).
62. WATERS, D.J., Private Communication (1970).
63. HAYHURST, A.N., and TELFORD, N.R., Combustion and Flame, 14 303, (1970).
64. PEI, D.C.T., Chem.Eng.Prog.Symp. 61, (59), 57, (1965).
65. SNELLEMAN, W., A Flame as a Standard of Temperature, PhD. Thesis, University of Utrecht, (1965).
66. NACHTSCHEIM, P.R., Proceedings of the Heat Transfer and Fluid Mechanics Institute. University of California (1967).
67. ROSNER, D.E., Discussion on a paper by MERCONEY, R.N., and GIEDT, W.H., ASME J. Heat Transfer, 89, 205, (1967).
68. ALLEN, D., and HARKER, J.H., The Chemical Engineer. No. 231, 160, (1969).